

Subharmonic solutions for a class of predator-prey models with degenerate weights in periodic environments *

JULIÁN LÓPEZ-GÓMEZ

Universidad Complutense de Madrid

Instituto de Matemática Interdisciplinar (IMI)

Departamento de Análisis Matemático y Matemática Aplicada

Plaza de las Ciencias 3, 28040 Madrid, Spain

E-mail: julian@mat.ucm.es

EDUARDO MUÑOZ-HERNÁNDEZ

Universidad Complutense de Madrid

Instituto de Matemática Interdisciplinar (IMI)

Departamento de Análisis Matemático y Matemática Aplicada

Plaza de las Ciencias 3, 28040 Madrid, Spain

E-mail: eduardmu@ucm.es

FABIO ZANOLIN

Università degli Studi di Udine

Dipartimento di Scienze Matematiche, Informatiche e Fisiche

Via delle Scienze 2016, 33100 Udine, Italy

E-mail: fabio.zanolin@uniud.it

December 23, 2022

Abstract

This paper deals with the existence, multiplicity, minimal complexity and global structure of the subharmonic solutions to a class of planar Hamiltonian systems with periodic coefficients, being the classical predator-prey model of V. Volterra its most paradigmatic example. By means of a topological approach based on techniques from global bifurcation theory, the first part of the paper ascertains their nature, multiplicity and minimal complexity, as well as their global minimal structure, in terms of the configuration of the function coefficients in the setting of the model. The second part of the paper introduces a dynamical system approach based on the theory of topological horseshoes that permits to detect, besides subharmonic solutions, “chaotic-type” solutions. As a byproduct of our analysis, the simplest predator-prey prototype models in periodic environments can provoke chaotic dynamics. This cannot occur in cooperative and quasi-cooperative dynamics, as a consequence of the ordering imposed by the maximum principle.

*This paper has been written under the auspices of the Ministry of Science, Technology and Universities of Spain, under Research Grant PID2021-123343NB-I00, and of the IMI of Complutense University. The second author, ORCID 0000-0003-1184-6231, has been also supported by contract CT42/18-CT43/18 of Complutense University of Madrid.

2010 Mathematics Subject Classification: 34C25, 37B55, 37E40, 37J12.

Keywords and Phrases. Periodic predator-prey Volterra model. Subharmonic coexistence states. Global structure. Minimal complexity. Chaotic dynamics.

1 Introduction

The analysis of subharmonic solutions to differential systems with periodic coefficients is a classical research topic which has been widely investigated also with respect to its relevant significance in several applications, including the study of differential equations models arising from Celestial Mechanics and Engineering. Generally speaking, given a first-order differential system

$$z' = F(t, z), \quad (1.1)$$

for $z = (z_1, \dots, z_d) \in \Omega$, where Ω is an open domain of \mathbb{R}^d and $F : \mathbb{R} \times \Omega \rightarrow \mathbb{R}^d$ is a sufficiently regular vector field which is T -periodic in the t -variable, by a *subharmonic solution of order $n \geq 2$* to system (1.1) we mean a nT -periodic solution of the system which is not kT -periodic for all integers $k \in \{1, \dots, n-1\}$. As pointed out by P. H. Rabinowitz in [100]:

“This latter quest is complicated by the fact that any T -periodic solution is a fortiori kT -periodic. Thus an additional argument is required to show that any subharmonics are indeed distinct.”

In particular, it will also be important to check whether a subharmonic solution of order n has indeed nT as its minimal period. This is a difficult task that nevertheless can be overcome in some circumstances thanks to the special structure of the vector field F . Some sufficient conditions have been already proposed in the literature (see, e.g., Michalek and Tarantello [82]).

The general aim of this work is to investigate, as deeply as possible, the subharmonics to a class of Lotka–Volterra systems under seasonal effects. Precisely, the model is a planar Hamiltonian system of the form

$$\begin{cases} x' = -\lambda\alpha(t)f(y), \\ y' = \lambda\beta(t)f(x), \end{cases} \quad (1.2)$$

where $f : \mathbb{R} \rightarrow \mathbb{R}$ is a locally Lipschitz continuous function with $f(0) = 0$ and $f(s)s > 0$ for $s \neq 0$ such that f is bounded on $(-\infty, 0]$ and has a superlinear growth at $+\infty$. The assumptions on f are motivated by the paradigmatic case

$$f(s) = e^s - 1, \quad (1.3)$$

coming from the original Volterra’s equations.

In 1926, Vito Volterra in [118] proposed a mathematical model for the predator-prey interactions as an answer to the statistics on the fishing data in Northern Adriatic sea,

provided by the biologist Umberto D'Ancona. His model, extraordinarily famous today, since it is discussed in most of textbooks on Ordinary Differential Equations and Ecology, has shown to be a milestone for the development of more realistic predator-prey models in Environmental Sciences and Population Dynamics (see, e.g., Begon, Harper and Townsend [7]). It can be formulated as follows

$$\begin{cases} N'_1 = N_1(a - bN_2), \\ N'_2 = N_2(-c + dN_1), \end{cases} \quad (1.4)$$

where $N_1(t) > 0$ and $N_2(t) > 0$ represent, respectively, the density of the prey and the predator populations at time t . In (1.4), the coefficients, a , b , c and d , are assumed to be positive (see Braun [12]). The same system had been already introduced few years before by Alfred J. Lotka from a hypothetical chemical reaction exhibiting periodic behavior in the chemical concentrations (see Murray [86, §3.1]), which reveals how the same models can mimic a variety of phenomenologies of a different nature. After these pioneering contributions, differential equations involving the interaction of two or more species are usually named as Lotka–Volterra systems and are represented in the general form

$$N'_i = N_i \left(a_i - \sum_{j=1}^N b_{ij} N_j \right), \quad i = 1, \dots, n, \quad (1.5)$$

though in this paper we will focus attention on those satisfying $b_{ii} = 0$. The choice of the sign of the coefficients a_i and b_{ij} allows describing different kinds of interactions, as competition, cooperation, or parasitism.

Although Volterra [119] and Lotka [77] considered the possibility of some varying in time coefficients, an extensive study of the Lotka–Volterra systems with periodic coefficients has not been carried out until more recently (see, e.g., Butler and Freedman [16], Cushing [23, 24] and Rosenblat [102], for some early works in this direction). However, in the past four decades, the researches in this area have originated a great number of contributions, also in connection with the study of periodically perturbed Hamiltonian systems and Reaction–Diffusion systems arising in genetics and population dynamics, beginning with the influential monograph of P. Hess [51] and the refinements of López–Gómez [64], where a general class of spatially heterogeneous diffusive Lotka–Volterra systems with periodic coefficients was studied. To understand the role played by the spatial heterogeneities in these models the reader is sent to the early works of López–Gómez [65] and Hutson et al. [52], as well as to the monographs [67, 68]. Further models covering more general spatial interactions, outside the Lotka–Volterra World, were introduced by López–Gómez and Molina–Meyer [70, 69].

Although the assumption that the coefficients of the model are periodic with a common period might seem restrictive, it is based on the natural assumption that the species are affected by identical seasonal effects, which is rather natural as they interact in the same environment. Precisely, the interest of this paper focuses into the following periodic

counterpart of the autonomous system (1.4)

$$\begin{cases} N'_1 = N_1(a(t) - b(t)N_2) \\ N'_2 = N_2(-c(t) + d(t)N_1) \end{cases} \quad (1.6)$$

where, typically, $a, b, c, d : \mathbb{R} \rightarrow \mathbb{R}$ are T -periodic functions such that

$$b(t) \geq 0, \quad d(t) \geq 0, \quad \int_0^T a(t) dt > 0, \quad \int_0^T c(t) dt > 0.$$

In this case, by [74, Th. A.1], the system (1.6) has a component-wise positive T -periodic solution, $(\tilde{N}_1(t), \tilde{N}_2(t))$, and the change of variables

$$N_1(t) = u(t)\tilde{N}_1(t), \quad N_2(t) = v(t)\tilde{N}_2(t),$$

leads to the study of the equivalent system

$$\begin{cases} u' = \lambda\alpha(t)u(1-v) \\ v' = \lambda\beta(t)v(-1+u) \end{cases} \quad (1.7)$$

where $(\tilde{N}_1(t), \tilde{N}_2(t))$ becomes $(1, 1)$ (see the Appendix of [74] for any further details). In (1.7), $\lambda > 0$ is regarded as a parameter, while $\alpha(t) \geq 0$ and $\beta(t) \geq 0$ are T -periodic function coefficients, where $T > 0$ is their minimal period. The component-wise *positive* periodic solutions of (1.7) are called (periodic) *coexistence states* and, obviously, are relevant in population dynamics, as they represent states where none of the interacting species is driven to extinction by the other.

Among the periodic coexistence states, the subharmonics are of particular interest. Focussing attention into the simplest prototype model with constant coefficients (1.4), it is folklore since Volterra [119] that all its positive solutions are periodic and oscillate around the equilibrium $P_0 \equiv (c/d, a/b)$ in the counterclockwise sense, lying on the “energy levels”

$$E(N_1, N_2) := dN_1 - c \log N_1 + bN_2 - a \log N_2 = \text{constant} = k,$$

for $k \in (k_0, +\infty)$, where

$$k_0 := E(P_0) = c \left(1 - \log \frac{c}{d}\right) + a \left(1 - \log \frac{a}{b}\right).$$

Therefore, P_0 is a global center in the open first quadrant. The fact that the period of the orbit at the level k , $\tau(k)$, is an increasing function of k is a more recent finding of Rothe [103], Shaaf [105] and Waldvogel [120], where it was also shown that

$$\lim_{k \downarrow k_0} \tau(k) = \frac{2\pi}{\sqrt{ac}} =: \tau_0 \quad \text{and} \quad \lim_{k \uparrow \infty} \tau(k) = +\infty.$$

Thus, for every $T \in (0, \tau_0)$, the equilibrium point P_0 is the unique T -periodic coexistence state (harmonic solution), though there are infinitely many nontrivial subharmonic coexistence states corresponding to the energy levels k for which $\tau(k) = mT$ for sufficiently

large $m \geq 2$. This classical example also illustrates how subharmonics can be packaged in equivalence classes (two subharmonics are equivalent when they are a time-shift of the other). This also holds for *nonautonomous systems*. Indeed, if $z(t)$ is a nT -periodic solution of (1.1), then $z(t + jT)$ is also a nT -periodic solution for every $j = 0, 1, \dots, n - 1$. Michalek and Tarantello [82] referred to the set

$$\Theta(z) = \{z(\cdot + jT) : j = 0, 1, \dots, n - 1\}$$

as the \mathbb{Z}_n -orbit of z . Hence, searching subharmonics in *nonautonomous* systems is a task fraught with a number of difficulties.

The main goals of this paper are the following:

- finding out nT -periodic solutions having nT as *minimal period*, namely *subharmonics of order n* ;
- among the subharmonics having the same order, ascertaining whether, or not, they belong to the same periodicity class.

Previous results on the existence and multiplicity of harmonic and subharmonic solutions in periodically perturbed predator-prey systems have been obtained by Hausrath [48] and Liu [62], as a consequence of the Moser twist theorem, and by Hausrath and Manásevich [49], Ding and Zanolin [29, 30] and Boscaggin [10] from the Poincaré–Birkhoff fixed point theorem. The latest results have been recently extended by Fonda and Toader [40] to systems in \mathbb{R}^{2n} by means of a (previous) higher-dimensional version of the Poincaré–Birkhoff theorem due to Fonda and Ureña [41]. More recently, Boscaggin and Muñoz-Hernández [11] have also analyzed the subharmonic solutions in a class of planar Hamiltonian systems including (1.7).

López-Gómez, Ortega and Tineo [76] and López-Gómez [66, §5] carried out a thorough investigation of the positive coexistence states for the generalized Lotka–Volterra system with periodic coefficients

$$\begin{cases} N'_1 = N_1(a_1(t) - c_1(t)N_1 - b_1(t)N_2), \\ N'_2 = N_2(a_2(t) + b_2(t)N_1 - c_2(t)N_2), \end{cases} \quad (1.8)$$

which includes the presence of logistic terms incorporating to the model setting some interspecific competition effects. This model has, in addition, semi-trivial coexistence states of the form $(\hat{N}_1(t), 0)$ and $(0, \hat{N}_2(t))$, where \hat{N}_i stands for the (unique) positive T -periodic solution of the logistic equation

$$N'_i = N_i(a_i(t) - c_i(t)N_i), \quad i = 1, 2.$$

As in the periodic-parabolic counterpart of (1.8), already analyzed by Hess [51] and López-Gómez [64], the local character of the semitrivial positive solutions plays a crucial role in determining the dynamics of (1.8), being a challenging task to ascertain the stability, or instability, of the coexistence states.

Ortega, López-Gómez and Tineo [76] made the crucial observation that, for the special choice

$$\alpha(t) \equiv 0, \quad \text{for } t \in [T/2, T], \quad \beta(t) \equiv 0, \quad \text{for } t \in [0, T/2], \quad (1.9)$$

(1.7) has a (unique) linearly unstable coexistence state, though the system can admit two coexistence states (see [76, Rem. 7.5]). This is strong contrast with some previous one-dimensional uniqueness results available for the diffusive counterparts of these models (see the detailed discussion of [66]). Actually, this prototype model has shown to be rather paradigmatic for analyzing the local character and the multiplicity of harmonic and subharmonic coexistence states. Indeed, setting

$$A := \int_0^T \alpha(t) dt, \quad B := \int_0^T \beta(t) dt, \quad (1.10)$$

it follows from [76, Pr. 7.1] that $P_0 \equiv (1, 1)$ is linearly unstable if

$$\lambda > \frac{2}{\sqrt{AB}}. \quad (1.11)$$

Moreover, by [66, Th. 5.3], the instability of P_0 guarantees the existence of three coexistence states for (1.8) within the appropriate ranges of values of its function coefficients. It turns out that, besides the unique (harmonic) coexistence state P_0 , there are, at least, two additional $2T$ -periodic coexistence states if (1.11) holds. After two decades, López-Gómez and Muñoz-Hernández [73] were able to construct nT -periodic solutions for every $n \geq 2$, providing simultaneously with a sharp estimate of their minimal cardinals. Figure 1 shows the (minimal) global bifurcation diagram of subharmonics of (1.7) found in [73] for an arbitrary choice of $\alpha(t)$ and $\beta(t)$ satisfying the *orthogonality condition* (1.9).

These findings should be also true, at least, when $\alpha(t)$ and $\beta(t)$ are *nearly orthogonal*, in the sense that the product $\alpha\beta$ is sufficiently small in $[0, T]$, and actually they might be also true for very general classes of weight functions $\alpha(t)$ and $\beta(t)$ far from satisfying (1.9). Thus, it is rather natural to investigate the structure of the set of subharmonics of (1.7) for more general configurations of $\alpha(t)$ and $\beta(t)$ than those satisfying (1.9). Besides its intrinsic interest, this analysis might reveal some new important features, based, e.g., on the shapes of $\alpha(t)$ and $\beta(t)$, that might be significative in population dynamics. Indeed, as already discussed by the authors in [74], when $\beta \equiv 0$, one is considering a seasonal time-interval where predator is still aggressive with respect to the prey but does not take advantage of the harvest, which may simulate the difference between the hunting and the gathering period. Analog interpretations may be given for the time-intervals when $\alpha \equiv 0$.

From the mathematical analysis of (1.7) it becomes apparent that its dynamics might vary according to the measure of the intersection of the supports of α and β . To differentiate the two extreme cases, we will name as “degenerate” the case when $|\text{supp } \alpha \cap \text{supp } \beta| = 0$, while the case when

$$|\text{supp } \alpha \cap \text{supp } \beta| > 0.$$

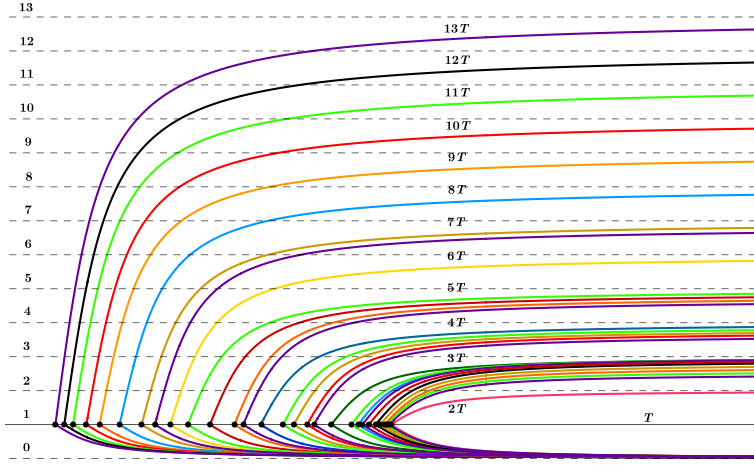


Figure 1: Admissible global bifurcation diagram under (1.9), after [73].

will be referred to as the “non-degenerate” case. In [74, 75], the authors have already shown the applicability of the Poincaré–Birkhoff theorem in searching subharmonics in both cases (see also the recent refinements of Boscaggin and Muñoz-Hernández [11]).

As a sharp analysis of (1.7) seems imperative to classify all the possible dynamics associated to a general predator-prey system with periodic coefficients, throughout this paper we will focus our attention into the simplest prototype model (1.7), with special emphasis towards the problem of analyzing its subharmonic solutions depending on whether, or not, the chosen configuration of $\alpha(t)$ and $\beta(t)$ is degenerate.

Among the various existing approaches in finding out subharmonics in Hamiltonian systems, the most successful ones are the following:

- variational methods (critical point theory),
- Kolmogorov–Arnold–Moser (KAM) theory, Moser twist theorem, and Poincaré–Birkhoff theorem,
- symbolic dynamics associated to Smale’s horseshoe-type structures, and
- reduction via symmetry and bifurcation theory.

As we are going to invoke the last three in this paper, we will shortly revisit them in the next few paragraphs.

Variational methods (critical point theory): In this framework, a number of different arguments have been given to show that the periodic solutions that are critical points of the associated functional are indeed subharmonics of large period. For instance, Rabinowitz [100] achieves it by analyzing the critical levels of the functional (see also Fonda and Lazer

[38] and Serra, Tarallo and Terracini [106]), whereas Michalek and Tarantello [82] apply a combination of estimates on critical levels and \mathbb{Z}_p -index theory. Assuming an additional non-degeneracy condition on the solutions, Conley and Zehnder [20] can get subharmonics through their Morse indices (see also Abbondandolo [1] and the references therein).

KAM theory, Moser twist theorem, and Poincaré–Birkhoff theorem: In this setting, a typical approach consists in constructing an annular region enclosed by two curves, Γ_{int} and Γ_{out} , which are invariant by the Poincaré map associated to the given planar system. Recall that the Poincaré map is the homeomorphism $\Phi = \Phi_0^T$ transforming an initial point z_0 to $\zeta(T; 0, z_0)$, where $\zeta(\cdot; 0, z_0)$ stands for the solution of (1.1) with $z(0) = z_0$. The associated flow is area-preserving when $\text{div}_z F(t, z) \equiv 0$, a condition which is always satisfied by Hamiltonian systems. Then, introducing a suitable *rotation number*, $\text{rot}([0, nT], z_0)$, the Poincaré–Birkhoff fixed point theorem guarantees the existence of at least two fixed points for Φ^n in the interior of the annulus as soon as the following *twist condition*

$$\text{rot}([0, nT], z_0) \begin{cases} < j \text{ [resp] } > j \text{ for all } z_0 \in \Gamma_{\text{int}} \\ > j \text{ [resp] } < j \text{ for all } z_0 \in \Gamma_{\text{out}} \end{cases} \quad (1.12)$$

holds for some integer j . In such situation, the fixed points of Φ^n have j as an associated rotation number. This actually entails the existence of subharmonics of order n if n and j are co-prime integers. Theorems 2.1 and 3.1 of Neumann [88] give some sufficient conditions so that these subharmonic solutions belong to different periodicity classes.

A typical definition of rotation number can be given by passing to polar coordinates and counting the number of turns (counterclockwise, or clockwise) that the solution $\zeta(t; 0, z_0)$ makes around the origin in a given time-interval. The choice of the origin as a “pivotal point” is merely conventional, but it fits well for systems like (1.2), where $F(t, 0) \equiv 0$. Adopting this methodology, for any given interval $[t_0, t_1]$, we will set

$$\text{rot}([t_0, t_1], z_0) := \delta \frac{1}{2\pi} \int_{t_0}^{t_1} \frac{F(t, \zeta(t; t_0, z_0)) \wedge \zeta(t; t_0, z_0)}{\|\zeta(t; t_0, z_0)\|^2} dt \quad (1.13)$$

where $\delta = \pm 1$. Boscaggin [10] and Boscaggin and Muñoz-Hernández [11] give some other equivalent notions.

Ding [31], Fonda and Ureña [41], Frank [42], Qian and Torres [97] and Rebelo [101] have found some refinements of the Poincaré–Birkhoff fixed point theorem adapted to more general settings where the boundary invariance of the underlying annular region is lost. Dalbono and Rebelo [25] and more recently Fonda, Sabatini and Zanolin [39] have reviewed a series of results on the applicability of the Poincaré–Birkhoff theorem in non-invariant annuli.

According to some recent findings of Boscaggin and Muñoz-Hernández [11], there is a link between the variational approach discussed in the previous paragraph and the rotation number estimates necessary to apply the Poincaré–Birkhoff theorem based on the Conley–Zehnder–Maslov index (see Abbondandolo [1] and Long [63]).

Nevertheless, establishing the existence of the invariant curves is a hard task that typically requires to invoke the KAM theory or some of its variants (see Laederich and Levi [58]), like, e.g., the Moser twist theorem [84], as in Dieckerhoff and Zehnder [28] and Levi [59] for the scalar second order differential equation

$$x'' + V_x(x, t) = 0,$$

or as in Haurath [48] and Liu [62] for the most sophisticated predator-prey system.

Symbolic dynamics associated with horseshoe-type structures: In connection with the previous discussion, subharmonics can be also detected by applying to the Poincaré map and its iterates various methods coming from the theory of dynamical systems, the most paradigmatic being the celebrated Smale's horseshoe (see Smale [108, 109], Moser [85, Ch. III] and Wiggins [121]). Essentially, it consists of a toy-diffeomorphism stretching and bending, recursively, a square onto a horseshoe-type domain.

In this paper, we will work in a slightly weaker setting entering into the theory of *topological horseshoes* as developed, adapting different perspectives, by Carbinatto, Kwapisz and Mischaikow [18], Mischaikow and Mrozek [83], Srzednicki [111], Srzednicki and Wójcik [112], Wójcik and Zgliczyński [122], Zgliczyński [123] and Zgliczyński and Gidea [124], just to quote some of the most illustrative contributions among a vast literature on this topic. The theory of topological horseshoes, as discussed by Burns and Weiss [14] and Kennedy and Yorke [53], consists of a series of methods introduced to extend the classical geometry of the Smale horseshoe to more general dynamical situations involving topological crossings and, crucially, avoiding any hyperbolicity assumptions on the diffeomorphism, as it might be a challenge to verify them in applications.

In particular, in this paper we will benefit of a topological approach developed by Papini and Zanolin [92, 93] and Pascoletti, Pireddu and Zanolin [94] leading to the following notion of *chaos in the coin-tossing sense*.

Definition 1.1. Let X be a metric space and $\Phi : \mathcal{Q} \rightarrow X$ be a homeomorphism. It is said that Φ has a topological horseshoe in the set \mathcal{Q} if there are $\ell \geq 2$ non-empty pairwise disjoint compact sets $\mathcal{H}_0, \dots, \mathcal{H}_{\ell-1} \subset \mathcal{Q}$ such that, for every two-sided sequence of ℓ symbols,

$$\mathbf{s} = (s_i)_{i \in \mathbb{Z}} \in \Sigma_\ell := \{0, \dots, \ell - 1\}^{\mathbb{Z}},$$

there exists $z \in \mathcal{Q}$ such that $z_i := \Phi^i(z) \in \mathcal{H}_{s_i}$ for all $i \in \mathbb{Z}$ and, whenever $(s_i)_i$ is a n -periodic sequence, then z can be chosen so that the sequence of iterates $(z_i)_i$ is as well n -periodic. In this case, it is also said that Φ *induces chaotic dynamics on ℓ symbols* in \mathcal{Q} .

Definition 1.1 is inspired in the concept of chaotic dynamics as a situation where a deterministic map can reproduce, along its iterates, all the possible outcomes of a coin-flipping experiment, as discussed by Smale [110] (see also Kirchgraber and Stoffer [54]). According to Medio, Pireddu and Zanolin [81], any map Φ inducing chaotic dynamics on ℓ symbols in \mathcal{Q} is *semi-conjugate* to the Bernoulli shift automorphism

$$\sigma : \Sigma_\ell \rightarrow \Sigma_\ell, \quad \sigma(s_i)_i := (s_{i+1})_i \quad \text{for all } i \in \mathbb{Z},$$

in the sense that there exist a compact subset, $\Lambda \subset \bigcup_{i=0, \dots, \ell-1} \mathcal{H}_i \subset \mathcal{Q}$, invariant for Φ , whose set of periodic points, $\text{Per } \Phi$, is dense in Λ , and a *continuous and surjective map* $g : \Lambda \rightarrow \Sigma_\ell$ such that:

- i) $g \circ \Phi = \sigma \circ g$, and
- ii) for every periodic sequence $\mathbf{s} \in \Sigma_\ell$, the set $g^{-1}(\mathbf{s})$ contains a periodic point of Φ with the same period.

Property ii) corresponds to the one introduced by Zgliczyński in [123, Th. 4.1]. Thus, adopting Definition 1.1 we are entering into a genuine classical definition of chaotic dynamics of Block–Coppel type, as discussed by Aulbach and Kieninger [5]. Hence, according to Adler, Konheim and McAndrew [2], Φ has a positive topological entropy. The semi-conjugation property provides a weaker form of chaos with respect to the original Smale’s horseshoe, where $g : \Lambda \rightarrow \Sigma_\ell$ is assumed to be a homeomorphism and, so, $\Phi|_\Lambda$ is *conjugate* to the Bernoulli shift. The conjugation property provides us with a stronger type of chaotic dynamics as, in such case, Φ inherits on the invariant set Λ all the properties of the automorphism σ . Therefore, all the existing notions of chaos, such as those introduced by Devaney [27], Li and Yorke [60], Aulbach and Kieninger [5] and Kirchgraber and Stoffer [54] hold simultaneously. Although there are series of results ensuring the conjugation, as, e.g., the celebrated Melnikov theorem, which requires the delicate task of analyzing perturbations of homoclinic, or heteroclinic, configurations, or the theory of linked twist maps developed by Devaney [26] and Sturman, Ottino and Wiggins [113], except in concrete special examples, it is a challenge to make sure that these sufficient conditions hold.

Clearly, for any map Φ satisfying the requirements of Definition 1.1, one can infer the existence of periodic points of arbitrary minimal period, and hence subharmonics if Φ is the Poincaré map of an ODE with periodic coefficients. For instance, if $\ell = 2$, given any periodic sequence in $\{0, 1\}$ of minimal period n , there is also a periodic point of Φ in \mathcal{Q} with minimal period n . Similar notions of “chaos” can be given by means of a number of topological methods, based on the Conley index, fixed point theories, or topological degree (see, e.g., Carbinatto, Kwapisz and Mischaikow [18], Mischaikow and Mrozek [83], Srzednicki [111], Srzednicki and Wójcik [112], Wójcik and Zgliczyński [122], Zgliczyński [123] and Zgliczyński and Gidea [124]). Typically, in any setting entailing Definition 1.1, it is possible to detect a larger number of subharmonics than merely applying the Poincaré–Birkhoff theorem (see Feltrin [35, Rem. 4.1]).

Among the main advantages of using the theory of topological horseshoes, instead of the methods discussed in the two previous items, it is worth-mentioning that, besides the system is not required to inherit any Hamiltonian structure, there are not constraints on the dimension.

Reduction via symmetry and bifurcation theory: Another successful approach for solving a huge variety of nonlinear differential equations, both ODEs and PDEs, relies on the topological degree through local and global bifurcation theory. Essentially, in the context of bifurcation theory, the continuation methods in parametric models do substitute the Implicit

Function Theorem in the presence of degenerate solutions, provided that a change of degree occurs as the parameter, λ , crosses some critical value, λ_0 . The relevance of bifurcation theory in studying nonlinear differential equations was first understood by Krasnosel'skii [55], who was able to show that any eigenvalue of the linearization at a given state with an odd (classical) algebraic multiplicity is a nonlinear eigenvalue. By a nonlinear eigenvalue we mean a bifurcation value from the given state, regardless the nature of the nonlinear terms of the differential equation. In other words, nonlinear eigenvalues are those for which the fact that bifurcation occurs is *based on the linear part*, as discussed by Chow and Hale [19]. Some years later, Rabinowitz [98, 99] established his celebrated global alternative within the setting of the Krasnosel'skii's theorem founding Global Bifurcation Theory. According to the Rabinowitz's global alternative, the global connected component, \mathfrak{C} , bifurcating from the given state at an eigenvalue with an odd (classical) algebraic multiplicity must be either unbounded, or it bifurcates from the given state at, at least, two different values of λ . The relevant fact that if \mathfrak{C} is bounded, then the number of bifurcation points from the given state with an odd algebraic multiplicity must be even was observed by Nirenberg [90].

However, the precise role played by the classical spectral theory in the context of the emerging bifurcation theory remained a real mystery for two decades. That was a mystery is confirmed by the astonishing circumstance that the extremely popular transversality condition of Crandall and Rabinowitz [21, 22] for bifurcation from simple eigenvalues was not known to entail a change of the Leray–Schauder degree until Theorem 5.6.2 of López–Gómez [67] could be derived through the generalized algebraic multiplicity, χ , of Esquinas and López–Gómez [34, 33, 67]. The multiplicity χ is far more general than the one introduced in [21, 22] for algebraically simple eigenvalues and it was used, e.g., by López–Gómez and Mora Corral [72], to characterize the existence of the Smith canonical form. According to [67, Ch.4], the oddity of χ characterizes whether, or not, λ_0 is a nonlinear eigenvalue of the problem, and this occurs if, and only if, the local degree changes as λ crosses λ_0 . And this regardless if we are dealing with the Leray–Schauder degree, or with degree for Fredholm operators of Fitzpatrick, Pejsachowicz and Rabier [36, 37], or Benevieri and Furi [8, 9], which are almost equivalent. Therefore, by Corollary 2.5 of López–Gómez and Mora–Corral [71], the local theorem of Crandall and Rabinowitz [21] is actually global. This important feature was later *rediscovered* by Shi and Wang [107] in a much less general context.

Some more specific important information in the context of dynamical bifurcation theory and singularity theory can be found in the textbooks of Guckenheimer and Holmes [47] and Golubitsky and Shaeffer [46]. Essentially, singularity theory tries to classify canonically all the possible local structures at the bifurcation values, while dynamical bifurcation theory focuses attention in bifurcation phenomena not involving only equilibria.

These abstract developments have tremendously facilitated the mathematical analysis of a huge variety of nonlinear bvp's related to a huge variety of nonlinear differential equations and systems (see, e.g., the monographs of López–Gómez [67, 68], Cantrell and Cosner [17] and Ni [89], as well as their abundant lists of references). However, the underlying mathematical analysis is more involved when dealing with periodic conditions, instead of mixed boundary conditions, especially when searching for branches of subhar-

monic solutions bifurcating from a given state. Indeed, although the pioneering strategy for constructing coexistence states as bifurcating from the semitrivial solution branches in Reaction-Diffusion systems of Lotka–Volterra type was developed by Cushing [23, 24] for their classical periodic counterparts, rather astonishingly, except for certain technicalities inherent to Nonlinear PDEs, the level of difficulty in establishing the existence of the coexistence states in the diffusive prototype models inherits the same order of magnitude as getting them in their classical periodic counterparts. Not to talk about finding out infinitely many subharmonics of large order. Although some additional contributions in this direction were done by Táboas [114], the analysis of the periodic-parabolic counterparts of these classical models, extraordinarily facilitated by the pioneering results of Cushing [23, 24] for the non-spatial models, was already ready to be developed by Hess [51] and López-Gómez [64].

Nevertheless, in spite of the huge amount of literature on bifurcation for Reaction-Diffusion Systems in population dynamics, almost no reference is available about harmonic and subharmonic solutions for predator-prey systems of Volterra type, except for those already discussed in this section, beginning with [76] and [66], and continuing, after two decades, with [73], where the weight functions $\alpha(t)$ and $\beta(t)$ were assumed to have non-overlapping supports so that the underlying Poincaré map associated with (1.7) could take a special form to allow solving the periodic problem via a one-dimensional reduction.

As already told above, the main goal of this paper is to analyze the existence, multiplicity and structure of subharmonic solutions to planar systems, including the periodic Volterra’s predator-prey model (1.7). Naturally, as the underlying Poincaré maps play a crucial role in this analysis, we will benefit of a number of methods and tools among those already described in the previous paragraphs. As a consequence of our analysis, the richness of the dynamics of (1.7) will become apparent even for the simplest configurations of $\alpha(t)$ and $\beta(t)$. Some recent applications of the Poincaré–Birkhoff fixed point theorem to equations directly related to (1.7) have been given by Boscaggin [10], Ding and Zanolin [29, 30], Fonda and Toader [40], Hausrath and Manásevich [49] and Rebelo [101]. In the more recent papers [73, 74, 75] the authors have studied in detail some simple prototype models, non-degenerate and degenerate. Essentially, this paper continues the research program initiated in [73, 74, 75] trying to understand how the relative position of the supports of the weight functions $\alpha(t)$ and $\beta(t)$ might influence the dynamics of (1.7) and the global structure of the set its subharmonics.

These goals will be achieved in Section 2 for the degenerate case by means of the bifurcation approach introduced in [73]. Precisely, we will consider the general case of weight functions having multiple non-overlapping humps as in Figure 2. Then, depending on the mutual distributions of the supports of $\alpha(t)$ and $\beta(t)$, some sharp estimates on the parameter λ ensuring the existence of nontrivial subharmonics will be given. These objectives will be accomplished in Theorems 2.1-2.5, up to deal with the most general configuration admissible for the validity of these results.

Further, in Section 3, we will analyze some simple prototype models, not previous considered in the literature, for which the associated Poincaré consists of a superposition of a

stretching and a twist producing a horseshoe-type geometry. The new findings have been collected in Theorems 3.1 and 3.2. As this topic is more sophisticated technically and not well understood by most of experts in Reaction-Diffusion systems, we will begin the proof of Theorem 3.1 by giving a rather direct proof for stepwise-constant functions $\alpha(t)$ and $\beta(t)$ before completing the proof in the general case. At a further step we will discuss the problem of the semi-conjugation/conjugation of the Poincaré map to the Bernoulli shift, which, essentially, depends on the shape of the weight functions. Finally, we will close Section 3 describing in full detail the geometric horseshoe nature of the Poincaré map associated with the periodic Volterra predator-prey system. This provides us with a (new) simple mechanism to mimic the Smale's horseshoe from one of the most paradigmatic models in population dynamics.

As a byproduct of our mathematical analysis it becomes apparent how the evolution in seasonal environments where predator-prey interaction plays a role might be random. To catch the attention of experts in Reaction-Diffusion systems and population dynamics, note that, actually, the harmonics and subharmonics of (1.7) are the non-spatial periodic harmonic and subharmonic solutions of the following Reaction-Diffusion periodic-parabolic problem

$$\begin{cases} \frac{\partial u}{\partial t} - d_1 \Delta u = \lambda \alpha(t) u (1 - v) & \text{in } \Omega \times (0, +\infty), \\ \frac{\partial v}{\partial t} - d_2 \Delta v = \lambda \beta(t) v (-1 + u) & \text{in } \Omega \times (0, +\infty), \\ \frac{\partial u}{\partial n_x} = \frac{\partial v}{\partial n_x} = 0 & \text{on } \partial\Omega \times (0, +\infty), \end{cases} \quad (1.14)$$

where Ω stands for a \mathcal{C}^2 bounded domain of \mathbb{R}^N , $N \geq 1$, n_x stands for the outward normal vector-field to Ω on its boundary, d_1 and d_2 are two positive constants, and Δ stands for the Laplace's operator in \mathbb{R}^N . Therefore, the findings of this paper seem extremely relevant from the point of view of population dynamics. As a byproduct of our analysis, non-cooperative systems in periodic environments can provoke chaotic dynamics. This cannot occur in cooperative and quasi-cooperative dynamics, as a consequence of the ordering imposed by the maximum principle. Therefore, it is just the lack of a maximum principle for the predator-prey models the main mechanism provoking chaos in these models, though this sharper analysis will be accomplished in a forthcoming paper.

To avoid unnecessary repetitions, throughout this paper we will assume that $\alpha, \beta : \mathbb{R} \rightarrow \mathbb{R}^+ := [0, +\infty)$ are continuous and T -periodic functions, though our results are easily extended to the Carathéodory setting with coefficients measurable and integrable in $L^1([0, T], \mathbb{R}^+)$. In particular, the bounded and piecewise-continuous α, β fall within our functional setting. Hence, piece-constant coefficients are admissible in Section 3.

2 A bifurcation approach: Minimal complexity of subharmonics for a class of degenerate predator-prey models

We consider the non-autonomous Volterra predator-prey model

$$\begin{cases} u' = \lambda\alpha(t)u(1-v) \\ v' = \lambda\beta(t)v(-1+u) \end{cases} \quad (2.1)$$

where $\lambda > 0$ is regarded as a real parameter, and the intersection of the supports of the non-negative weight functions α and β , denoted by

$$Z := \text{supp } \alpha \cap \text{supp } \beta,$$

is assumed to have Lebesgue measure zero, $|Z| = 0$. This is the reason why the model (2.1) is said to be *degenerate*. In (2.1), given a real number $T > 0$, α and β are T -periodic continuous functions such that

$$A := \int_0^T \alpha > 0, \quad B := \int_0^T \beta > 0.$$

These kind of degenerate Volterra predator-prey models were introduced in [76] and [66] and, then, deeply analyzed in [73]. Actually, these references dealt with the very special, but interesting, case when

$$\text{supp } \alpha \equiv [0, T/2], \quad \text{supp } \beta \equiv [T/2, T],$$

where we could benefit of the degenerate character of the model to ascertain the global structure of the set of nT -periodic coexistence states of (2.1). In the non-degenerate case when $|Z| \neq 0$, the techniques developed in [73] do not work. In such case the existence of high order subharmonics can be established through the celebrated Poincaré–Birkhoff twist theorem, or appropriate variants of it (see, e.g., [32, 41, 43, 45, 78], as well as [74] for a specific application to (2.1)). However, the twist theorem cannot provide us with the global bifurcation diagram of subharmonics constructed in [73]. The main goal of this section is sharpening and generalizing as much as possible the main findings of [73].

Precisely, we analyze the existence of nT -periodic coexistence states of (2.1) for any integer $n \geq 1$ under the following structural constraints on the weight functions α and β . For some integers $k, \ell \geq 1$, with $|k - \ell| \leq 1$, it is assumed the existence of $k + \ell$ continuous functions in the interval $[0, T]$, $\alpha_i \geq 0$, $1 \leq i \leq k$, and $\beta_j \geq 0$, $1 \leq j \leq \ell$, such that

$$\alpha = \alpha_1 + \alpha_2 + \cdots + \alpha_k, \quad \beta = \beta_1 + \beta_2 + \cdots + \beta_\ell,$$

with

$$\text{supp } \alpha_i \subseteq [t_0^i, t_1^i] \text{ and } \text{supp } \beta_j \subseteq [t_2^j, t_3^j], \quad (2.2)$$

for some partition of $[0, T]$

$$0 \leq t_0^1 < t_1^1 \leq t_2^1 < t_3^1 \leq t_0^2 < t_1^2 \leq t_2^2 < t_3^2 \leq \cdots \leq t_0^k < t_1^k \leq t_2^k < t_3^k \leq T$$

if $k = \ell$, or

$$0 \leq t_0^1 < t_1^1 \leq t_2^1 < t_3^1 \leq t_0^2 < t_1^2 \leq t_2^2 < t_3^2 \leq \cdots \leq t_0^k < t_1^k \leq T$$

if $k = \ell + 1$. Similarly, we also consider the case when, instead of (2.2),

$$\text{supp } \beta_j \subseteq [t_0^j, t_1^j] \text{ and } \text{supp } \alpha_i \subseteq [t_2^i, t_3^i], \quad (2.3)$$

for some partition of $[0, T]$

$$0 \leq t_0^1 < t_1^1 \leq t_2^1 < t_3^1 \leq t_0^2 < t_1^2 \leq t_2^2 < t_3^2 \leq \cdots \leq t_0^\ell < t_1^\ell \leq t_2^\ell < t_3^\ell \leq T$$

if $\ell = k$, or

$$0 \leq t_0^1 < t_1^1 \leq t_2^1 < t_3^1 \leq t_0^2 < t_1^2 \leq t_2^2 < t_3^2 \leq \cdots \leq t_0^\ell < t_1^\ell \leq T$$

if $\ell = k + 1$.

Moreover, we refer to an α -interval (resp. β -interval) as a maximal interval where $\beta \equiv 0$ (resp. $\alpha \equiv 0$) and we set

$$A_i := \int_0^T \alpha_i, \quad B_j := \int_0^T \beta_j. \quad (2.4)$$

Figure 2 shows a series of examples satisfying the previous requirements. Note that the support of the α_i 's and the β_j 's on each of the intervals $[t_r^i, t_{r+1}^i]$, $1 \leq i \leq k$, and $[t_r^j, t_{r+1}^j]$, $1 \leq j \leq \ell$, might not be connected.

There are two fundamental aims in this section. The first one is to show that the complexity of the global bifurcation diagram of subharmonics of (2.1) when $k = \ell$ depends on the size of k , rather than on the particular structure of the α_i 's and the β_j 's on each of the intervals of the partition of $[0, T]$. In fact, all admissible global bifurcation diagrams when $k = \ell$ can be constructed systematically, through a certain algorithm, from the one already found in [73], regardless the particular locations of each of the points of the partitions, t_r^s 's. The second aim of this section is to determine a lower bound for the number of nT -periodic coexistence states of model (2.1).

It is elementary to show that, for any initial point $z_0 := (u_0, v_0)$ (with $u_0, v_0 > 0$) and each initial time τ_0 , there exists a unique solution $(u(t; \tau_0, z_0), v(t; \tau_0, z_0))$ to system (2.1) which is globally defined in time. In the sequel, by convention, when studying nT -periodic solutions (for any $n \geq 1$), we will be looking for the fixed and periodic points of the Poincaré map with $\tau_0 = 0$, i.e.,

$$z_0 = (u_0, v_0) \mapsto (u(t; 0, z_0), v(t; 0, z_0)).$$

This does not exclude the possibility of the existence of other fixed points for the Poincaré maps defined with a different initial point τ_0 . Typically, the corresponding solutions will be equivalent through an appropriate time translation and hence, they will be not considered in counting the multiplicity of the solutions.

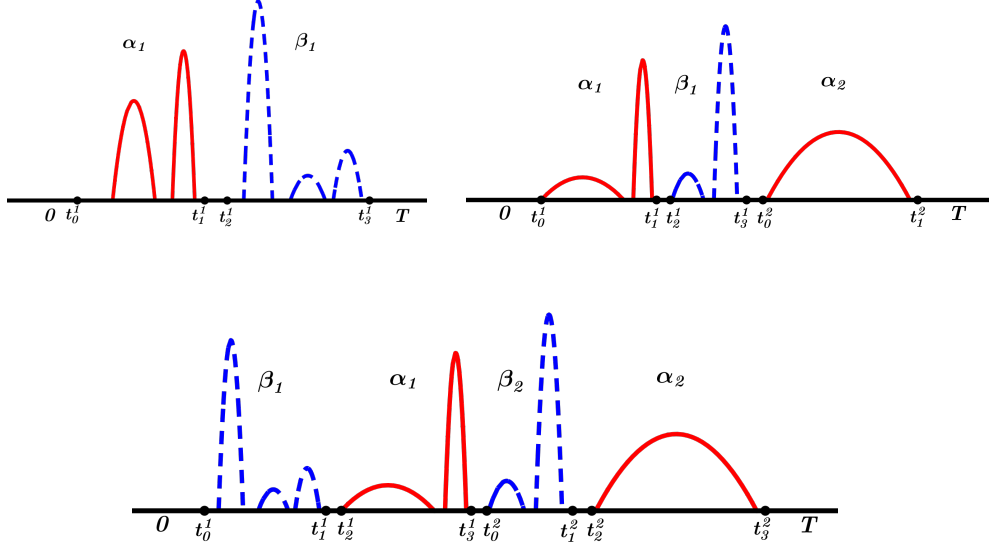


Figure 2: Some admissible examples of weight functions α and β .

2.1 The case when $k = \ell = 1$ and $\text{supp } \alpha_1 \subseteq [t_0^1, t_1^1]$

Then,

$$\text{supp } \alpha_1 \subseteq [t_0^1, t_1^1] \text{ and } \text{supp } \beta_1 \subseteq [t_2^1, t_3^1], \quad (2.5)$$

where

$$0 \leq t_0^1 < t_1^1 \leq t_2^1 < t_3^1 \leq T.$$

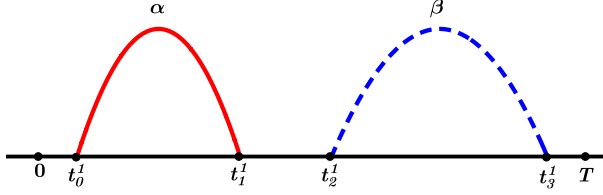
Figure 3 illustrates this case.

Under condition (2.5), the next result holds.

Theorem 2.1. *Assume (2.5). Then, the equilibrium $(1, 1)$ is the unique T -periodic coexistence state of (2.1). Thus, (2.1) cannot admit non-trivial T -periodic coexistence states. Moreover, (2.1) possesses exactly two non-trivial $2T$ -periodic coexistence states for every*

$$\lambda > \frac{2}{\sqrt{A_1 B_1}},$$

where A_1 and B_1 are those defined in (2.4). Furthermore, in the special case when $A_1 = B_1$

Figure 3: α and β satisfying (2.5)

and $u(0) = v(0)$, for every $\lambda > \frac{2}{A_1}$ and $n \geq 2$, (2.1) has, at least, n non-trivial nT -periodic coexistence states if n is even, and $n - 1$ if n is odd.

Proof. Thanks to (2.5), (2.1) can be integrated. Indeed, for any given $(u_0, v_0) \in \mathbb{R}^2$, the (unique) solution of (2.1) such that $(u(0), v(0)) = (u_0, v_0)$ is given by

$$u(t) = u_0 e^{(1-v_0)\lambda \int_0^t \alpha(s) ds}, \quad v(t) = v_0 e^{(-1+u(T))\lambda \int_0^t \beta(s) ds}, \quad t \in [0, T].$$

Thus, the associated T -time and $2T$ -time Poincaré maps are defined through

$$(u_1, v_1) := \mathcal{P}_1(u_0, v_0) := (u(T), v(T)) = (u_0 e^{(1-v_0)\lambda A_1}, v_0 e^{(-1+u_1)\lambda B_1})$$

and

$$\begin{aligned} (u_2, v_2) := \mathcal{P}_2(u_0, v_0) &= \mathcal{P}_1(u_1, v_1) = (u_1 e^{(1-v_1)\lambda A_1}, v_1 e^{(-1+u_2)\lambda B_1}) \\ &= (u_0 e^{(2-v_0-v_1)\lambda A_1}, v_0 e^{(-2+u_1+u_2)\lambda B_1}). \end{aligned}$$

It is apparent that the unique T -periodic coexistence state, i.e., the unique solution of (2.1) such that $u_0, v_0 > 0$ and $\mathcal{P}_1(u_0, v_0) = (u_0, v_0)$, is the equilibrium (1,1). Similarly, the $2T$ -periodic coexistence states are the solutions such that $u_0, v_0 > 0$ and $\mathcal{P}_2(u_0, v_0) = (u_0, v_0)$, i.e., those solutions satisfying

$$u_0, v_0 > 0, \quad 2 - u_0 = u_1 = u_0 e^{(1-v_0)\lambda A_1}, \quad 2 - v_0 = v_1 = v_0 e^{(1-u_0)\lambda B_1}. \quad (2.6)$$

Thus, expressing $x \equiv v_0$ in terms of u_0 , setting $(A, B) \equiv (A_1, B_1)$, and adapting the corresponding argument on [73, p. 41] it is easily seen that the $2T$ -periodic coexistence states are given by the zeroes of the function

$$\varphi(x) = x \left(e^{\frac{e^{(1-x)\lambda A} - 1}{e^{(1-x)\lambda A} + 1} \lambda B} + 1 \right) - 2.$$

This function has been already analyzed on [73, Th. 2.1], where it was established that it possesses exactly two zeros different from the equilibrium $x = 1$ for every $\lambda > \frac{2}{\sqrt{AB}}$. This proves the first part of the theorem.

By iterating n times, it follows that the nT -time map is defined through

$$\begin{aligned} (u_n, v_n) &:= \mathcal{P}_n(u_0, v_0) = \mathcal{P}_1^n(u_0, v_0) \\ &= (u_0 e^{(n-v_0-v_1-\cdots-v_{n-1})\lambda A}, v_0 e^{(u_1+u_2+\cdots+u_n-n)\lambda B}). \end{aligned} \quad (2.7)$$

Hence, due to (2.7), a solution $(u(t), v(t))$ of (2.1) provides us with a nT -periodic coexistence state if, and only if, $u_0 > 0$, $v_0 > 0$ and

$$\begin{cases} n = v_0 + v_1 + \cdots + v_{n-1}, \\ n = u_0 + u_1 + \cdots + u_{n-1}. \end{cases} \quad (2.8)$$

Thus, assuming that $A = B$ and $u_0 = v_0 = x$, the system (2.8) reduces to one equation (cf. [73, Le. 3.1]). Hence, setting

$$E_n(\lambda, x) := \begin{cases} \exp\left(\left[\frac{n+1}{2} - x \sum_{\substack{i=0 \\ i \in 2\mathbb{N}}}^{n-1} E_i(\lambda, x)\right]\lambda A\right), & n \in 2\mathbb{N} + 1, \\ \exp\left(\left[x \sum_{\substack{i=1 \\ i \in 2\mathbb{N}+1}}^{n-1} E_i(\lambda, x) - \frac{n}{2}\right]\lambda A\right), & n \in 2\mathbb{N}, \end{cases} \quad (2.9)$$

where $E_0(\lambda, x) = 1$, it follows from [73, Th. 3.3] that, for every $n \geq 1$,

$$\varphi_n(x) = \varphi_{n-1}(x) - 1 + xE_{n-1}(\lambda, x)$$

and $\varphi_0 \equiv 0$, where these φ_n 's are the functions whose zeroes provide us with the nT -periodic coexistence states of (2.1) that were constructed in [73]. Therefore, we are within the setting of [73], where it was inferred from these features (see Sections 2–6 of [73]) the existence of, at least, n non-trivial nT -periodic coexistence states if n is even and $n - 1$ if n is odd. This concludes the proof. \square

Note that in [73] we dealt with continuous non-negative weight functions α and β such that

$$\text{supp } \alpha \equiv [0, \frac{T}{2}] \text{ and } \text{supp } \beta \equiv [\frac{T}{2}, T],$$

whereas in Theorem 2.1 the weight functions α and β are two arbitrary non-negative continuous functions with disjoint supports. As the set of subharmonics obeys identical equations as in [73], it is apparent that, much like in [73], also in this more general case the global bifurcation diagram of the positive subharmonics of (2.1) follows the general patterns sketched in Figure 1, which has been reproduced from [73]. Similarly, at the light shared by the analysis of [73], Theorem 2.1 establishes that the global topological structure of the bifurcation diagram sketched in Figure 1 remains invariant regardless the concrete values of $t_0^1, t_1^1, t_2^1, t_3^1$ and the number and distribution of the components of the supports of the weight functions $\alpha(t)$ and $\beta(t)$ on each of the intervals of the partition of $[0, T]$ induced by these values. Naturally, much like in [73], Figure 1 shows an ideal global bifurcation diagram, for as the local behavior of most of the bifurcations from $(1, 1)$ is unknown, except for $n \in \{2, 3, 4\}$.

2.2 The case when $k = \ell = 1$ and $\text{supp } \beta_1 \subseteq [t_0^1, t_1^1]$

Then,

$$\text{supp } \beta_1 \subseteq [t_0^1, t_1^1] \text{ and } \text{supp } \alpha_1 \subseteq [t_2^1, t_3^1], \quad (2.10)$$

where

$$0 \leq t_0^1 < t_1^1 \leq t_2^1 < t_3^1 \leq T.$$

Figure 4 shows a simple example within this case.

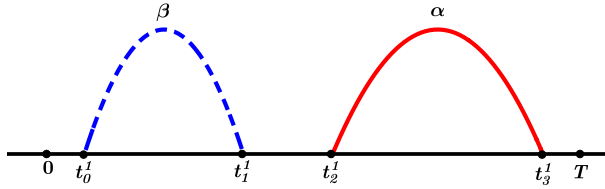


Figure 4: α and β satisfying (2.10).

Remark 2.1. Based on Theorem 2.1, one can get, very easily, solutions of (2.1) satisfying (2.10) in the interval $[0, T]$. Indeed, if (u_0, v_0) is the initial value to an nT -periodic solution of (2.1) for the weight distribution (2.5), then, a solution with initial values $(u_0 e^{(1-v_0)A_1}, v_0)$ provides us with an nT -periodic solution of (2.1) for the configuration (2.10). Next section goes further by establishing that, for the distribution (2.10), there are periodic solutions of (2.5) with initial data on the line $u = v$ by means of similar symmetry reductions and techniques as in the proof of Theorem 2.1. Equivalently, fixing a time $\tau_0 \in (t_1^1, t_2^1)$, and setting

$$\tilde{\alpha}(t) := \alpha(t + \tau_0), \quad \tilde{\beta}(t) := \beta(t + \tau_0),$$

the pair $(\tilde{\alpha}, \tilde{\beta})$ lies within the configuration of Figure 3. Thus, Theorem 2.1 applies. Note that this is equivalent to consider the Poincaré map with τ_0 as initial time.

The next result focuses attention into the case when condition (2.10) holds. A genuine situation where this occurs is represented in Figure 4. As this case was left outside the general scope of [73], it is a novelty here.

Theorem 2.2. *Under condition (2.10), the equilibrium $(1, 1)$ is the unique T -periodic co-existence state of (2.1). Moreover, (2.1) possesses exactly two non-trivial $2T$ -periodic co-existence states for every*

$$\lambda > \frac{2}{\sqrt{A_1 B_1}}. \quad (2.11)$$

If, in addition, $A_1 = B_1$, then the problem (2.1) has, for every $\lambda > \frac{2}{A_1}$ and $n \geq 3$, at least $n - 1$ non-trivial nT -periodic coexistence states with $u_0 = v_0$ if n is odd, whereas if n is even, then (2.1) possesses, at least, $n - 2$ non-trivial nT -periodic coexistence states with $u_0 = v_0$, and exactly two with $u_0 + v_0 = 2$.

The main difference between Theorems 2.1 and 2.2 relies on the fact that all the solutions of (2.1) when $A_1 = B_1$ and n is even have been constructed to satisfy $u_0 = v_0$ under condition (2.5), while (2.1) only admits $n - 2$ solutions with $u_0 = v_0$ and 2 solutions with $u_0 + v_0 = 2$ when (2.10) holds.

Proof. Since, for every $(u_0, v_0) \in \mathbb{R}^2$, the unique solution of (2.1) with $(u(0), v(0)) = (u_0, v_0)$ is given through

$$u(t) = u_0 e^{(1-v(T))\lambda \int_0^t \alpha(s) ds}, \quad v(t) = v_0 e^{(-1+u_0)\lambda \int_0^t \beta(s) ds}, \quad t \in [0, T],$$

the T -time and $2T$ -time Poincaré maps of (2.1) are given by

$$(u_1, v_1) := \mathcal{P}_1(u_0, v_0) := (u(T), v(T)) = (u_0 e^{(1-v_1)\lambda A_1}, v_0 e^{(-1+u_0)\lambda B_1})$$

and

$$\begin{aligned} (u_2, v_2) := \mathcal{P}_2(u_0, v_0) &= \mathcal{P}_1(u_1, v_1) = (u_1 e^{(1-v_2)\lambda A_1}, v_1 e^{(-1+u_1)\lambda B_1}) \\ &= (u_0 e^{(2-v_1-v_2)\lambda A_1}, v_0 e^{(-2+u_0+u_1)\lambda B_1}). \end{aligned}$$

It is easily seen that $(u_0, v_0) = (1, 1)$ is the unique fixed point of \mathcal{P}_1 . Moreover, a solution of (2.1), $(u(t), v(t))$, is a $2T$ -periodic coexistence state if, and only if, $u_0 > 0$, $v_0 > 0$ and

$$(u_2, v_2) = \mathcal{P}_2(u_0, v_0) = (u_0, v_0).$$

In other words,

$$u_0, \quad v_0 > 0, \quad 2 - u_0 = u_1 = u_0 e^{(v_0-1)\lambda A_1}, \quad 2 - v_0 = v_1 = v_0 e^{(u_0-1)\lambda B_1}. \quad (2.12)$$

Setting $(A, B) \equiv (A_1, B_1)$ and arguing as in the proof of Theorem 2.1, it becomes apparent that the non-trivial $2T$ -periodic coexistence states of (2.1) are given by the zeroes of the map

$$\psi(x) := x \left(e^{\frac{1-e^{(x-1)\lambda A}}{1+e^{(x-1)\lambda A}} \lambda B} + 1 \right) - 2 \quad (2.13)$$

with $x = v_0 \neq 1$. By definition, it is obvious that

$$\psi(x) < 0 \text{ for all } x \leq 0, \quad \psi(1) = 0, \quad \psi(x) > 0 \text{ for all } x \geq 2.$$

Moreover, by differentiating with respect to x , after rearranging terms, yields

$$\begin{aligned} \psi'(x) &= e^{\frac{1-e^{(x-1)\lambda A}}{1+e^{(x-1)\lambda A}} \lambda B} \left[1 - 2\lambda^2 ABx \frac{e^{(x-1)\lambda A}}{(1+e^{(x-1)\lambda A})^2} \right] + 1, \\ \psi''(x) &= e^{\frac{1-e^{(x-1)\lambda A}}{1+e^{(x-1)\lambda A}} \lambda B} \left[x \left(\frac{2\lambda^2 AB e^{(x-1)\lambda A}}{(1+e^{(x-1)\lambda A})^2} \right)^2 - \frac{4\lambda^2 AB e^{(x-1)\lambda A}}{(1+e^{(x-1)\lambda A})^2} + \frac{2\lambda^3 A^2 B x e^{(x-1)\lambda A} (e^{(x-1)2\lambda A} - 1)}{(1+e^{(x-1)\lambda A})^4} \right], \end{aligned}$$

for all $x \geq 0$. In particular,

$$\psi'(1) = 2 - \lambda^2 \frac{AB}{2}.$$

Thus, owing to (2.11), $\psi'(1) < 0$. Summarizing, (2.11) implies that

$$\psi(0) = -2 < 0, \quad \psi(1) = 0, \quad \psi'(1) < 0, \quad \psi(2) > 0.$$

Hence, the function ψ possesses, at least, one zeroes in each of the intervals $(0, 1)$ and $(1, 2)$. Therefore, (2.1) has, at least, two $2T$ -periodic coexistence states. Moreover, adapting the analysis carried out in [73, Sec. 2], from the previous value of $\psi''(x)$, it is easily seen that any critical point, x_c , of ψ satisfies $\psi''(x_c) < 0$ if $x_c \in (0, 1)$ and $\psi''(x_c) > 0$ if $x_c \in (1, 2)$. Consequently, (2.1) possesses exactly two $2T$ -periodic coexistence states under condition (2.11). This ends the proof of the first assertion.

Subsequently, we assume that

$$A = B, \quad u_0 = v_0 = x. \quad (2.14)$$

In this case the nT -time map is defined as follows

$$\begin{aligned} (u_n, v_n) &:= \mathcal{P}_n(u_0, v_0) = \mathcal{P}_1^n(u_0, v_0) \\ &= (u_0 e^{(n-v_1-v_2-\dots-v_n)\lambda A}, v_0 e^{(u_0+u_1+\dots+u_{n-1}-n)\lambda A}). \end{aligned}$$

Thus, $(u_n, v_n) = (u_0, v_0)$, i.e., (u_0, v_0) provides us with a subharmonic of order $n \geq 1$ of (2.1), if and only if

$$\begin{cases} n = v_0 + v_1 + \dots + v_{n-1}, \\ n = u_0 + u_1 + \dots + u_{n-1}. \end{cases} \quad (2.15)$$

Adapting the argument of the proof of [73, Lem. 3.1], it is easily seen that the two equations of (2.15) coincide under condition (2.14). Thus, the solutions of the system (2.15) are the zeroes of the function

$$\psi_n(x) := x + u_1(x) + \dots + u_{n-1}(x) - n, \quad x > 0.$$

Consequently, the nT -periodic coexistence states of (2.1) are given through $\psi^{-1}(0)$.

Arguing as in the proof of [73, Prop. 3.2], it becomes apparent that

$$(u_n, v_n) := \mathcal{P}_n(x, x) = (xE_{2n}(-\lambda, x), xE_{2n-1}(-\lambda, x))$$

for all $n \geq 1$. Hence,

$$(1, 1) = \mathcal{P}_n(1, 1) = (E_{2n}(-\lambda, 1), E_{2n-1}(-\lambda, 1)) \quad (2.16)$$

for all $n \geq 1$. Further, by the proof of [73, Th. 3.3], we find that

$$\psi_n(\lambda, x) = x \sum_{j=0}^{n-1} E_j(-\lambda, x) - n = \psi_{n-1}(x) - 1 + xE_{n-1}(-\lambda, x)$$

for all $x > 0$. Note that ψ_n also depends on the parameter $\lambda > 0$. To make explicit this dependence, we will subsequently write $\psi_n(\lambda, x)$, instead of $\psi_n(x)$, for all $n \geq 1$.

By (2.16), differentiating with respect to x and particularizing at $x = 1$ yields

$$q_n(\lambda) := \frac{\partial \psi_n}{\partial x}(\lambda, 1) = n + \sum_{j=1}^{n-1} E'_j(-\lambda, 1). \quad (2.17)$$

Adapting the induction argument of the proof of [73, Lemma 4.1], it follows from the definition of the E_j 's that the function $q_n(\lambda)$ is a polynomial for all $n \geq 1$.

The next result relates the sequence $\{q_n\}_{n \geq 1}$ with the corresponding sequence $\{p_n\}_{n \geq 1}$ constructed in [73] under condition (2.5).

Proposition 2.1. *For every $n \geq 1$,*

$$q_{2n-1}(\lambda) = p_{2n-1}(\lambda), \quad \frac{q_{2n}(\lambda)}{2 + A\lambda} = \frac{p_{2n}(\lambda)}{2 - A\lambda}, \quad (2.18)$$

and

$$q_n(\lambda) = [2 + (-1)^n A\lambda] q_{n-1}(\lambda) - q_{n-2}(\lambda). \quad (2.19)$$

Proof. According to [73, (4.6)], p_n is defined as

$$p_n(\lambda) := \frac{\partial \varphi_n}{\partial x}(\lambda, 1) = n + \sum_{j=1}^{n-1} E'_j(\lambda, 1).$$

Thus, by (2.18), $q_n(\lambda) = p_n(-\lambda)$. By [73, Cor. 4.7], $p_{2n-1}(\lambda)$ and $\frac{p_{2n}(\lambda)}{2 - A\lambda}$ are even functions in λ . Hence,

$$q_{2n-1}(\lambda) = p_{2n-1}(\lambda) \quad \text{and} \quad q_{2n}(\lambda) = p_{2n}(-\lambda) = \frac{p_{2n}(-\lambda)}{2 - A(-\lambda)}(2 + A\lambda) = \frac{p_{2n}(\lambda)}{2 - A\lambda}(2 + A\lambda).$$

This concludes the proof of (2.18).

On the other hand, by [73, Th. 4.6], we already know that

$$p_{2n-1}(\lambda) = (2 + A\lambda)p_{2n-2}(\lambda) - p_{2n-3}(\lambda) \quad (2.20)$$

and

$$\frac{p_{2n}(\lambda)}{2 - A\lambda} = p_{2n-1}(\lambda) - \frac{p_{2n-2}(\lambda)}{2 - A\lambda}. \quad (2.21)$$

Therefore, owing to (2.18), (2.20) and (2.21), we find that, for every $n \geq 1$,

$$\frac{q_{2n-1}(\lambda)}{2 - A\lambda} = \frac{p_{2n-1}(\lambda)}{2 - A\lambda} = (2 + A\lambda) \frac{p_{2n-2}(\lambda)}{2 - A\lambda} - \frac{p_{2n-3}(\lambda)}{2 - A\lambda} = q_{2n-2}(\lambda) - \frac{q_{2n-3}(\lambda)}{2 - A\lambda}$$

and

$$\frac{q_{2n}(\lambda)}{2 + A\lambda} = \frac{p_{2n}(\lambda)}{2 - A\lambda} = p_{2n-1}(\lambda) - \frac{p_{2n-2}(\lambda)}{2 - A\lambda} = q_{2n-1}(\lambda) - \frac{q_{2n-2}(\lambda)}{2 + A\lambda}.$$

So, (2.19) holds, and the proof is complete. \square

As a direct consequence of (2.18), the corresponding sets of bifurcation points from the curve $(\lambda, x) = (\lambda, 1)$ coincide under conditions (2.5) and (2.10) as soon as $u_0 = v_0 (= x)$ and $A = B$, except for the bifurcation point $(\lambda, x) = (2/A, 1)$, because

$$2/A \in p_{2n}^{-1}(0) \setminus q_{2n}^{-1}(0) \quad \text{for all } n \geq 1.$$

Moreover, also by (2.18), the mathematical analysis carried out in Sections 5 and 6 of [73] applies *mutatis mutandis* to cover the case when (2.10) holds, instead of (2.5). As a byproduct, also in the case when (2.10) holds, all the zeroes of the polynomials $q_n(\lambda)$ are simple. Thus, the Crandall–Rabinowitz theorem [21] provides us with a local analytic curve of nT -periodic solutions. Moreover, since the generalized algebraic multiplicity of Esquinas and López-Gómez [34] equals one, according to [67, Th. 6.2.1] and the unilateral theorem [67, Th. 6.4.3], these local curves of subharmonics can be extended to maximal connected components of the set of nT -subharmonics of (2.1). This proves the theorem when $u_0 = v_0 = x$ and $A = B$, regardless the oddity of $n \geq 1$.

Finally, assume that $2 = u_0 + v_0$ and $A = B$. As we already know that a solution $(u(t), v(t))$ is $2T$ -periodic if, and only if,

$$2 = u_0 + v_0 \quad 2 = v_0 + v_1 = v_0 + v_0 e^{(u_0-1)\lambda A},$$

it becomes apparent that the non-trivial $2T$ -periodic coexistence states of (2.1) are the zeroes of the function

$$\varphi_2(x) = x[e^{(1-x)\lambda A} + 1] - 2, \quad x \in (0, 2) \setminus \{1\}.$$

As, according to the proof of Theorem 2.1, φ_2 possesses exactly two zeroes, the proof of Theorem 2.2 is completed. \square

Since, according to (2.18), we already know that

$$\{r \in q_n^{-1}(0) : r > 0, n \geq 1\} = \{r \in p_n^{-1}(0) : r > 0, n \geq 1\} \setminus \{2\},$$

the global bifurcation diagram of subharmonics of (2.1) when (2.10), instead of (2.5), holds true, can be obtained from the global bifurcation diagram plotted in Figure 1 by removing the component of subharmonics of order two. However, even the local behavior of the corresponding components of subharmonics of order n in each of the cases (2.5) and (2.10) might be different, because, in general, $\varphi_n \neq \psi_n$ for all $n \geq 2$ and, hence, the identity $\varphi_n^{-1}(0) = \psi_n^{-1}(0)$ cannot be guaranteed.

By (2.6), $0 < v_0 < 1$ if $0 < u_0 < 1$. Similarly, $1 < v_0 < 2$ if $1 < u_0 < 2$. Thus, the $2T$ -periodic coexistence states of (2.1) under condition (2.5) are localized in the shadowed region of the left plot in Figure 5. Moreover, by (2.12), $1 < v_0 < 2$ if $0 < u_0 < 1$, and $0 < v_0 < 1$ if $1 < u_0 < 2$. Thus, under condition (2.10), the $2T$ -periodic coexistence states of (2.1) lie in the shadowed area of the right plot of Figure 5. This explains why (2.1) cannot admit a subharmonic of order two if $u_0 = v_0$.

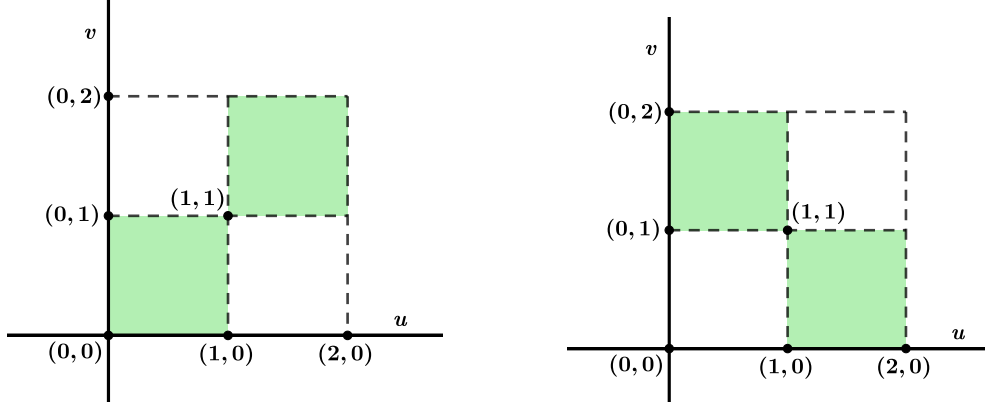


Figure 5: The shadow regions on each of these figures represent the quadrants of the phase-plane containing the initial data to $2T$ -periodic coexistence states of (2.1) under the conditions (2.5) (left) and (2.10) (right).

2.3 The case when $k = \ell \geq 2$

Then, either

$$\text{supp } \alpha_j \subseteq [t_0^j, t_1^j] \quad \text{and} \quad \text{supp } \beta_j \subseteq [t_2^j, t_3^j] \quad \text{for every } j \in \{1, 2, \dots, k\}, \quad (2.22)$$

or

$$\text{supp } \beta_j \subseteq [t_0^j, t_1^j] \quad \text{and} \quad \text{supp } \alpha_j \subseteq [t_2^j, t_3^j] \quad \text{for every } j \in \{1, 2, \dots, k\}, \quad (2.23)$$

for some

$$0 \leq t_0^1 < t_1^1 \leq t_2^1 < t_3^1 \leq \dots \leq t_0^k < t_1^k \leq t_2^k < t_3^k \leq T.$$

As in Theorems 2.1 and 2.2, to analyze the higher order subharmonics of (2.1) we need to impose the constraints

$$A_1 := \int_0^T \alpha_1 = \dots = \int_0^T \alpha_k = \int_0^T \beta_1 = \dots = \int_0^T \beta_k, \quad u_0 = v_0 > 0. \quad (2.24)$$

Even in the simplest case when $k = \ell = 1$ it is far from evident that the analysis of [73] will be possible to refine as to sharpen Theorems 2.1 and 2.2 to cover the general case when

$$\int_0^T \alpha \neq \int_0^T \beta.$$

Essentially, (2.24) reduces the problem of finding out the subharmonics of (2.1) to the problem of getting the zeroes of a sequence of real functions, instead of vectorial ones, much

like in the simplest case when $k = \ell = 1$ already covered by Sections 2.1 and 2.2. The next lemma is pivotal in the proof of the main theorem of this section. We observe that it holds independently of (2.24).

Lemma 2.1. *Assume*

$$A_1 := \int_0^T \alpha_1 = \dots = \int_0^T \alpha_k \quad \text{and} \quad B_1 := \int_0^T \beta_1 = \dots = \int_0^T \beta_k.$$

Then, under condition (2.22) (resp. (2.23)), for any integers $n, m, q, r \geq 1$ such that

$$nm = qr,$$

the Poincaré map of (2.1) at time nT for $k = \ell = m$, denoted by $\mathcal{P}_n^{m,\alpha,\beta}$ (resp. $\mathcal{P}_n^{m,\beta,\alpha}$), equals the Poincaré map of (2.1) at time qT for $k = \ell = r$; denoted, naturally, by $\mathcal{P}_q^{r,\alpha,\beta}$ (resp. $\mathcal{P}_q^{r,\beta,\alpha}$).

Proof. Assume (2.22) and $k = \ell = m$. Then, integrating in $[0, t_0^2]$ yields

$$u(t) = u_0 e^{(1-v(t_0^1))\lambda \int_0^t \alpha_1(s)ds}, \quad v(t) = v_0 e^{(u(t_0^2)-1)\lambda \int_0^t \beta_1(s)ds},$$

for all $t \in [0, t_0^2]$, because $v(t_0^1) = v_0$ and $u(t_0^2) = u(t_0^1)$. Arguing by induction, assume that

$$u(t) = u_0 e^{\sum_{j=1}^{m-1} (1-v(t_0^j))\lambda \int_0^t \alpha_j(s)ds}, \quad v(t) = v_0 e^{\sum_{j=2}^m (u(t_0^j)-1)\lambda \int_0^t \beta_{j-1}(s)ds},$$

for all $t \in [0, t_0^m]$. Then, integrating in $[t_0^m, T]$, it becomes apparent that

$$\begin{aligned} u(t) &= u_0 e^{\sum_{j=1}^m (1-v(t_0^j))\lambda \int_0^t \alpha_j(s)ds}, \\ v(t) &= v_0 e^{\sum_{j=2}^m (u(t_0^j)-1)\lambda \int_0^t \beta_{j-1}(s)ds + (u(t_0^1+T)-1) \int_0^t \beta_m(s)ds} \end{aligned}$$

for all $t \in [0, T]$. Thus, iterating n times, we find that, for every $t \in [0, nT]$,

$$\begin{cases} u(t) = u_0 e^{\sum_{i=0}^{n-1} \sum_{j=1}^m (1-v(t_0^j+iT))\lambda \int_0^t \alpha_j(s)ds} \\ v(t) = v_0 e^{\sum_{i=0}^{n-1} [\sum_{j=2}^m (u(t_0^j+iT)-1)\lambda \int_0^t \beta_{j-1}(s)ds + (u(t_0^1+(i+1)T)-1) \int_0^t \beta_m(s)ds]} \end{cases} \quad (2.25)$$

for all $t \in [0, nT]$. Moreover, the interval $[0, nT]$ can be viewed as an interval consisting of nm pairs of α and β intervals, instead of made of n copies of $[0, T]$. Thus, setting for every $1 \leq j \leq m$ and $0 \leq i \leq n-1$,

$$t_0^j + iT \equiv j + mi, \quad (u(t_0^j + iT), v(t_0^j + iT)) \equiv (u_{j+mi}, v_{j+mi}),$$

and

$$\alpha_j(t) = \alpha_j(t + iT) \equiv \alpha_{j+mi}(t), \quad \beta_j(t) = \beta_j(t + iT) \equiv \beta_{j+mi}(t),$$

(2.25) can be equivalently expressed as

$$u(t) = u_0 e^{\sum_{h=1}^{nm} (1-v_h) \lambda \int_0^t \alpha_h(s) ds}, \quad v(t) = v_0 e^{\sum_{h=2}^{nm+1} (u_h-1) \lambda \int_0^t \beta_{h-1}(s) ds},$$

for all $t \in [0, nT]$. Thus, it becomes apparent that

$$\begin{aligned} \mathcal{P}_n^{m,\alpha,\beta}(u_0, v_0) &:= (u(nT), v(nT)) \\ &= \left(u_0 e^{(nm - \sum_{h=1}^{nm} v_h) \lambda A_1}, v_0 e^{(\sum_{h=2}^{nm+1} u_h - nm) \lambda B_1} \right). \end{aligned} \quad (2.26)$$

As in (2.26) n and m are arbitrary integer numbers, it is apparent that

$$\mathcal{P}_q^{r,\alpha,\beta} = \mathcal{P}_n^{m,\alpha,\beta}$$

for all integers $q, r \geq 1$ such that $nm = qr$,

Lastly, assume (2.23) and $k = \ell = m$. Then, arguing as above yields

$$\begin{aligned} \mathcal{P}_n^{m,\beta,\alpha}(u_0, v_0) &:= (u(nT), v(nT)) \\ &= \left(u_0 e^{(\sum_{h=2}^{nm+1} v_h - nm) \lambda A_1}, v_0 e^{(nm - \sum_{h=1}^{nm} u_h) \lambda B_1} \right) \end{aligned}$$

and, therefore, taking integers $q, r \geq 1$ such that $nm = qr$, we find that

$$\mathcal{P}_q^{r,\beta,\alpha} = \mathcal{P}_n^{m,\beta,\alpha}.$$

The proof is complete. \square

Since $\mathcal{P}_q^{r,\alpha,\beta} = \mathcal{P}_n^{m,\alpha,\beta}$, their fixed points are the same. Thus, if $nm = qr$, then, the set of positive fixed points of the Poincaré map of (2.1) at time nT for $k = \ell = m$ equals the set of positive fixed points of the Poincaré map of (2.1) at time qT for $k = \ell = r$. The main result of this section invokes this feature to estimate the number of subharmonics of arbitrary order of (2.1) in any of the cases (2.22) and (2.23).

Theorem 2.3. *Suppose (2.24), $u_0 = v_0 > 0$, and $k = \ell = m \geq 2$, and set*

$$\nu(z) := \begin{cases} z & \text{if } z \in 2\mathbb{N}, \\ z-1 & \text{if } z \in 2\mathbb{N}+1, \end{cases} \quad \mu(z) := \begin{cases} z-2 & \text{if } z \in 2\mathbb{N}, \\ z-1 & \text{if } z \in 2\mathbb{N}+1. \end{cases} \quad (2.27)$$

Then, for every integer $n \geq 1$ and $\lambda > 2/A_1$, (2.1) has $\nu(nm)$ (resp. $\mu(nm)$) nT -periodic coexistence states under condition (2.22) (resp. (2.23)).

Proof. Assume (2.22). By the semigroup property of the flow, Lemma 2.22 implies that

$$(\mathcal{P}_n^{1,\alpha,\beta})^m := \mathcal{P}_{nm}^{1,\alpha,\beta} = \mathcal{P}_n^{m,\alpha,\beta}.$$

Thus, the set of positive fixed points of $\mathcal{P}_{nm}^{1,\alpha,\beta}$, already described by Theorem 2.1, equals the set of positive fixed points of $\mathcal{P}_n^{m,\alpha,\beta}$. As, due to Theorem 2.1, the map $\mathcal{P}_{nm}^{1,\alpha,\beta}$ has, at least, $\nu(nm)$ positive fixed points, the map $\mathcal{P}_n^{m,\alpha,\beta}$ also admits, at least, $\nu(nm)$ positive fixed points for all $\lambda > 2/A_1$. When, instead of (2.22), the condition (2.23) holds, then one should invoke to Theorem 2.2, instead of Theorem 2.1. As the proof follows the same patterns, we will omit any further technical detail. \square

Crucially, since $\mathcal{P}_n^{m,\alpha,\beta} = \mathcal{P}_q^{r,\alpha,\beta}$, the global bifurcation diagram of the nT -periodic coexistence states for $k = \ell = m$ coincides with the global bifurcation diagram of the qT -periodic coexistence states for $k = \ell = r$ if $nm = qr$. For instance, if $m = 2$, then the set of components of nT -periodic coexistence states provides us with the set of components of $2nT$ -periodic coexistence states for $m = 1$. Thus, for $m = 2$ the global bifurcation diagram of subharmonics can be obtained by removing from Figure 1 the set of components filled in by odd order subharmonics. Therefore, the global bifurcation diagram sketched in Figure 1 provides us with all the global bifurcation diagrams for every $k = \ell = m \geq 2$ by choosing the appropriate subharmonic components in that diagram.

Finally, the next result ascertains the number of coexistence states with minimal period nT among those given by Theorem 2.3. By minimal period nT it is meant that the coexistence states are nT -periodic but not mT -periodic if $m < n$. To state that result, we first need to deliver two well-known facts on number theory. For every integer $n \geq 1$, the Euler *totient function* is defined as

$$\Phi(n) := \text{card}(\{1 \leq m \leq n \mid \text{gcd}(n, m) = 1\}).$$

According to Gauss [44, p. 21], the Euler totient function satisfies the next identity

$$n = \sum_{d|n} \Phi(d). \quad (2.28)$$

The next result relates, through (2.28), the Euler totient function with a very special class of univariate polynomials.

Proposition 2.2. *Let $\mathbb{K}[X]$ be the univariate polynomials ring over a zero characteristic field, \mathbb{K} . Then, for every sequence $\{h_n\}_{n \geq 2} \subset \mathbb{K}[X]$ satisfying:*

1. $\deg(h_n) = n - 1$,
2. $\text{card}\{r \in \mathbb{R} : h_n(r) = 0\} = n - 1$, and
3. $h_{n_1}|h_{n_2}$ if, and only if, $n_1|n_2$,

the following identity holds

$$\Phi(n) = \text{card}\{r \in \mathbb{R} : h_n(r) = 0 \text{ and } h_d(r) \neq 0 \text{ if } d|n\}.$$

Proof. Setting

$$\begin{aligned} \mathcal{C}_h(n) &:= \text{card}\{r \in \mathbb{R} : h_n(r) = 0\}, \\ \mathcal{C}_h^{\min}(n) &:= \text{card}\{r \in \mathbb{R} : h_n(r) = 0 \text{ and } h_d(r) \neq 0 \text{ if } d|n\}, \end{aligned}$$

it is apparent that

$$\mathcal{C}_h^{\min}(n) = \mathcal{C}_h(n) - \sum_{\substack{d|n \\ d \neq 1, n}} \mathcal{C}_h^{\min}(d).$$

By definition, $\mathcal{C}_h^{\min}(p) = \Phi(p)$ for every prime integer $p \geq 2$, because $\mathcal{C}_h^{\min}(p) = \mathcal{C}_h(p) = p-1$. Moreover, for any given prime integers $p_1, p_2 \geq 2$,

$$\mathcal{C}_h^{\min}(p_1 p_2) = \begin{cases} \mathcal{C}_h(p_1 p_2) - \mathcal{C}_h^{\min}(p_1) - \mathcal{C}_h^{\min}(p_2) = p_1 p_2 - 1 - \Phi(p_1) - \Phi(p_2) & \text{if } p_1 \neq p_2, \\ \mathcal{C}_h(p_1 p_2) - \mathcal{C}_h^{\min}(p_1) = p_1 p_2 - 1 - \Phi(p_1) & \text{if } p_1 = p_2. \end{cases}$$

Thus, by (2.28), $\mathcal{C}_h^{\min}(p_1 p_2) = \Phi(p_1 p_2)$. Now, given $i \geq 2$, assume as a complete induction hypothesis, that, for every $j \in \{1, 2, \dots, i\}$,

$$\mathcal{C}_h^{\min}(p_1 p_2 \dots p_j) = \Phi(p_1 p_2 \dots p_j). \quad (2.29)$$

Then, denoting $\gamma := p_1 p_2 \dots p_{j+1}$, it follows from (2.29) that

$$\mathcal{C}_h^{\min}(\gamma) = \mathcal{C}_h(\gamma) - \sum_{\substack{d|\gamma \\ d \neq 1, \gamma}} \mathcal{C}_h^{\min}(d) = \gamma - 1 - \sum_{\substack{d|\gamma \\ d \neq 1, \gamma}} \Phi(d) = \gamma - \sum_{\substack{d|\gamma \\ d \neq \gamma}} \Phi(d).$$

Therefore, by (2.28), $\mathcal{C}_h^{\min}(\gamma) = \Phi(\gamma)$, which concludes the induction. As any integer, n , can be factorized as a (unique) finite product of prime integers, it becomes apparent that $\mathcal{C}_h^{\min}(n) = \Phi(n)$. This ends the proof. \square

Next theorem is a direct consequence of Proposition 2.2.

Theorem 2.4. *Assume (2.24), $k = \ell = m \geq 1$, and either (2.22), or (2.23). Then, (2.1) possesses, at least, $\Phi(nm)$ coexistence states with minimal period nT for all $nm > 2$.*

Proof. First, assume that (2.22). Then, by Lemma 4.3 and Theorem 5.2 of [73], the sequence of polynomials p_{nm} whose positive roots are the bifurcation points to the nT -periodic coexistence states, satisfies the hypothesis of Proposition 2.2. Thus,

$$\mathcal{C}_p^{\min}(nm) = \Phi(nm).$$

Subsequently, we denote by

$$\mathcal{C}_{p,+}^{\min}(nm) := \text{card}\{r \in \mathbb{R}, r > 0 : p_{nm}(r) = 0 \text{ and } p_d(r) \neq 0 \text{ if } d|nm\}$$

the cardinality of the set of bifurcation points of (2.1) to minimal nT -periodic coexistence states. As, thanks to [73, Cor. 4.7], we already know that $\frac{p_{2nm}(\lambda)}{2-A\lambda}$ and $p_{2nm+1}(\lambda)$ are even polynomials, it is apparent that

$$\mathcal{C}_{p,+}^{\min}(nm) = \frac{\Phi(nm)}{2}.$$

Thus, as they emerge at least two solutions from each positive root, there are, at least, $\Phi(nm)$ coexistence states with minimal period nT for $nm > 2$.

Finally, assume (2.23). Then, owing to (2.18),

$$\mathcal{C}_{q,+}^{\min}(nm) = \mathcal{C}_{p,+}^{\min}(nm) = \frac{\Phi(nm)}{2}.$$

Therefore, the same conclusion holds. This ends the proof. \square

Now we will ascertain, under the assumptions of Theorem 2.4, the classes of periodicity of the subharmonics of (2.1). Recall that, thanks to Lemma 2.1, $\mathcal{P}_n^m = \mathcal{P}_{nm}^1$. Thus, for $k = \ell = m$, the nT -periodic coexistence states of (2.1) are the same as the nmT -periodic coexistence states for $k = \ell = 1$. Remember that, in case $k = \ell = 1$, we already know from Lemma 3.1 of [73] that

$$u_h = v_{nm-h} \quad \text{for all } h \in \{1, 2, \dots, nm-1\}. \quad (2.30)$$

Proposition 2.3. *Assume (2.24), $k = \ell = 1$, and either (2.22), or (2.23), and let (u, v) be a minimal nmT -periodic coexistence state of (2.1) with $nm > 2$. Then,*

$$u_h = v_h \text{ if and only if } nm \in 2\mathbb{N} \text{ and } h = \frac{nm}{2}. \quad (2.31)$$

Therefore:

1. *The $\Phi(nm)$ subharmonics of order nm of (2.1) given by Theorem 2.4 lie in different periodicity classes if $nm \in 2\mathbb{N} + 1$, $nm \geq 3$, and*
2. *At least $\Phi(nm)/2$ of these subharmonics lie in different periodicity classes if $nm \in 2\mathbb{N}$, $nm \geq 2$.*

Proof. The proof of (2.31) proceeds by contradiction. Assume that $u_h = v_h$ for some $h \neq nm/2$. Then, by (2.30),

$$v_{nm-h} = u_h = v_h = u_{nm-h} \quad \text{for all } h \in \{1, 2, \dots, nm-1\},$$

which, in particular, implies that

$$z_h := (u_h, v_h) = (u_{nm-h}, v_{nm-h}) =: z_{nm-h}. \quad (2.32)$$

Note that, by the structure of (2.1),

$$z_h \neq z_{h+1} \quad \text{for all } h \in \{1, 2, \dots, nm-2\}. \quad (2.33)$$

Subsequently, we set

$$\omega_{\min} := \min\{h, nm-h\}, \quad \omega_{\max} := \max\{h, nm-h\}, \quad \omega^* := \omega_{\max} - \omega_{\min}.$$

Thanks to (2.32), by the T -periodicity of (2.1), we find that, for every $k \in \mathbb{N}$,

$$z_{\omega_{\max}} = z_{\omega_{\min} + k\omega^*} \pmod{nm}.$$

Suppose $\gcd(\omega^*, nm) = 1$. Then, by the Bézout's Identity, there exists an integer $k_0 \geq 1$ such that $(k_0 + 1)\omega^* = \omega^* + 1 \pmod{nm}$, which contradicts (2.33). Thus, $\gcd(\omega^*, nm) > 1$ and, hence, there exists $k < nm$ such that $k\omega^* = 0 \pmod{nm}$. Therefore,

$$\omega_{\min} + k\omega^* = \omega_{\min} \pmod{nm}$$

which implies that the solution is kT -periodic with $k < nm$. This contradicts the minimality of the period and ends the proof. \square

We conclude this section with a quick comparison with the previous results of the authors in [75] though the Poincaré–Birkhoff theorem. According to [75], if $nm \geq 3$ and $n = 3h+i \geq 1$ for some $h \geq 0$ and $i \in \{0, 1, 2\}$, then there exists $\lambda_n > 0$ such that, for every $\lambda > \lambda_n$, (2.1) possesses, at least,

$$\sigma(n) = 2 \left(hm + \left[\frac{im}{3} \right] \right) \quad (2.34)$$

nT -periodic solutions. Moreover, setting

$$\gamma(n) := \min \left\{ \gamma \geq 0 : \gcd \left(n, \frac{\sigma(n)}{2} - \gamma \right) = 1 \right\}, \quad (2.35)$$

it turns out that, for every $\lambda > \lambda_n$, (2.1) has, at least, $\sigma(n) - 2\gamma(n)$ periodic solutions with minimal period nT . Next, we will compare, in some special cases, the lower bounds on the number of independent subharmonics provided by Proposition 2.3 and Theorem 4 of [75]. Assuming that n and m prime numbers, the Euler totient function Φ satisfies

$$\Phi(nm) = \begin{cases} (n-1)(m-1) & \text{if } n \neq m, \\ n(n-1) & \text{if } n = m, \\ nm - 1 & \text{if } nm \text{ is prime.} \end{cases}$$

Thus, thanks to (2.34), there exists a constant $c > 0$ such that

$$\Phi(nm) - (\sigma(n) - 2\gamma(n)) \geq \frac{nm}{3} - c(n+m) + 2\gamma(n),$$

which is positive for sufficiently large n and m . Therefore, within this rank, under the strong assumptions on the weight functions and on the initial values imposed in this section, Proposition 2.3 is sharper than [75, Th. 4]. However, in some other circumstances the previous difference might be negative, being in these cases deeper [75, Th.4] than Proposition 2.3. It remains an open problem here to find out the eventual relationships between Φ and $\sigma - 2\gamma$, if any.

In [88] (see also [11, Sec.4.1.2]), where the Poincaré–Birkhoff theorem was improved from several perspectives, another lower bound, also related to $\Phi(n)$, was given for the number of subharmonics of order n of (2.1).

2.4 The case when $k \neq \ell$

Necessarily, either $k = \ell + 1$, or $\ell = k + 1$. Moreover, setting $m := \min\{k, \ell\}$, there exist

$$0 \leq t_0^1 < t_1^1 \leq t_2^1 < t_3^1 \leq \cdots \leq t_0^m < t_1^m \leq t_2^m < t_3^m \leq t_1^{m+1} < t_2^{m+1} \leq T,$$

such that

$$\text{supp } \alpha_i \subseteq [t_0^i, t_1^i] \quad \text{and} \quad \text{supp } \beta_j \subseteq [t_2^j, t_3^j] \quad (2.36)$$

if $k = \ell + 1$, whereas

$$\text{supp } \beta_j \subseteq [t_0^j, t_1^j] \quad \text{and} \quad \text{supp } \alpha_i \subseteq [t_2^i, t_3^i] \quad (2.37)$$

if $\ell = k + 1$.

The next result shows that also in this case (2.1) has as many subharmonics as in the context of Theorem 2.3 with $k = \ell$.

Theorem 2.5. *Assume*

$$A_1 := \int_0^T (\alpha_1 + \alpha_{m+1}) = \int_0^T \alpha_2 = \cdots = \int_0^T \alpha_m = \int_0^T \beta_1 = \int_0^T \beta_2 = \cdots = \int_0^T \beta_m \quad (2.38)$$

if (2.36) holds, and

$$B_1 := \int_0^T (\beta_1 + \beta_{m+1}) = \int_0^T \beta_2 = \cdots = \int_0^T \beta_m = \int_0^T \alpha_1 = \int_0^T \alpha_2 = \cdots = \int_0^T \alpha_m \quad (2.39)$$

under condition (2.37). Then, much like in Theorem 2.3, for every integer $n \geq 1$ and $\lambda > 2/A_1$, (2.1) has $\nu(nm)$ (resp. $\mu(nm)$) nT -periodic coexistence states under condition (2.36) (resp. (2.37)).

Proof. Assume (2.36) and (2.38), and let denote the Poincaré map in the time interval $[s_1, s_2]$ by $\mathcal{P}_{[s_1, s_2]}^{k=\ell}$ if $k = \ell$, and by $\mathcal{P}_{[s_1, s_2]}^{k=\ell+1}$ if $k = \ell + 1$. Then, the value $\int_0^T \alpha_1$ in case $k = \ell$ equals $\int_0^T (\alpha_1 + \alpha_{m+1})$ in case $k = \ell + 1$.

Let (u_0, v_0) be a fixed point of $\mathcal{P}_{[0, nT]}^{k=\ell} = \mathcal{P}_{[0, t_3^{nm}]}^{k=\ell}$. Then, the point $(u_0 e^{(1-v_0) \int_0^T \alpha_{m+1}}, v_0)$ is a fixed point of $\mathcal{P}_{[0, nT]}^{k=\ell+1} = \mathcal{P}_{[0, t_1^{nm+1}]}^{k=\ell+1}$. Indeed, by the structure of (2.1),

$$\begin{aligned} \mathcal{P}_{[0, t_1^1]}^{k=\ell+1}(u_0 e^{(1-v_0) \int_0^T \alpha_{m+1}}, v_0) &= (u_0 e^{(1-v_0) \int_0^T (\alpha_{m+1} + \alpha_1)}, v_0) \\ &= (u_0 e^{(1-v_0) A_1}, v_0) = \mathcal{P}_{[0, t_1^1]}^{k=\ell}(u_0, v_0). \end{aligned}$$

Moreover, thanks to (2.38), we also have that $\mathcal{P}_{[t_1^1, t_3^{nm}]}^{k=\ell+1} = \mathcal{P}_{[t_1^1, t_3^{nm}]}^{k=\ell}$. Thus, since (u_0, v_0) is a fixed point of $\mathcal{P}_{[0, t_3^{nm}]}^{k=\ell}$, it becomes apparent that

$$\mathcal{P}_{[0, t_3^{nm}]}^{k=\ell+1}(u_0 e^{(1-v_0) \int_0^T \alpha_{m+1}}, v_0) = (u_0, v_0).$$

Therefore,

$$\mathcal{P}_{[0, t_1^{nm+1}]}^{k=\ell+1}(u_0 e^{(1-v_0) \int_0^T \alpha_{m+1}}, v_0) = (u_0 e^{(1-v_0) \int_0^T \alpha_{m+1}}, v_0),$$

i.e., $(u_0 e^{(1-v_0) \int_0^T \alpha_{m+1}}, v_0)$ is an nT -periodic coexistence state. This establishes a bijection between the nT -coexistence states of (2.1) in cases $\ell = k$ and $k = \ell + 1$, and shows that (2.1) has $\nu(nm)$ nT -periodic coexistence states under condition (2.36).

As the proof when $\ell = k + 1$ can be accomplished similarly, we will omit its technical details here. \square

Our next result gives some sufficient conditions for non-existence.

Lemma 2.2. *The following non-existence results hold:*

- (i) (2.1) *cannot admit any non-trivial nT -periodic coexistence state, $n \in \mathbb{N}$, if $k + \ell = 1$.*
- (ii) (2.1) *cannot admit any non-trivial T -periodic coexistence state if $k + \ell = 3$.*

Proof. If $k + \ell = 1$, then either $k = 1$ and $\ell = 0$, or $\ell = 1$ and $k = 0$. Thus, either u , or v , are constant for all $t \in [0, T]$, which ends the proof.

Now, suppose that $k + \ell = 3$. Then, there exist

$$0 \leq t_0^1 < t_1^1 \leq t_2^1 < t_3^1 \leq t_0^2 \leq t_1^2 \leq T,$$

such that either

$$\text{supp } \alpha_1 \subseteq [t_0^1, t_1^1], \quad \text{supp } \beta_1 \subseteq [t_2^1, t_3^1], \quad \text{supp } \alpha_2 \subseteq [t_0^2, t_1^2],$$

or

$$\text{supp } \beta_1 \subseteq [t_0^1, t_1^1], \quad \text{supp } \alpha_1 \subseteq [t_2^1, t_3^1], \quad \text{supp } \beta_2 \subseteq [t_0^2, t_1^2],$$

as illustrated in Figure 6.

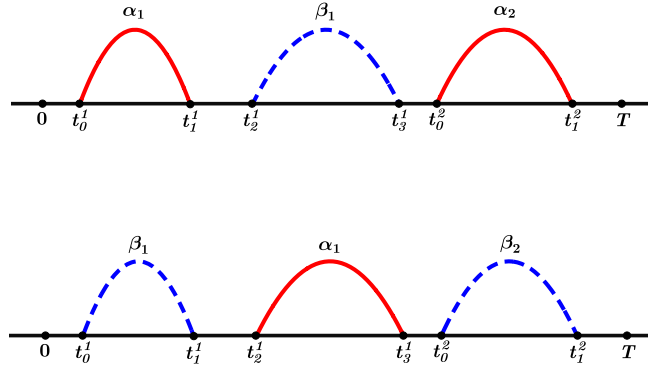


Figure 6: Two admissible examples with $k = 2, \ell = 1$, and $k = 1, \ell = 2$.

By the special structure of (2.1), where $\alpha\beta = 0$, the orbit of any solution in the interval $[0, T]$ consists of three lines, two of them parallel in the phase-plane to one of the axis, while the third one is parallel to the other axis. So, these orbits cannot be closed. Therefore, (2.1) cannot admit any T -periodic solution. \square

The next theorem summarizes the results found in the previous four sections. It characterizes the existence of T -periodic coexistence states, and subharmonics of all orders of (2.1), in terms of the number of α -intervals and β -intervals in $[0, T]$.

Theorem 2.6. *The system (2.1) admits, for sufficiently large λ , some T -periodic coexistence state if, and only if, $k + \ell \geq 4$. Moreover, for every $\lambda > 2/A_1$, under the appropriate symmetry properties, (2.1) has subharmonics of all orders, $n \geq 2$, if, and only if, $k + \ell \geq 2$.*

2.5 The limiting T -periodic case $k = \ell = 2$

According to Theorem 2.6, the condition $k + \ell \geq 4$ is necessary and sufficient so that (2.1) can admit a T -periodic coexistence state. In this section, we deal with the limiting case when $k = \ell = 2$ and ascertain the bifurcation directions to T -periodic coexistence states. Note that when $k = \ell \geq 2$, then there exist

$$0 \leq t_0^1 < t_1^1 \leq t_2^1 < t_3^1 \leq t_0^2 < t_1^2 \leq t_2^2 < t_3^2 \leq T.$$

such that either

$$\text{supp } \alpha_1 \subseteq [t_0^1, t_1^1], \quad \text{supp } \beta_1 \subseteq [t_2^1, t_3^1], \quad \text{supp } \alpha_2 \subseteq [t_0^2, t_1^2], \quad \text{supp } \beta_2 \subseteq [t_2^2, t_3^2], \quad (2.40)$$

or

$$\text{supp } \beta_1 \subseteq [t_0^1, t_1^1], \quad \text{supp } \alpha_1 \subseteq [t_2^1, t_3^1], \quad \text{supp } \beta_2 \subseteq [t_0^2, t_1^2], \quad \text{supp } \alpha_2 \subseteq [t_2^2, t_3^2]. \quad (2.41)$$

Figure 7 shows two admissible configurations.

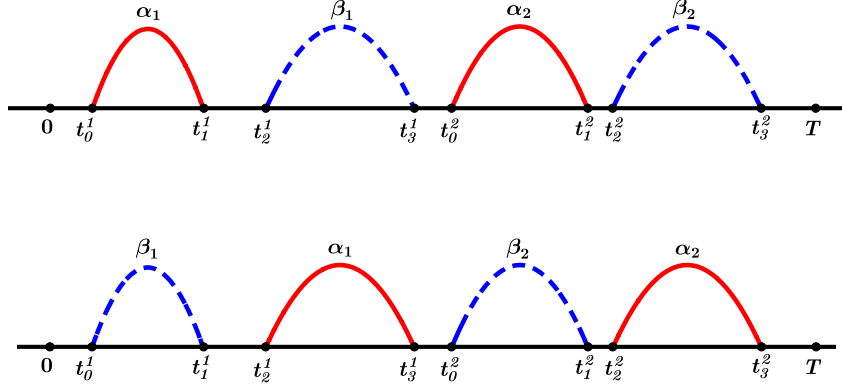


Figure 7: Two examples, with $k = \ell = 2$, satisfying (2.40) (above) and (2.41) (below).

Theorem 2.7. *Under the assumption (2.40), or (2.41), (2.1) has, at least, two T -periodic coexistence states for every $\lambda > \lambda_0$, where*

$$\lambda_0 := \sqrt{\frac{(A_1 + A_2)(B_1 + B_2)}{A_1 A_2 B_1 B_2}}, \quad A_i := \int_{\text{supp } \alpha_i} \alpha_i, \quad B_i := \int_{\text{supp } \beta_i} \beta_i, \quad i = 1, 2. \quad (2.42)$$

In general, although $\lambda > \lambda_0$ is a sufficient condition, it is far from necessary. Actually, regarding λ as the main bifurcation parameter, λ_0 provides with a bifurcation value to T -periodic coexistence states of (2.1) from the line $(\lambda, u, v) = (\lambda, 1, 1)$, and there are some ranges of values of the parameters, $A_j, B_j, j \in \{1, 2\}$, for which this bifurcation is trans-critical.

Proof. Assume (2.40). Then, integrating (2.1) yields

$$u(T) = u_0 e^{(1-v_0)\lambda A_1 + (1-v(t_0^2))\lambda A_2}, \quad v(T) = v_0 e^{(-1+u(t_0^2))\lambda B_1 + (-1+u(T))\lambda B_2}. \quad (2.43)$$

Thus, a solution $(u(t), v(t))$ of (2.1) with initial data (u_0, v_0) is a T -periodic coexistence state if, and only, if $u_0, v_0 > 0$ and $\mathcal{P}_1(u_0, v_0) = (u_0, v_0)$, i.e, by (2.43), if, and only, if $u_0, v_0 > 0$ and

$$(1 - v_0)A_1 = (v(t_0^2) - 1)A_2, \quad (1 - u_0)B_2 = (u(t_0^2) - 1)B_1,$$

which, again integrating (2.1), is equivalent to

$$\begin{cases} (1 - v_0)A_1 = (v_0 e^{(-1+u_0 e^{(1-v_0)\lambda A_1})\lambda B_1} - 1)A_2, \\ (1 - u_0)B_2 = (u_0 e^{(1-v_0)\lambda A_1} - 1)B_1. \end{cases} \quad (2.44)$$

Hence, eliminating u_0 from the second equation of (2.44),

$$u_0 = \frac{B_1 + B_2}{B_2 + B_1 e^{(1-v_0)\lambda A_1}}. \quad (2.45)$$

So, substituting (2.45) into the first equation of (2.44), it follows that

$$(1 - v_0)A_1 = (v_0 e^{(-1+\frac{B_1+B_2}{B_2+B_1 e^{(1-v_0)\lambda A_1}} e^{(1-v_0)\lambda A_1})\lambda B_1} - 1)A_2.$$

Consequently, naming $x \equiv v_0$ and setting

$$\Phi(x) := x(A_2 e^{\frac{B_2(e^{(1-x)\lambda A_1}-1)}{B_1 e^{(1-x)\lambda A_1}+B_2}\lambda B_1} + A_1) - (A_1 + A_2), \quad (2.46)$$

it is apparent that $\Phi^{-1}(0)$ provides us with the set of T -periodic coexistence states of (2.1). As $\Phi(x) < 0$ for all $x \leq 0$, its zeroes are always positive. Since

$$\Phi(0) = -(A_1 + A_2) < 0, \quad \Phi(1) = 0,$$

$$\Phi(x) > 0 \quad \text{if} \quad x \geq M := 1 + A_2/A_1,$$

and

$$\Phi'(1) = A_1 + A_2 - \lambda^2 \frac{A_1 A_2 B_1 B_2}{B_1 + B_2},$$

we find that $\Phi'(1) < 0$ if and only if, $\lambda > \lambda_0$ (see (2.42)). Therefore, (2.1) possesses two T -periodic solutions, (λ, x_{\pm}) , with $0 < x_- < 1$ and $1 < x_+ < M$. This ends the proof when (2.40) holds. Note that $x_{\pm} \in (0, M)$.

Assume (2.41). Then, repeating the previous argument it is apparent that the T -periodic coexistence states of (2.1) are the zeroes of the map

$$\Psi(x) := x(B_2 e^{\frac{A_2(1-e^{(x-1)\lambda B_1})}{A_1 e^{(x-1)\lambda B_1 + A_2}} \lambda A_1} + B_1) - (B_1 + B_2). \quad (2.47)$$

As above, since $\Psi(x) < 0$ for all $x \leq 0$, its zeroes are always positive. Thus, as $\Psi(x)$ satisfies

$$\begin{aligned} \Psi(0) &= -(B_1 + B_2) < 0, & \Psi(1) &= 0, \\ \Psi(x) &> 0 \quad \text{if} \quad x \geq N := 1 + B_2/B_1, \end{aligned}$$

and

$$\Psi'(1) = B_1 + B_2 - \lambda^2 \frac{A_1 A_2 B_1 B_2}{A_1 + A_2},$$

it is apparent that $\Psi'(1) < 0$ if $\lambda > \lambda_0$. Therefore, in this case, (2.1) admits, at least, two T -periodic coexistence states, (λ, x^\pm) , with $0 < x^+ < 1$ and $1 < x^- < N$. Note that $x^\pm \in (0, N)$. This concludes the proof that $\lambda > \lambda_0$ is sufficient for the existence of, at least, two T -periodic coexistence states.

It remains to determine the bifurcation directions from $(\lambda, x) = (\lambda_0, 1)$ in both cases. Now, it is appropriate to make explicit the dependence of the functions Φ and Ψ not only on x but also on λ , for as λ will be though as a bifurcation parameter.

Assume (2.40) and let $\Phi(\lambda, x)$ denote the function defined by (2.46). Then, the linearization of this function at $(\lambda, 1)$ is given by

$$\mathfrak{L}(\lambda) := \frac{\partial \Phi}{\partial x}(\lambda, 1) = A_1 + A_2 - \lambda^2 \frac{A_1 A_2 B_1 B_2}{B_1 + B_2}. \quad (2.48)$$

Thus, using the notations of [67], we find that, by the definition of λ_0 ,

$$\mathfrak{L}_0 := \mathfrak{L}(\lambda_0) = \frac{\partial \Phi}{\partial x}(\lambda_0, 1) = 0, \quad \mathfrak{L}_1 := \frac{d\mathfrak{L}}{d\lambda}(\lambda_0).$$

We claim that the next algebraic transversality condition holds

$$\mathfrak{L}_1(N[\mathfrak{L}_0]) \oplus R[\mathfrak{L}_0] = \mathbb{R}. \quad (2.49)$$

Indeed, since $\mathfrak{L}_0 = 0$, it is apparent that $R[\mathfrak{L}_0] = [0]$ and hence, $N[\mathfrak{L}_0] = \mathbb{R} = \text{span}[1]$. Moreover, differentiating with respect to λ (2.48) yields

$$\mathfrak{L}_1 = -\frac{2\lambda_0 A_1 A_2 B_1 B_2}{B_1 + B_2} \neq 0.$$

Therefore, $\mathfrak{L}_1 \notin R[\mathfrak{L}_0]$ and (2.49) holds. Consequently, by Theorem 7.1 of Crandall and Rabinowitz [21], there exist $\varepsilon > 0$ and two analytic functions $\lambda, x : (-\varepsilon, \varepsilon) \rightarrow \mathbb{R}$ such that, for some $\lambda_1 \in \mathbb{R}$ to be determined,

$$\lambda(s) = \lambda_0 + \lambda_1 s + \mathcal{O}(s^2), \quad x(s) = 1 + s + \mathcal{O}(s^2), \quad \text{as } s \rightarrow 0,$$

and $\Phi(\lambda(s), x(s)) = 0$ for all $s \in (-\varepsilon, \varepsilon)$. Moreover, besides $(\lambda, 1)$, these are the unique solutions of (2.1) in a neighborhood of $(\lambda_0, 1)$.

Setting

$$\varphi(s) := \Phi(\lambda(s), x(s)), \quad |s| < \varepsilon,$$

it is apparent that

$$0 = \varphi(s) = \varphi(0) + \varphi'(0)s + \frac{1}{2}\varphi''(0)s^2 + \mathcal{O}(s^3) \quad |s| < \varepsilon,$$

where ' stands for differentiation with respect to s . So,

$$\varphi(0) = \varphi'(0) = \varphi''(0) = 0.$$

By construction,

$$0 = \varphi(0) = \Phi(\lambda_0, 1) = 0, \quad \frac{\partial \Phi}{\partial x}(\lambda_0, 1).$$

Moreover, differentiating (2.46) with respect to λ , it becomes apparent that

$$\frac{\partial \Phi}{\partial \lambda}(\lambda_0, 1) = 0.$$

Thus, since $\lambda'(0) = \lambda_1$,

$$\varphi'(0) = \frac{\partial \Phi}{\partial \lambda}(\lambda_0, 1)\lambda_1 + \frac{\partial \Phi}{\partial x}(\lambda_0, 1) = 0$$

does not provide any information on the sign of λ_1 . So, we must analyze the second order terms of $\Phi(\lambda, x)$ at $(\lambda_0, 1)$. By differentiating Φ , after some straightforward, but tedious, manipulations, we find that

$$\frac{\partial^2 \Phi}{\partial x^2}(\lambda_0, 1) = \lambda_0^2 \frac{A_1 A_2 B_1 B_2}{(B_1 + B_2)^2} [(B_1 + B_2)(\lambda_0 A_1 - 2) + \lambda_0 A_1 B_1 (\lambda_0 B_2 - 2)],$$

$$\frac{\partial^2 \Phi}{\partial x \partial \lambda}(\lambda_0, 1) = -2\lambda_0 \frac{A_1 A_2 B_1 B_2}{B_1 + B_2}, \quad \frac{\partial^2 \Phi}{\partial \lambda^2}(\lambda_0, 1) = 0.$$

Consequently, differentiating and substituting the previous values of the second derivatives, it is apparent that

$$\begin{aligned} 0 = \varphi''(0) &= 2\lambda_1 \frac{\partial^2 \Phi}{\partial x \partial \lambda}(\lambda_0, 1) + \frac{\partial^2 \Phi}{\partial x^2}(\lambda_0, 1) + \frac{\partial^2 \Phi}{\partial \lambda^2}(\lambda_0, 1) \\ &= \lambda_1 \left(-4\lambda_0 \frac{A_1 A_2 B_1 B_2}{B_1 + B_2} \right) + \lambda_0^2 \frac{A_1 A_2 B_1 B_2}{(B_1 + B_2)^2} [(B_1 + B_2)(\lambda_0 A_1 - 2) + \lambda_0 A_1 B_1 (\lambda_0 B_2 - 2)] \end{aligned}$$

and therefore,

$$\lambda_1 = \frac{\lambda_0}{4(B_1 + B_2)} [(B_1 + B_2)(\lambda_0 A_1 - 2) + \lambda_0 A_1 B_1 (\lambda_0 B_2 - 2)]. \quad (2.50)$$

It is clear that (2.50) can reach both positive and negative values depending on the values of the several parameters A_1 , A_2 , B_1 and B_2 . For instance, if

$$2A_1 < A_2, \quad 2B_2 < B_1, \quad \frac{2}{3} < \frac{B_2}{A_1} < \frac{3}{2}, \quad (2.51)$$

then,

$$\lambda_0^2 A_1^2 = \frac{(A_1 + A_2)(B_1 + B_2)}{A_2 B_1 B_2} A_1 = \left(\frac{A_1}{A_2} + 1 \right) \left(1 + \frac{B_2}{B_1} \right) \frac{A_1}{B_2} < \left(\frac{3}{2} \right)^3 < 4.$$

Similarly,

$$\lambda_0^2 B_2^2 = \frac{(A_1 + A_2)(B_1 + B_2)}{A_1 A_2 B_1} B_2 = \left(\frac{A_1}{A_2} + 1 \right) \left(1 + \frac{B_2}{B_1} \right) \frac{B_2}{A_1} < \left(\frac{3}{2} \right)^3 < 4.$$

Since the estimates (2.51) are satisfied, for example, if $B_2 = A_1$, $B_1 = A_2$ and $2B_2 < B_1$, it becomes apparent that (2.51) holds for wide open ranges of values of the several parameters involved in the setting of (2.1).

Now, assume (2.41), instead of (2.40). Then, the T -periodic coexistence states are given by the zeros of the map $\Psi(\lambda, x)$ defined in (2.47). In this case, the linearization of $\Psi(\lambda, x)$ at $(\lambda, 1)$ is given by

$$\mathfrak{M}(\lambda) := \frac{\partial \Psi}{\partial x}(\lambda, 1) = B_1 + B_2 - \lambda^2 \frac{A_1 A_2 B_1 B_2}{A_1 + A_2}.$$

Thus, setting

$$\mathfrak{M}_0 := \mathfrak{M}(\lambda_0) = 0, \quad \mathfrak{M}_1 := \frac{d\mathfrak{M}}{d\lambda}(\lambda_0),$$

and adapting the argument given above, it is apparent that the transversality condition

$$\mathfrak{M}_1(N[\mathfrak{M}_0]) \oplus R[\mathfrak{M}_0] = \mathbb{R}$$

holds true. Moreover, also

$$\frac{\partial \Psi}{\partial x}(\lambda_0, 1) = 0 = \frac{\partial \Psi}{\partial \lambda}(\lambda_0, 1).$$

Hence, to find out the bifurcation direction, we must proceed as in the previous case. A rather straightforward, but tedious, calculation shows that

$$\frac{\partial^2 \Psi}{\partial x^2}(\lambda_0, 1) = \lambda_0^2 \frac{A_1 A_2 B_1 B_2}{(A_1 + A_2)^2} [(A_1 + A_2)(-\lambda_0 B_1 - 2) + \lambda_0 A_1 B_1 (\lambda_0 A_2 - 2)],$$

$$\frac{\partial^2 \Psi}{\partial x \partial \lambda}(\lambda_0, 1) = -2\lambda_0 \frac{A_1 A_2 B_1 B_2}{A_1 + A_2}, \quad \frac{\partial^2 \Psi}{\partial \lambda^2}(\lambda_0, 1) = 0.$$

Therefore,

$$\lambda_1 = \frac{\lambda_0}{4(A_1 + A_2)} [-(B_1 + B_2)(\lambda_0 A_1 + 2) + \lambda_0 A_1 B_1 (\lambda_0 B_2 - 2)],$$

which can reach negative values also in this case. Indeed, if

$$B_2 < A_1 < B_1, \quad A_1 < A_2,$$

then

$$\lambda_0^2 B_2^2 = \frac{(A_1 + A_2)(B_1 + B_2)}{A_1 A_2 B_1} B_2 < 4$$

and consequently $\lambda_1 < 0$. This concludes the proof. \square

Note that Theorem 2.7 generalizes Theorems 2.1 and 2.2. Indeed, if $A_1 = A_2$ and $B_1 = B_2$, then $\varphi(x) = \Phi(x)$ and $\psi(x) = \Psi(x)$. Thus,

$$\lambda_0 = \frac{2}{\sqrt{A_1 B_1}},$$

which provides us with Theorems 2.1 and 2.2. Moreover, by Lemma 2.2, Theorem 2.7 holds also for the cases

$$\text{supp } \alpha_i \subseteq [t_0^i, t_1^i] \text{ and } \text{supp } \beta_j \subseteq [t_2^j, t_3^j], \quad (2.52)$$

and

$$\text{supp } \beta_i \subseteq [t_0^i, t_1^i] \text{ and } \text{supp } \alpha_j \subseteq [t_2^j, t_3^j], \quad (2.53)$$

with $i \in \{1, 2, 3\}$, $j \in \{1, 2\}$ and for some

$$0 \leq t_0^1 < t_1^1 \leq t_2^1 < t_3^1 \leq t_0^2 < t_1^2 \leq t_2^2 < t_3^2 \leq t_0^3 < t_1^3 \leq T.$$

If (2.52) holds, then

$$\lambda_0 = \sqrt{\frac{(B_1 + B_2 + B_3)(A_1 + A_2)}{B_2(B_1 + B_3)A_1 A_2}},$$

while

$$\lambda_0 = \sqrt{\frac{(A_1 + A_2 + A_3)(B_1 + B_2)}{A_2(A_1 + A_3)B_1 B_2}}$$

if (2.53) holds.

3 Chaotic dynamics

In this section we consider again the non-autonomous Volterra predator-prey model

$$\begin{cases} u' = \alpha(t)u(1 - v), \\ v' = \beta(t)v(-1 + u), \end{cases} \quad (3.1)$$

where $\alpha \geq 0$, $\beta \geq 0$ are T -periodic continuous functions for some $T > 0$, with the aim to prove the presence of chaotic-like dynamics.

As in Section 2, attention is focused on the *coexistence states*, namely the component-wise positive solutions of the system (3.1). As already explained in Section 1 (cf. (1.2)), in this kind of systems it is natural to perform the change of variables

$$x = \log u, \quad y = \log v,$$

which moves the equilibrium point $(1, 1)$ to the origin $(0, 0)$ of the phase-plane. In the new variables x and y , the model (3.1) turns into the next equivalent planar Hamiltonian system

$$\begin{cases} x' = -\alpha(t)(e^y - 1), \\ y' = \beta(t)(e^x - 1). \end{cases} \quad (3.2)$$

Thus, in this section, instead of looking for coexistence states of (3.1), we will simply look for solutions of (3.2).

The existence of complex dynamics for prey-predator equations has been studied since the Eighties, mostly from a numerical point of view (see Takeuchi and Adachi [115]). Evidence of chaos has been detected in numerical simulations for three-dimensional (or higher-dimensional) autonomous systems, for instance for the interaction of one predator with two preys or the case of a prey, a predator and a top predator, as well as introducing as a third variable a nutrient.

For the two-dimensional case results have been obtained for discrete models of Holling type, as, e.g., those of Agiza et al. [3], which are in line with the classical works of May [80] and Li and Yorke [60], when proving chaos for discrete single species logistic-type equations. Other examples of chaos for two-dimensional systems have been numerically produced by adding some delay effects in the equations, as in Nakaoka, Saito and Takeuchi [87].

But less results are available in the literature concerning chaotic-like solutions to planar predator-prey systems with periodic coefficients (see, for instance, Baek and Do [6], Broer et al. [13], Kuznetsov, Muratori and Rinaldi [56] and Volterra [117]). Typical features of these models is to add logistic and/or Holling growth effects on the prey population and assume that the intraspecific growth rate takes the form $r(1 + \varepsilon \sin(\omega t))$. The special choice of the periodic coefficient allows to study numerically the bifurcation diagrams to give evidence of complex dynamics for some choices of the parameters.

Up to the best of our knowledge, only very few results provide a complete analytic proof of the presence of chaotic dynamics, without the need of numeric support, for the classical Volterra predator-prey system with periodic coefficients. In Pireddu and Zanolin [95] the Volterra original system with harvesting effects was considered and it was proved that chaos may arise under special forms of a periodic harvesting; these authors also considered a case of intermittency in the predation in [96, pp.221-225]. Also in Ruiz-Herrera [104], a rigorous analysis of chaos for periodically perturbed planar systems, was performed for a case in which the Volterra system switches periodically to new system with logistic effects and no predation.

It is the aim of this section to show a simple mechanism producing chaotic dynamics for system (3.2), just assuming that the coefficient $\alpha(t)$ vanishes on some interval, regardless the length of the vanishing interval, which might have dramatic consequences from the point

of view of the applications. Actually, we will prove the following main result which holds for the more general system (cf. (1.2))

$$\begin{cases} x' = -\lambda\alpha(t)f(y), \\ y' = \lambda\beta(t)g(x), \end{cases} \quad (3.3)$$

where $f, g : \mathbb{R} \rightarrow \mathbb{R}$ are C^1 -continuous functions with $f(0) = g(0) = 0$, $f'(0), g'(0) > 0$ and $f(s)s > 0, g(s)s > 0$ for $s \neq 0$. We also assume that at least one of the two functions is bounded in a neighborhood of $+\infty$ or $-\infty$. To be more specific and just to fix a possible case, we will suppose that f is bounded on $(-\infty, 0]$. In the application to the predator-prey model we have

$$f(s) = g(s) = e^s - 1.$$

The introduction of the parameter $\lambda > 0$ in (3.3) is not relevant from the mathematical point of view. For us it is convenient in order to make a comparison to the result about subharmonic solutions obtained by the authors in [74].

Theorem 3.1. *Assume that there exists $T_0 \in (0, T)$ such that:*

- (c₁) $\alpha \geq 0, \beta \geq 0$ on $[0, T_0]$ and there exists $\hat{t} \in [0, T_0]$ with $\alpha(\hat{t})\beta(\hat{t}) > 0$;
- (c₂) $\alpha \equiv 0$ and $\beta \geq 0$ on $[T_0, T]$.

Then, for every $\ell \geq 2$, there exists $\lambda^ = \lambda_\ell^*$ such that, for each $\lambda > \lambda^*$, there exists a constant K_λ such that, if*

$$\int_{T_0}^T \beta(t) dt > K_\lambda, \quad (3.4)$$

then, the Poincaré map associated with (3.3) induces chaotic dynamics on ℓ -symbols on some compact subset, \mathcal{Q} , of the first quadrant.

The proof of Theorem 3.1 is postponed to a next subsection. From the proof, it will become apparent how to determine the constants λ^* and K_λ . The assumption that f and g are C^1 can be weakened, by assuming, as in [74], that f, g are locally Lipschitz with

$$0 < \liminf_{s \rightarrow 0} \frac{f(s)}{s} \leq \limsup_{s \rightarrow 0} \frac{f(s)}{s} < +\infty, \quad 0 < \liminf_{s \rightarrow 0} \frac{g(s)}{s} \leq \limsup_{s \rightarrow 0} \frac{g(s)}{s} < +\infty. \quad (3.5)$$

Up to the best of our knowledge, this is the most general result available for complex dynamics to the predator-prey equations with periodic coefficients. In fact, the previous theorems of Pireddu and Zanolin [95, 96] and Ruiz-Herrera [104] required very specific structural assumptions on the coefficients, which were assumed to be stepwise, in order to transform Volterra equation to a switched system. Nevertheless, we will also present a less general version of Theorem 3.1 where $\beta = \text{constant} > 0$, α is a piecewise constant function vanishing on $[T_0, T]$, according to (c₂), and $f(s) = g(s) = e^s - 1$. This more elementary and special case is introduced in the following subsection in order to better explain the geometry

and the dynamics associated to our system. Actually, for expository reasons, this section has been split into three parts. In the first subsection, we perform a detailed analysis of the equation with a stepwise coefficient. Then, we show how the the same geometrical ideas can be adapted to prove Theorem 3.1. Finally, in the last subsection, we will recall some of the main features of the Smale's horseshoe, adapted to our situation here, in order to discuss a possible further improvement of our results from a numerical point of view.

3.1 The simplest model of type (3.2) with chaotic dynamics

In this section we consider a special case of Theorem 3.1 that already exhibits all the significant geometrical features of the main result. Precisely, for a given $T_0 \in (0, T)$, we will consider the T -periodic functions $\alpha(t)$ and $\beta(t)$ defined by

$$\beta(t) := \begin{cases} \beta_0 > 0 & \text{if } t \in [0, T_0), \\ \beta_1 > 0 & \text{if } t \in [T_0, T), \end{cases} \quad \text{and} \quad \alpha(t) := \begin{cases} \alpha > 0 & \text{if } t \in [0, T_0), \\ 0 & \text{if } t \in [T_0, T), \end{cases} \quad (3.6)$$

where the positive constants α and β_0, β_1 and the exact values of T_0 and T are going to be made precise later. Also, we will set $T_1 := T - T_0$. Thus, the dynamics of (3.2) on each of the intervals $[0, T_0]$ and $[T_0, T]$ are those of the associated autonomous Volterra predator-prey systems in the intervals $[0, T_0]$ and $[0, T_1]$, respectively.

Although the function $\alpha(t)$, and possibly $\beta(t)$, has a jump at $t = T_0$, for any given $z := (x_0, y_0) \in \mathbb{R}^2$, the Poincaré map associated to the system (3.2) in the interval $[0, T]$ is well-defined as

$$\begin{aligned} \Phi : \mathbb{R}^2 &\rightarrow \mathbb{R}^2 \\ z &\mapsto \Phi(z) := (x(T; z), y(T; z)), \end{aligned}$$

where $(x(t; z), y(t; z))$ stands for the unique solution of (3.2) such that $(u(0; z), y(0; z)) = z$, and it is a diffeomorphism. Under the assumption (3.6), the action of system (3.2) can be regarded as a composition of the actions of the systems

$$\begin{aligned} \text{(I)} \quad & \begin{cases} x' = \alpha(1 - e^y) \\ y' = -\beta_0(1 - e^x) \end{cases} & \text{(II)} \quad & \begin{cases} x' = 0 \\ y' = -\beta_1(1 - e^x) \end{cases} \end{aligned} \quad (3.7)$$

on each of the intervals $[0, T_0]$ and $[T_0, T]$, respectively. In this manner, system (3.2) turns out to be a *switched system* with a T -periodic *switching signal* and with (3.7)-(I) and (3.7)-(II) as *active subsystems*, according to the terminology adopted by Liberzon [61]. In other words, the Poincaré map Φ is the composition of the two Poincaré maps associated to each of these systems,

$$\Phi := \Phi_{T_1} \circ \Phi_{T_0},$$

where Φ_{T_0} and Φ_{T_1} stand for the Poincaré maps associated to the first and second systems of (3.7) on the intervals $[0, T_0]$ and $[0, T_1]$, respectively.

Subsequently, we denote by $\theta(t, z)$ the angular polar coordinate at time $t \geq 0$ of the solution $(x(t; z), y(t; z))$ for system (3.7)-(I). Then, for any given $\varrho > 0$, the rotation number of the solution in the interval $[0, \varrho]$ is defined through

$$\text{rot}([0, \varrho], z) := \frac{\theta(\varrho, z) - \theta(0, z)}{2\pi}.$$

It is an algebraic counter, modulo 2π , of the winding number of the solution around the origin. It can be equivalently expressed using (1.13) on the first subsystem.

Dynamics of (3.2) in the interval $[0, T_0]$

We begin by analyzing the dynamics of (3.2) on $[0, T_0]$ under the action of Φ_{T_0} , i.e., the dynamics of (3.7)-(I). It is folklore that the phase-portrait of the (autonomous) system is a global nonlinear center around the origin, i.e., every solution different from the equilibrium $(0, 0)$ is periodic and determines a closed curve around the origin; the *first integral*, or *energy function*, of the system being

$$\mathcal{E}(x, y) = \alpha(e^y - y) + \beta_0(e^x - x). \quad (3.8)$$

Thus, setting

$$\omega := \mathcal{E}(0, 0) = \alpha + \beta_0 = \min_{\mathbb{R}^2} \mathcal{E},$$

for every $\ell > \omega$, the corresponding level line of the first integral, $\Gamma(\ell) = \mathcal{E}^{-1}(\ell)$, is a closed orbit of a periodic solution. Moreover, by simply having a glance at the system, it is easily realized that the solutions run counterclockwise around the origin.

Subsequently, for every $\ell > \omega$, we will denote by $\tau(\ell)$ the (minimal) period of the orbit $\Gamma(\ell)$. Thanks to a result of Waldvogel [120], the fundamental period map $\tau : (\omega, +\infty) \rightarrow \mathbb{R}$ is increasing and it satisfies

$$\lim_{\ell \downarrow \omega} \tau(\ell) = \frac{2\pi}{\sqrt{\alpha\beta_0}}, \quad \lim_{\ell \uparrow +\infty} \tau(\ell) = +\infty.$$

For the rest of this section, we fix $\ell_1 > \omega$ and choose

$$T_0 := 2\tau(\ell_1). \quad (3.9)$$

If a solution of the system (3.7)-(I) crosses entirely the third quadrant, then, there exists an interval $[t_0, t_1] \subseteq [0, T_0]$, with $x(t_0) < 0$, $y(t_0) = 0$, $x(t_1) = 0$ and $y(t_1) < 0$, such that $x(t) < 0$ and $y(t) < 0$ for all $t \in (t_0, t_1)$. Thus, for every $t \in [t_0, t_1]$, we have that

$$\begin{aligned} |y(t)| &= \left| \int_{t_0}^t \beta_0(e^{x(s)} - 1) ds \right| \leq \int_{t_0}^{t_1} \beta_0 ds \leq \beta_0 T_0 =: M, \\ |x(t)| &= \left| \int_t^{t_1} \alpha(1 - e^{y(s)}) ds \right| \leq \int_{t_0}^{t_1} \alpha ds \leq \alpha T_0 =: N. \end{aligned}$$

Hence, if there exists a $\tilde{t} \in [0, T_0]$ such that

$$x(\tilde{t}) < 0, \quad y(\tilde{t}) < 0, \quad x^2(\tilde{t}) + y^2(\tilde{t}) > M^2 + N^2,$$

then the solution cannot cross entirely the third quadrant in $[0, T_0]$, though, as all the solutions are periodic around the origin, all must cross the third quadrant in a sufficiently large time. Therefore, given (x_2, y_2) such that

$$x_2 < 0, \quad y_2 < 0, \quad x_2^2 + y_2^2 > M^2 + N^2$$

and setting $\ell_2 := \mathcal{E}(x_2, y_2)$ (and, without loss of generality, with $\ell_2 > \ell_1$), it becomes apparent that, if $z = (0, y_0) \in \Gamma(\ell_2)$ with $y_0 > 0$, then

$$\theta(t, z) \in [\pi/2, 3\pi/2] \quad \text{for all } 0 \leq t \leq T_0,$$

because the orbit through (x_2, y_2) , $\Gamma(\ell_2)$, cannot cross the entire third quadrant in the time interval $[0, T_0]$. Consequently, by (3.9), we find that

$$\begin{cases} \text{rot}([0, T_0], z) = 2 & \text{if } z \in \Gamma(\ell_1), \\ \text{rot}([0, t], z) < 1/2 \quad \forall t \in [0, T_0] & \text{if } z = (0, y_0) \in \Gamma(\ell_2), y_0 > 0. \end{cases} \quad (3.10)$$

Subsequently, in order to analyze the Poincaré map Φ_{T_0} , we will focus attention into the annular region, \mathcal{A} , of the phase-plane enclosed by the orbits $\Gamma(\ell_1)$ and $\Gamma(\ell_2)$, where (3.10) holds, which has been represented in Figure 8, i.e.,

$$\mathcal{A} := \{(x, y) \in \mathbb{R}^2 : \ell_1 \leq \mathcal{E}(x, y) \leq \ell_2\} = \bigcup_{\ell_1 \leq \ell \leq \ell_2} \Gamma(\ell).$$

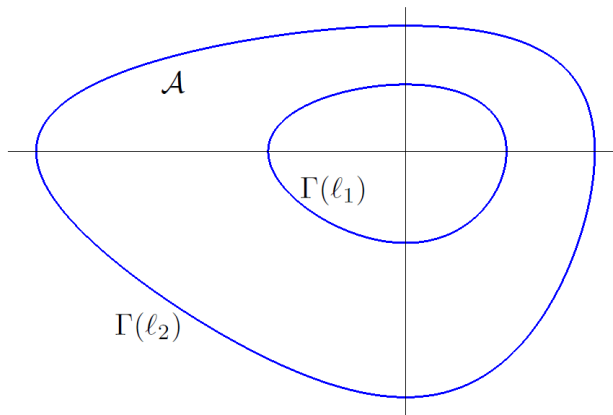


Figure 8: The region \mathcal{A} enclosed by curves $\Gamma(\ell_1)$ and $\Gamma(\ell_2)$ with $\omega < \ell_1 < \ell_2$.

For graphical purposes, the aspect ratios in Figure 8 have been slightly modified.

By the dynamical properties of (3.7)-(I), the Poincaré map Φ_{T_0} transforms the portion of \mathcal{A} on the positive y -axis, i.e., the segment

$$\sigma_0 := \mathcal{A} \cap \{(0, y) \in \mathbb{R}^2 : y > 0\} = \{(0, y) \in \mathbb{R} \times (0, \infty) : \ell_1 \leq \mathcal{E}(0, y) \leq \ell_2\}, \quad (3.11)$$

into the spiraling line plotted in Figure 9(a). The unique $(0, y_1)$ such that $\mathcal{E}(0, y_1) = \ell_1$ remains invariant by Φ_{T_0} because $T_0 = 2\tau(\ell_1)$. Thus, $(0, y_1)$ gives two rounds around the orbit $\Gamma(\ell_1)$ as $t \in [0, T_0]$. Since the period map $\tau(\ell)$ is increasing with respect to ℓ , the points $(0, y) \in \sigma_0$ with $y > y_1$ close to y_1 cannot complete two rounds around the origin, though close to get it. The bigger is taken $y > y_1$, the bigger is the gap $\frac{\pi}{2} + 4\pi - \theta(T_0, (0, y))$, until y approximates y_2 , the unique value of y such that $\mathcal{E}(0, y_2) = \ell_2$, where, according to the choice of $\Gamma(\ell_2)$, we already know that $\theta(T_0, (0, y)) < 3\pi/2$. Similarly, defining $(x_+(\ell_1), 0)$ as the intersection of $\Gamma(\ell_1)$ with the positive x -axis, Figure 9(b) shows a plot of the parallel (vertical) segment

$$\sigma_1 := \mathcal{A} \cap (\{x_+(\ell_1)\} \times [0, \infty)) = \{(x_+(\ell_1), y) \in \mathbb{R} \times [0, \infty) : \ell_1 \leq \mathcal{E}(x_+(\ell_1), y) \leq \ell_2\}. \quad (3.12)$$

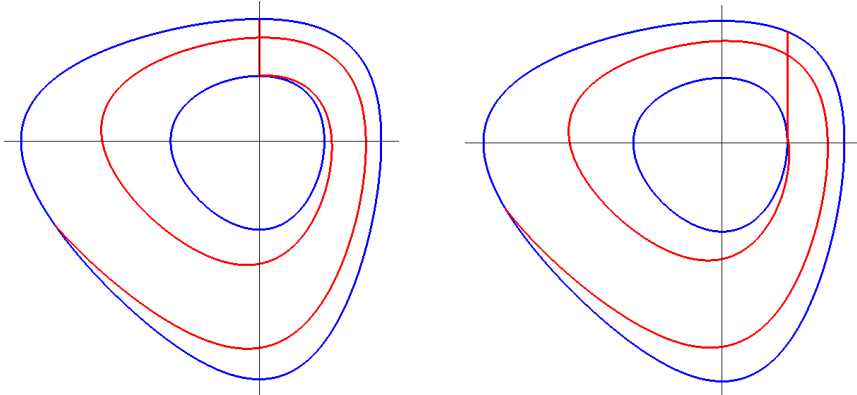


Figure 9: The segments σ_i and the curves $\Phi_{T_0}(\sigma_i)$ for $i = 0$ (left) and $i = 1$ (right).

The curves $\Phi_{T_0}(\sigma_i)$ look like sort of logarithmic spirals with the angular polar coordinate increasing along their trajectories. As illustrated by Figure 9(b), $\Phi_{T_0}(\sigma_1)$ is a curve looking like $\Phi_{T_0}(\sigma_0)$.

Throughout the rest of this section, we consider the topological square, \mathcal{Q} , enclosed by the segments σ_0 and σ_1 in \mathcal{A} , i.e.,

$$\mathcal{Q} := \{(x, y) \in \mathcal{A} : 0 \leq x \leq x_+(\ell_1), y > 0\}.$$

The plot of Figure 10 shows $\Phi_{T_0}(\mathcal{Q})$, which is the spiral-like region enclosed in the annulus \mathcal{A} and bounded by the curves $\Phi_{T_0}(\sigma_0)$ and $\Phi_{T_0}(\sigma_1)$. Subsequently, we will also consider the topological square

$$\mathcal{R} := \{(x, y) \in \mathcal{A} : 0 \leq x \leq x_1, y < 0\},$$

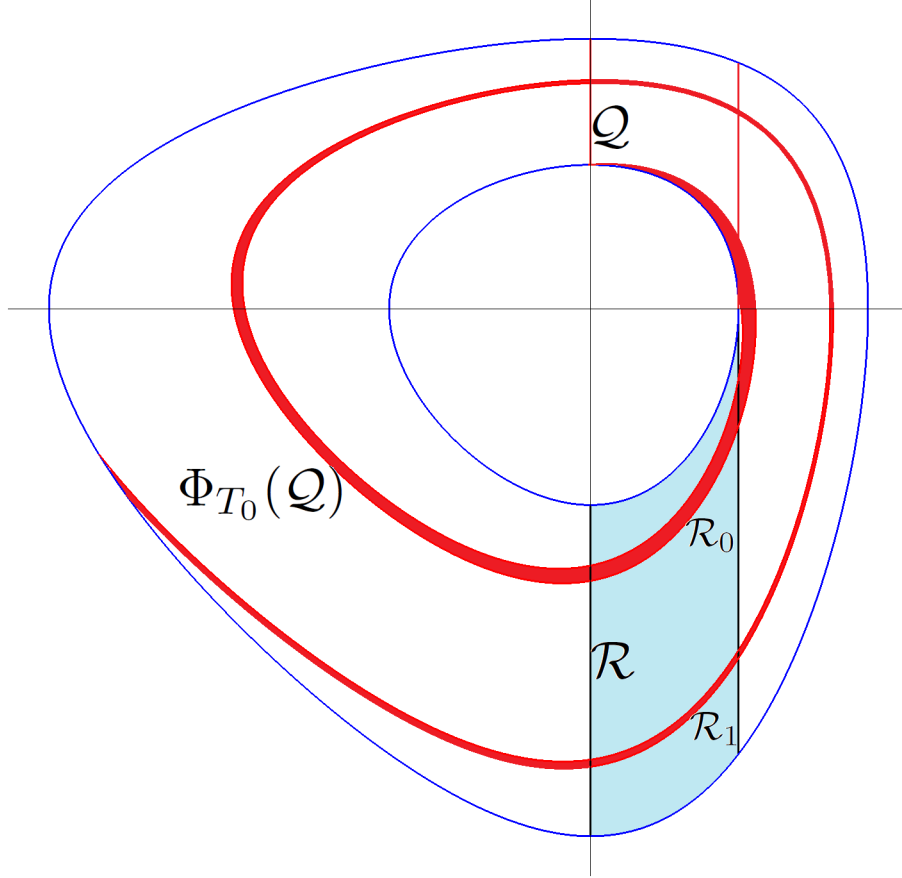


Figure 10: The regions \mathcal{Q} , \mathcal{R} , $\Phi_{T_0}(\mathcal{Q})$, \mathcal{R}_0 and \mathcal{R}_1 .

which has been also represented in Figure 10, where $\Phi_{T_0}(\mathcal{Q}) \cap \mathcal{R}$ consists of two smaller rectangular regions which have been named as \mathcal{R}_0 and \mathcal{R}_1 .

Remark 3.1. For convenience in the exposition, we have chosen ℓ_1 and T_0 to satisfy (3.10). But one can adjust the parameters to have $T_0 \geq j\tau\ell_1$ for some integer $j \geq 2$, of course. In this case, we should modify the choice of ℓ_2 in order to get the second condition of (3.10). Now, we will have $\text{rot}([0, T_0], z) \geq j$ if $z \in \Gamma(\ell_1)$ as first condition. Indeed, the intersection of $\Phi_{T_0}(\mathcal{Q})$ with \mathcal{R} consists of $j \geq 2$ rectangular regions.

Dynamics of (3.2) in the interval $[T_0, T] \equiv [0, T_1]$.

Throughout this paragraph we recall that $T_1 := T - T_0$ and consider the Poincaré map Φ_{T_1} . Choosing $\alpha = 0$ in the interval $[T_0, T]$ our main goal in this section is to show that, for sufficiently large $\beta_1 T_1 = \int_{T_0}^T \beta(t) dt > 0$, the region \mathcal{R} is mapped across \mathcal{Q} by the Poincaré

map Φ_{T_1} . Actually we have that $\Phi_{T_1}(\mathcal{R})$ intersects transversally \mathcal{Q} . Such transversality entails a complex behavior reminiscent of Smale's horseshoe.

Since $\alpha(t) = 0$ and $\beta(t) = \beta_1$ for all $t \in [0, T_1]$ in (3.7)-(II), we have that

$$x'(t) = 0 \text{ and } x(t) = x_0 \text{ for all } t \in [0, T_1]. \quad (3.13)$$

Thus,

$$y(T_1) - y(0) = \int_0^{T_1} \beta_1(e^{x_0} - 1)dt = \beta_1(e^{x_0} - 1)T_1. \quad (3.14)$$

By (3.13) and (3.14), we find that $\Phi_{T_1}(z) = z$ if $z = (0, y_0) \in \mathcal{R}$, and, hence,

$$\Phi_{T_1}(\{(x, y) \in \mathcal{R} : x = 0\}) = \{(x, y) \in \mathcal{R} : x = 0\}.$$

In other words, the left side of \mathcal{R} consists of fixed points of Φ_{T_1} .

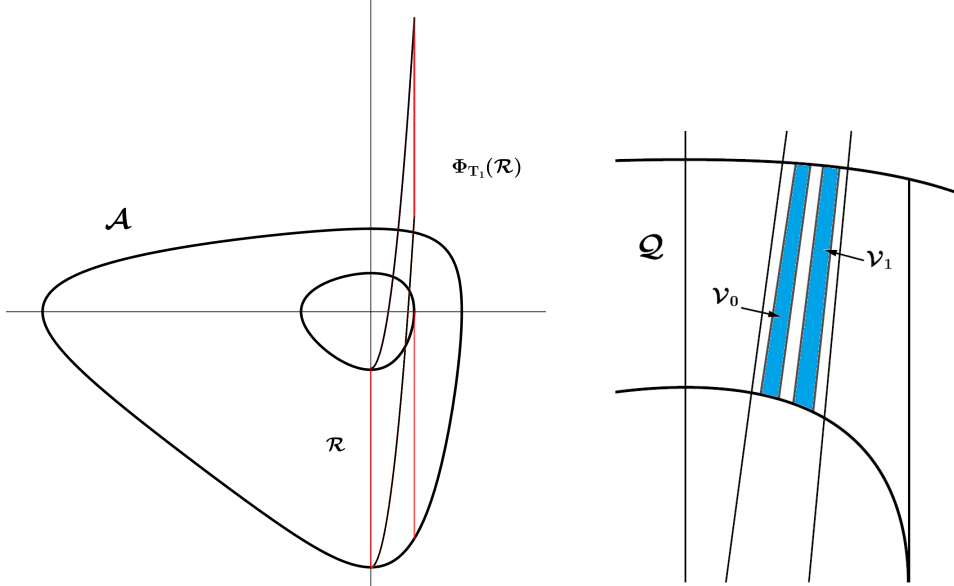


Figure 11: The topological squares \mathcal{R} and $\Phi_{T_1}(\mathcal{R})$ (left panel), as well as the squares $\mathcal{V}_0 := \Phi_{T_1}(\mathcal{R}_0) \cap \mathcal{Q}$ and $\mathcal{V}_1 := \Phi_{T_1}(\mathcal{R}_1) \cap \mathcal{Q}$ (right panel).

On the other hand, by (3.13), for every $z = (x_1, y) \in \mathcal{R}$, with $0 < x_1 \leq x_+(\ell_1)$, we have that $x(t) = x_1$ for all $t \in [0, T_1]$, and hence

$$y(T_1) - y(0) = \int_0^{T_1} \beta_1(e^{x_1} - 1)dt = \beta_1(e^{x_1} - 1)T_1.$$

Consequently, if we denote by $y_2^- < 0$ and $y_2^+ > 0$ the unique values of y such that $\mathcal{E}(0, y_2^\pm) = \ell_2$, then, setting $M^* = M^*(\ell_2) := \max\{|y_2^-|, |y_2^+|\}$ and choosing T_1 satisfying

$$T_1 > \frac{2M^*}{\beta_1(e^{x_+} - 1)}, \quad \text{for } x_+ := x_+(\ell_1), \quad (3.15)$$

it becomes apparent that $y(T_1) - y(0) > 2M^*$. So,

$$\Phi_{T_1}(\{(x, y) \in \mathcal{R} : x = x_+\}) \subsetneq \{x_+\} \times (y_2^+, \infty).$$

Therefore, for $i = 1, 2$, the topological rectangle $\mathcal{V}_i := \Phi_{T_1}(\mathcal{R}_i) \cap \mathcal{Q}$ crosses \mathcal{Q} , transversally, as represented in the second picture of Figure 11. As (3.15) holds for sufficiently large $\beta_1 > 0$, regardless the size of T_1 , as a rather direct consequence of the abstract theory of Papini and Zanolin [92, 93], it becomes apparent that, for every $T_0 \in (0, T)$, the problem (3.1), with the special choice (3.6), exhibits complex dynamics for sufficiently large $\beta_1 > 0$. Actually, the geometry of the problem is very similar to the one considered by Pascoletti, Pireddu and Zanolin [94, Figs. 6, 7, 8] and Labouriau and Sovrano [57, Def. 3.3], consisting of a twist map acting in an annular region, composed with a shift map on a strip. The type of chaotic dynamics which occurs is that stated in Definition 1.1 with the semi-conjugation to the Bernoulli shift on two symbols. Actually, we can produce a semi-conjugation with respect to a larger set of ℓ symbols by suitably adapting the parameters $(\alpha, \beta_0, \beta_1)$ as well as T_0 and T_1 , as already sketched in Remark 3.1. This concludes the proof of Theorem 3.1 for stepwise constant coefficients.

We omit the technical details regarding the application of the results from Papini and Zanolin [92, 93] for the special choice (3.6), since we will present this approach in a more thoroughly manner along the proof of Theorem 3.1. On the other hand, the case of stepwise constant coefficients in (3.6) and (3.7)-(I)&(II) suggests that, at least from a numerical point of view, we are in a situation where a stronger result about chaotic dynamics can be obtained, namely the *conjugation* to the Bernoulli automorphism, due to the presence of a Smale horseshoe. Indeed, the geometry that we have described above suggests a rather elementary mechanism to generate complex dynamics, by adopting the original methodology of Smale [108], as illustrated in the Conley–Moser approach in [85, Ch. III]. In the next subsection, we will prove Theorem 3.1 in its more general form, using the theory of topological horseshoes. Then, we will end this paper by discussing some possible sharper results in the frame of the original horseshoe geometry, by assuming (3.1) with the special choice of coefficients in (3.6).

3.2 Proof of Theorem 3.1

As already discussed recalled in Section 1, in order to prove the presence of chaotic dynamics according to Definition 1.1 there are various different approaches of topological nature, though these results provide a weaker form of chaos with respect to classical Smale’s horseshoe, because they guarantee the semi-conjugation to the Bernoulli shift automorphism, instead of the conjugation. However, the approaches based on the the so-called theory of topological horseshoes, guarantee a broader range of applications. Here we briefly recall some basic facts from the “stretching along the path method”, by specializing our presentation to planar homeomorphisms.

Let $\Phi : \mathbb{R}^2 \rightarrow \mathbb{R}^2$ be a planar homeomorphism and let \mathcal{M} be a compact set of the plane which is homeomorphic to the unit square. We select two disjoint compact arcs on the

boundary of \mathcal{M} that we conventionally denote $\mathcal{M}_{\text{left}}^-$ and $\mathcal{M}_{\text{right}}^-$ and call the left and right sides of \mathcal{M} . Then, setting $\mathcal{M}^- := \mathcal{M}_{\text{left}}^- \cup \mathcal{M}_{\text{right}}^-$, the pair $\widehat{\mathcal{M}} := (\mathcal{M}, \mathcal{M}^-)$ is called an oriented rectangle. Given two oriented rectangles $\widehat{\mathcal{M}}$ and $\widehat{\mathcal{N}}$ and a compact set $\mathcal{H} \subset \mathcal{M}$, we write

$$(\mathcal{H}, \Phi) : \widehat{\mathcal{M}} \Rightarrow \widehat{\mathcal{N}}$$

if the following property holds:

for every path $\gamma_0 : [0, 1] \rightarrow \mathcal{M}$ with $\gamma(0)$ and $\gamma(1)$ belonging to different components of \mathcal{M}^- , there exists a sub-path $\gamma_1 := \gamma_0|_{[s_0, s_1]}$ such that $\gamma_1(t) \in \mathcal{H}$ for all $t \in [s_0, s_1]$ and $\Phi(\gamma_1(t)) \in \mathcal{N}$ with $\gamma(s_0)$ and $\gamma(s_1)$ belonging to different components of \mathcal{N}^- .

If $\mathcal{H} = \mathcal{M}$, we just write $\Phi : \widehat{\mathcal{M}} \Rightarrow \widehat{\mathcal{N}}$. Moreover, for any integer $\ell \geq 2$, we will use the notation

$$\Phi : \widehat{\mathcal{M}} \Rightarrow^\ell \widehat{\mathcal{N}},$$

if there are ℓ pairwise disjoint (nonempty) compact sets $\mathcal{H}_0, \dots, \mathcal{H}_{\ell-1}$ in \mathcal{M} , such that

$$(\mathcal{H}_i, \Phi) : \widehat{\mathcal{M}} \Rightarrow \widehat{\mathcal{N}} \quad \text{for all } i = 0, \dots, \ell - 1.$$

In the proof of Theorem 3.1 the following result, adapted from Pascoletti, Pireddu and Zanolin [94]) will be used.

Lemma 3.1. *Assume that $\Phi = \Phi_2 \circ \Phi_1$ and let \widehat{Q} and \widehat{R} be two oriented rectangles such that*

- i) $\Phi_1 : \widehat{Q} \Rightarrow^\ell \widehat{R}$ for some $\ell \geq 2$,
- ii) $\Phi_2 : \widehat{R} \Rightarrow \widehat{Q}$.

Then, Φ induces chaotic dynamics on ℓ symbols in the set \mathcal{Q} .

We are in position now to prove Theorem 3.1, with Φ_1 and Φ_2 the Poincaré maps associated to the system (3.3) in the intervals $[0, T_0]$ and $[T_0, T]$, respectively. Clearly, $\Phi = \Phi_2 \circ \Phi_1$ is the Poincaré map on the interval $[0, T]$ and its n -periodic points corresponds to the nT -periodic solutions to the differential system.

For the sake of simplicity in the exposition, we restrict ourselves to the case of $\ell = 2$ symbols, conventionally $\{0, 1\}$. The case of an arbitrary $\ell \geq 2$ can be easily proved via a simple modification of our argument.

As a first step, we focus our attention in the time-interval $[0, T_0]$ where the supports of α and β intersect nontrivially on a set containing a non-degenerate interval, J , where, without loss of generality, we can suppose that

$$\min_{t \in J} \{\alpha(t), \beta(t)\} \geq \varsigma_0 > 0.$$

In $[0, T_0]$ we are precisely in the same situation as the authors in [74, §2]. Accordingly, we just recall some main facts from [74] which are needed for our proof and send the

reader for the technical details to the original article, if necessary. For a fixed $\eta > 0$ with $\min\{f'(0), g'(0)\} > \eta$, we can find a (small) radius $r_0 > 0$ such that

$$\theta(T_0, z_0) - \theta(0, z_0) \geq \lambda \eta \zeta_0 |J| \quad \text{for all } z_0 \text{ with } \|z_0\| = r_0$$

(see [74, Formula (13)]). Here, as in Section 3.1, we are denoting by $\theta(t, z_0)$ the angular coordinate associated with the solution of (3.3) with $z_0 \neq 0$ as initial point. Then, for

$$\lambda > \lambda^* := \frac{7\pi}{2\eta\zeta_0|J|}, \quad (3.16)$$

we have that

$$\theta(T_0, z_0) > 4\pi \quad \text{if } 0 \leq \theta(0, z_0) \leq \pi/2 \text{ with } \|z_0\| = r_0. \quad (3.17)$$

On the other hand, following the same argument as in the previous steps (3.9)-(3.10) (see also [74, p. 2401]), we can find a (large) radius $R_0 > r_0$ such that the solutions departing from the first quadrant outside the disc of radius R_0 cannot cross the third quadrant, that is

$$\theta(T_0, z_0) < \frac{3\pi}{2} \quad \text{if } 0 \leq \theta(0, z_0) \leq \pi/2 \text{ with } \|z_0\| = R_0. \quad (3.18)$$

Suppose now that $\lambda > \lambda^*$ is fixed. By the continuous dependence of the solutions from initial data (see also [74, Pr. 1]) there are two radii r_λ and R_λ with

$$0 < r_\lambda \leq r_0 < R_0 \leq R_\lambda$$

such that any solution $\zeta(t; z_0)$ of (3.3) with z_0 in the first quadrant and $r_0 \leq \|z_0\| \leq R_0$ satisfies $r_\lambda \leq \|\zeta(t; z_0)\| \leq R_\lambda$ for all $t \in [0, T_0]$.

Subsequently, we introduce the sets

$$\mathcal{Q} := \{z = (x, y) \in \mathbb{R}^2 : 0 \leq x \leq r_0, y \geq 0, r_0 \leq \|z\| \leq R_0\},$$

and

$$\mathcal{Q}_{\text{left}}^- := \mathcal{Q} \cap C_{r_0}, \quad \mathcal{Q}_{\text{right}}^- := \mathcal{Q} \cap C_{R_0},$$

where C_ρ denotes the circumference of center at the origin and radius $\rho > 0$, and

$$\mathcal{R} := \{z = (x, y) \in \mathbb{R}^2 : 0 \leq x \leq r_\lambda, y \leq 0, r_\lambda \leq \|z\| \leq R_\lambda\},$$

$$\mathcal{R}_{\text{left}}^- := \mathcal{R} \cap \{(x, y) : x = 0\}, \quad \mathcal{R}_{\text{right}}^- := \mathcal{R} \cap \{(x, y) : x = r_\lambda\}.$$

So that the oriented rectangles \widehat{Q} and \widehat{R} are defined, too. It is obvious that both \mathcal{Q} and \mathcal{R} are homeomorphic to the unit square. For instance, the map

$$(u, v) \mapsto (ur_0, (\varrho(v)^2 - u^2 r_0^2)^{1/2}),$$

with $\varrho(v) = r_0 + v(R_0 - r_0)$, provides a homeomorphism from the unit square $[0, 1]^2$ onto \mathcal{Q} , mapping $v = 0$ to $\mathcal{Q}_{\text{left}}^-$ and $v = 1$ to $\mathcal{Q}_{\text{right}}^-$ and, similarly, the map

$$(u, v) \mapsto (ur_\lambda, -(\varrho_\lambda(v)^2 - u^2 r_\lambda^2)^{1/2}),$$

with $\varrho_\lambda(v) = r_\lambda + v(R_\lambda - r_\lambda)$, provides a homeomorphism from the unit square onto \mathcal{R} , mapping $u = 0$ to $\mathcal{R}_{\text{left}}^-$ and $u = 1$ to $\mathcal{R}_{\text{right}}^-$. Thus, the definition of oriented rectangles is well posed.

We also introduce the pairwise disjoint compact (nonempty) subsets of \mathcal{Q}

$$\mathcal{H}_{1-j} := \{z \in \mathcal{Q} : \Phi_1(z) \in \mathcal{R}, 3\pi/2 + 2j\pi \leq \theta(T_0, z) \leq 2\pi + 2j\pi\} \quad \text{for } j = 0, 1.$$

By definition,

$$\mathcal{H}_0 \sqcup \mathcal{H}_1 \subset \mathcal{Q} \cap \Phi_1^{-1}(\mathcal{R}).$$

Figure 12 shows a possible hierarchy of the sets \mathcal{H}_0 and \mathcal{H}_1 within \mathcal{Q} .

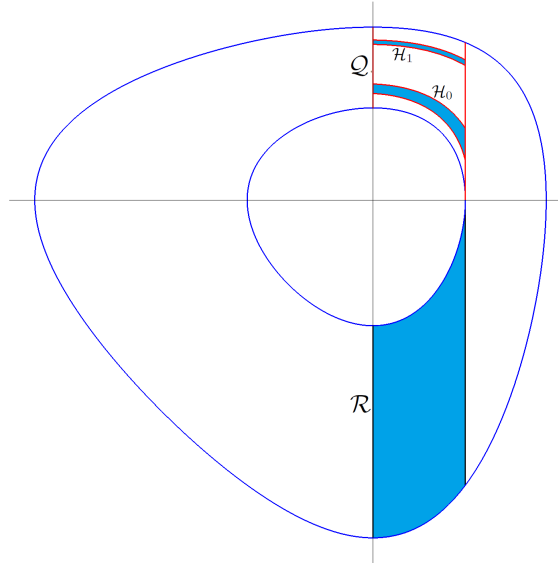


Figure 12: The sets \mathcal{H}_0 and \mathcal{H}_1 , as well as \mathcal{Q} and \mathcal{R} , for the stepwise constant coefficients studied in Section 3.1. Although in this special situation $\mathcal{H}_0 \sqcup \mathcal{H}_1 = \mathcal{Q} \cap \Phi_1^{-1}(\mathcal{R})$, by the choice of T_0 , in general, $\mathcal{Q} \cap \Phi_1^{-1}(\mathcal{R})$ might contain more components.

Let $\gamma : [0, 1] \rightarrow \mathcal{Q}$ be a continuous map such that $\gamma(0) \in \mathcal{Q}_{\text{left}}^-$ and $\gamma(1) \in \mathcal{Q}_{\text{right}}^-$ and let us consider the evolution of $\gamma(s)$ through the first Poincaré map Φ_1 . The angular coordinate $\theta(T_0, \gamma(s))$ as a function of the parameter $s \in [0, 1]$ is a continuous map which, according to (3.17) and (3.18) satisfies

$$\theta(T_0, \gamma(0)) > 4\pi, \quad \theta(T_0, \gamma(1)) \leq 3\pi/2.$$

Hence, the path $s \mapsto \theta(T_0, \gamma(s))$ crosses at least twice the portion of the fourth quadrant between C_{r_λ} and C_{R_λ} and therefore it also crosses (at least twice) the region \mathcal{R} from $x = 0$ to $x = r\lambda$.

By an elementary continuity argument, there are two subintervals, $[s_0, s_1]$ and $[s_3, s_4]$, with $0 < s_0 < s_1 < s_3 < s_4 < 1$, such that

$$\theta(T_0, \gamma(s_0)) = 4\pi, \quad \theta(T_0, \gamma(s_1)) = \frac{3\pi}{2} + 2\pi, \quad \frac{3\pi}{2} + 2\pi \leq \theta(T_0, \gamma(s)) \leq 4\pi \quad \forall s \in [s_0, s_1],$$

and

$$\theta(T_0, \gamma(s_3)) = 2\pi, \quad \theta(T_0, \gamma(s_4)) = \frac{3\pi}{2}, \quad \frac{3\pi}{2} \leq \theta(T_0, \gamma(s)) \leq 2\pi \quad \forall s \in [s_3, s_4].$$

Thus, the path $[s_0, s_1] \ni s \mapsto \theta(T_0, \gamma(s))$ crosses the fourth quadrant and hence there is a subinterval $[s'_0, s'_1] \subset [s_0, s_1]$ such that $\Phi_1(\gamma(s)) \in \mathcal{R}$ for all $s \in [s'_0, s'_1]$ with $\Phi_1(\gamma(s'_0)) \in \mathcal{R}_{\text{right}}^-$ and $\Phi_1(\gamma(s'_1)) \in \mathcal{R}_{\text{left}}^-$. By the definition of \mathcal{H}_0 , we have that $\gamma(s) \in \mathcal{H}_0$ for all $s \in [s'_0, s'_1]$. Therefore, we have proved that $(\mathcal{H}_0, \Phi_1) : \widehat{Q} \rightleftharpoons \widehat{R}$. In the same manner, we can find a subinterval $[s'_3, s'_4] \subset [s_3, s_4]$ such that $\Phi_1(\gamma(s)) \in \mathcal{R}$ for all $s \in [s'_3, s'_4]$, with $\Phi_1(\gamma(s'_3)) \in \mathcal{R}_{\text{right}}^-$ and $\Phi_1(\gamma(s'_4)) \in \mathcal{R}_{\text{left}}^-$. Therefore, by the definition of \mathcal{H}_1 we have that $\gamma(s) \in \mathcal{H}_1$ for all $s \in [s'_3, s'_4]$, thus proving that $(\mathcal{H}_1, \Phi_1) : \widehat{Q} \rightleftharpoons \widehat{R}$. This ends the proof of Lemma 3.1(i) for $\ell = 2$.

To have the result for an arbitrary $\ell \geq 2$, we have just to modify the choice of λ^* in (3.16) to $\lambda > \lambda^* := (4\ell - 1)\pi/(2\eta\varsigma_0|J|)$ and introduce corresponding subsets $\mathcal{H}_0, \dots, \mathcal{H}_{\ell-1}$ of $\mathcal{Q} \cap \Phi_1^{-1}(\mathcal{R})$.

Now, we consider the map Φ_2 by studying the equation (3.3) in the interval $[T_0, T]$, where $\alpha \equiv 0$ and hence

$$\Phi_2(x_0, y_0) = (x_0, y_0 + \lambda g(x_0) \int_{T_0}^T \beta(t) dt).$$

Thus, the dynamics is the same as that of (3.2) in the interval $[T_0, T]$ considered in Section 3.1, modulo a minor change in the parameters involved. It is clear that the points on $\mathcal{R}_{\text{left}}^-$ remain stationary, while those of $\mathcal{R}_{\text{right}}^-$ move upward at the new position

$$y_0 + \lambda g(x_\lambda) \int_{T_0}^T \beta(t) dt \geq -R_\lambda + \lambda g(x_\lambda) \int_{T_0}^T \beta(t) dt.$$

Therefore, if

$$\int_{T_0}^T \beta(t) dt > K_\lambda := \frac{2R_\lambda}{\lambda g(x_\lambda)}, \quad (3.19)$$

then Lemma 3.1(ii) holds. Indeed, any path in \mathcal{R} linking the two sides of \mathcal{R}^- is stretched to a path crossing entirely the set \mathcal{Q} (from $\mathcal{Q}_{\text{left}}^-$ to $\mathcal{Q}_{\text{right}}^-$) and remaining inside the strip $[0, r_\lambda] \times \mathbb{R}$. This concludes the proof of Theorem 3.1. \square

Remark 3.2. The chaotic dynamics associated with the Poincaré map $\Phi = \Phi_2 \circ \Phi_1$ comes from the composition of a twist rotation (due to Φ_1) with a shearing parallel to the y -axis (due to Φ_2). Clearly, if we consider the Poincaré map of initial time T_0 , we will obtain

$\Phi_1 \circ \Phi_2$ and, by a similar argument, through a symmetric counterpart of Lemma 3.1 where the order of the two maps is commuted, we may prove the existence of a horseshoe type structure inside the set \mathcal{R} . Moreover, using the fact that the shear map moves downward the points with $x < 0$ (in fact, $g(x) < 0$ for $x < 0$), we can also start from a set

$$\mathcal{Q} := \{z = (x, y) \in \mathbb{R}^2 : 0 \leq -r_0 \leq x \leq 0, y \leq 0, r_0 \leq \|z\| \leq R_0\}$$

and a target set

$$\mathcal{R} := \{z = (x, y) \in \mathbb{R}^2 : r_\lambda \leq x \leq 0, y \geq 0, r_\lambda \leq \|z\| \leq R_\lambda\},$$

again reversing the roles of \mathcal{Q} and \mathcal{R} by commuting Φ_1 with Φ_2 .

Furthermore, we can obtain a variant of Theorem 3.1 by keeping condition (c_1) and modifying condition (c_2) to

$$(c'_2) \quad \alpha \geq 0 \text{ and } \beta \equiv 0 \text{ on } [T_0, T].$$

In this situation, the assumption (3.4) should be replaced by a similar hypothesis involving $\int_{T_0}^T \alpha$. Under conditions $(c_1) - (c'_2)$, the Poincaré maps produce a dynamics where a twist rotation is composed with a shearing parallel to the x -axis.

Remark 3.3. Hénon proposed in [50], as a model problem, the mapping given by the quadratic equations

$$x_1 = x \cos \alpha - (y - x^2) \sin \alpha, \quad y_1 = x \sin \alpha + (y - x^2) \cos \alpha,$$

as a simple example of an area-preserving mapping which exhibits chaotic dynamics. The mapping in Hénon's model splits into a product of a shearing parallel to the y -axis and a rotation. It is interesting that the typical numerical features observed in the experiments in [50] appear also in Volterra's equations for the setting of Theorem 3.1, as shown in Figure 13.

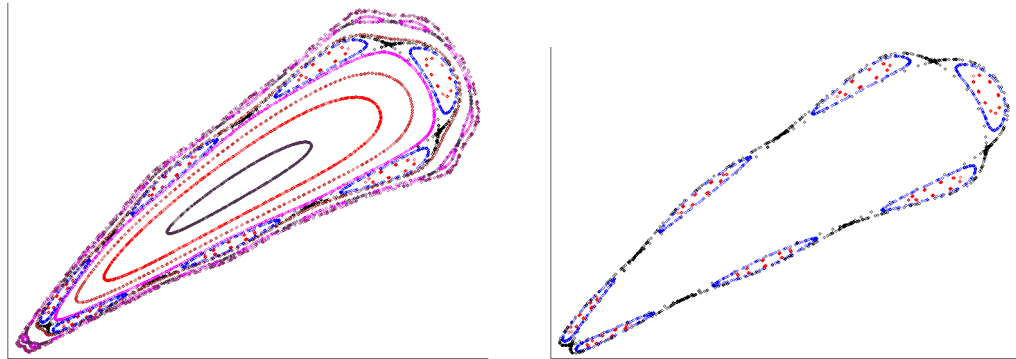


Figure 13: Some numerical experiments for a periodic Volterra system.

The left picture of Figure 13 shows the first 800 iterations of the Poincaré map for a Volterra system

$$\begin{cases} u' = \lambda\alpha(t)u(1-v), \\ v' = -\lambda\beta(t)v(1-u), \end{cases}$$

under the general assumptions of Theorem 3.1, starting from different initial points. The numerical experiments reveal the presence of stability regions (invariant curves around the constant coexistence state $(1, 1)$, according to Liu [62]), as well as some more complicated discrete orbits of “chaotic type”. The right figure highlights some special orbits, in particular, seven-fold island chains (according to Arrowsmith and Place [4, p.262]) separated away by heteroclinic connections and including higher order subharmonics. See also Hénon [50, Figs. 4, 5].

Chaotic dynamics in the degenerate case for system (3.3)

To conclude our analysis, we show now how to adapt the proof of Theorem 3.1 to deal with degenerate weights in system (3.3). This will be achieved by applying the estimates previously obtained by the authors in [75], where some results about the existence of periodic solutions for (3.3) were found when the functions α and β have a common support of zero measure. This case provides also a connection with the theorems in Section 2.

To fix ideas, we suppose that in the interval $[0, T_0]$ there are ℓ positive humps of α separated away by $k = \ell$ positive humps of β , as in (2.22), with the corresponding support intervals intersecting on sets of zero measure. The symmetric case when, instead of (2.22), the condition (2.33) holds, can be treated similarly by interchanging the roles of α and β and modifying the choice of the initial set \mathcal{Q} and the target set \mathcal{R} , as it will be explained in Remark 3.4 below.

Then the following result holds, where, as before, we suppose that $f, g : \mathbb{R} \rightarrow \mathbb{R}$ are C^1 -functions such that $f(0) = g(0) = 0$, $f'(0) > 0$, $g'(0) > 0$, and $f(s)s > 0$, $g(s)s > 0$ for $s \neq 0$. Moreover, at least one of the two functions, e.g., f , is bounded on $(-\infty, 0]$.

Theorem 3.2. *Assume that there exists $T_0 \in (0, T)$ such that:*

- (c₁) $\ell = k \geq 4$, with ℓ, k even integers;
- (c₂) $\alpha \equiv 0$ and $\beta \geq 0$ on $[T_0, T]$.

Then, there exists $\lambda^ = \lambda_\ell^*$ such that, for every $\lambda > \lambda^*$, there exists a constant K_λ for which, whenever*

$$\int_{T_0}^T \beta(t) dt > K_\lambda, \quad (3.20)$$

the Poincaré map associated with (3.3) induces chaotic dynamics on $\ell/2$ symbols on some compact set \mathcal{Q} contained in the first quadrant.

Proof. For simplicity in the exposition in the proof, we will focus attention in the case $\ell = k = 4$, where, starting on the region \mathcal{Q} we obtain two crossings of the region \mathcal{R} and, as a consequence, a complex dynamics on two symbols.

We will follow the same argument as in the proof of Theorem 3.1, just emphasizing the necessary modifications. As a first step, we will focus our attention in the time-interval $[0, T_0]$.

As the supports of α and β do not overlap, the associated dynamics is a composition of shear maps of the following form. If $\alpha \geq 0$, $\beta \equiv 0$ and $y > 0$ (resp. $y < 0$), the points are moved parallel to the x -axis from right to left (resp. from left to right). Similarly, when $\alpha \equiv 0$, $\beta \geq 0$ and $x < 0$ (resp. $x > 0$), then the points are moved parallel to the y -axis in a decreasing (resp. increasing) sense. Once passed two positive humps of α and an intermediate positive hump of β , the points in the first quadrant with $y_0 \geq \delta_0$ end in the fourth quadrant for sufficiently large $\lambda > 0$. Thus, after another interval where $\beta \geq 0$, we come back to the first quadrant and can repeat the process, as described in detail by the authors in [75]. Since the points on the x -axis (resp. the y -axis) do not move when $\beta \equiv 0$ (resp. when $\alpha \equiv 0$), in the proof of this theorem it is convenient to slightly modify the choice of \mathcal{Q} and \mathcal{R} as follows

$$\mathcal{Q} := \{z = (x, y) \in \mathbb{R}^2 : 0 \leq x \leq r_1, y \geq 0, r_0 \leq \|z\| \leq R_0\},$$

for $0 < r_1 < r_0$, and

$$\mathcal{Q}_{\text{left}}^- := \mathcal{Q} \cap C_{r_0}, \quad \mathcal{Q}_{\text{right}}^- := \mathcal{Q} \cap C_{R_0}.$$

In this manner, there is $\hat{y}_0 := (r_0^2 - r_1^2)^{1/2} > 0$ such that $y \geq \hat{y}_0$ for all $(x, y) \in \mathcal{Q}$. According to Lemmas 1, 2 and Theorem 3 of [75], for that choice, there exists λ^* such that the condition (3.17) is reestablished for every (fixed) $\lambda > \lambda^*$, i.e.,

$$\theta(T_0, z_0) > 4\pi \quad \text{if } z_0 \in \mathcal{Q} \cup C_{r_0}. \quad (3.21)$$

On the other hand, exactly as explained above, for sufficiently large $R_0 > r_0$, the solutions departing from the first quadrant outside the disc of radius R_0 cannot cross the third quadrant, that is

$$\theta(T_0, z_0) < \frac{3\pi}{2} \quad \text{if } z_0 \in \mathcal{Q} \cup C_{R_0}. \quad (3.22)$$

By continuous dependence, once fixed a $\lambda > \lambda^*$, one can find two radii r_λ and R_λ , with

$$0 < r_\lambda \leq r_1 < R_0 \leq R_\lambda,$$

such that any solution $\zeta(t; z_0)$ of (3.3) with $z_0 \in \mathcal{Q}$ lies in the set

$$\mathcal{R} := \{z = (x, y) \in \mathbb{R}^2 : 0 \leq x \leq r_\lambda, y \leq 0, r_\lambda \leq \|z\| \leq R_\lambda\},$$

for all $t \in [0, T_0]$.

Thus, much like in the proof of Theorem 3.1, we can also define

$$\mathcal{R}_{\text{left}}^- := \mathcal{R} \cap \{(x, y) : x = 0\}, \quad \mathcal{R}_{\text{right}}^- := \mathcal{R} \cap \{(x, y) : x = r_\lambda\}.$$

From now on, we have just to repeat the proof of Theorem 3.1 without any significant change in order to show that $\Phi_1 : \widehat{\mathcal{Q}} \rightleftarrows^2 \widehat{\mathcal{R}}$. The verification that $\Phi_2 : \widehat{\mathcal{R}} \rightleftarrows \widehat{\mathcal{Q}}$ proceeds exactly as before. Therefore, according to Lemma 3.1, we get the chaotic dynamics for $\Phi = \Phi_2 \circ \Phi_1$ on two symbols.

Note that, in order to produce a semi-conjugation on m -symbols, we need to make at least m -turns around origin, starting at \mathcal{Q} , in the time-interval $[0, T_0]$. This can be achieved, for sufficiently large λ , if both α and β are assumed to have, at least, $2m$ positive humps. The proof is complete. \square

Remark 3.4. If, instead of (2.22), the condition (2.23) holds, then we can assume (c'_2) , instead of (c_2) , and take \mathcal{Q} and \mathcal{R} to be *adjacent to the x-axis and opposite with respect to the y-axis*.

Chaotic dynamics when $\alpha(t)\beta(t) > 0$ for all $t \in [0, T]$.

So far, in this section we have studied the system (3.3) by assuming that either $\alpha \equiv 0$ and $\beta \geq 0$, or $\beta \equiv 0$ and $\alpha \geq 0$, on some time-interval. In both these cases, the dynamics is spanned by the superposition of a twist rotation with a shear map. In this section, we would like to stress the fact that a rich dynamics can be also produced, through a different mechanism, when α and β are throughout positive and appropriately separated away from each other, in a sense to be specified below. To analyze the simplest geometry, we restrict ourselves to consider the system (3.2) with stepwise constant function coefficients, $\alpha(t)$ and $\beta(t)$, as in Section 3.1. More precisely, we assume that $T = T_0 + T_1$ and

$$\beta(t) := \begin{cases} \beta_0 > 0 & \text{if } t \in [0, T_0), \\ \beta_1 > 0 & \text{if } t \in [T_0, T), \end{cases} \quad \alpha(t) := \begin{cases} \alpha_0 > 0 & \text{if } t \in [0, T_0), \\ \alpha_1 > 0 & \text{if } t \in [T_0, T), \end{cases} \quad (3.23)$$

where the positive constants $\alpha_0, \alpha_1, \beta_0, \beta_1$ and the exact values of T_0 and T_1 will be made precise later. In this case, the dynamical behaviors of (3.2) on each of the intervals $[0, T_0]$ and $[T_0, T] \equiv [0, T_1]$ are those of the associated autonomous Volterra-type systems

$$(I) \quad \begin{cases} x' = \alpha_0(1 - e^y) \\ y' = -\beta_0(1 - e^x) \end{cases} \quad (II) \quad \begin{cases} x' = \alpha_1(1 - e^y) \\ y' = -\beta_1(1 - e^x) \end{cases} \quad (3.24)$$

respectively. Note that the systems (3.24)-(I) and (3.24)-(II) have the same equilibrium point (the origin), and both describe a global center. However, for different choices of the pairs (α_0, β_0) and (α_1, β_1) the shape of the level lines of the Hamiltonian may change. Geometrically, this situation is reminiscent to that already studied by Takeuchi et al. in [116], where a predator-prey model with randomly varying coefficients was considered.

Now, making a choice so that

$$\frac{\beta_1}{\alpha_1} > \frac{\beta_0}{\alpha_0}, \quad (3.25)$$

or the converse inequality, it is possible to find level lines of the two systems crossing to each other.

From this, we can construct two annular domains \mathcal{A}_0 and \mathcal{A}_1 , filled by periodic orbits of (3.24)-(I) and (3.24)-(II), respectively, in such a manner that the annuli intersect into four rectangular regions, as illustrated in Figure 14, where the annulus \mathcal{A}_0 is obtained for $\alpha_0 = \beta_0 = 1$ and the level lines passing through the initial points $(0, 0.8)$ and $(0, 1.5)$, whereas \mathcal{A}_2 is obtained for $\alpha_1 = 0.1, \beta_1 = 5$ and the level lines passing through the initial points $(0, 1.7)$ and $(0, 2.5)$. From a numerical point of view, the larger is the gap in condition (3.25), the wider are the linked annuli which can be constructed.

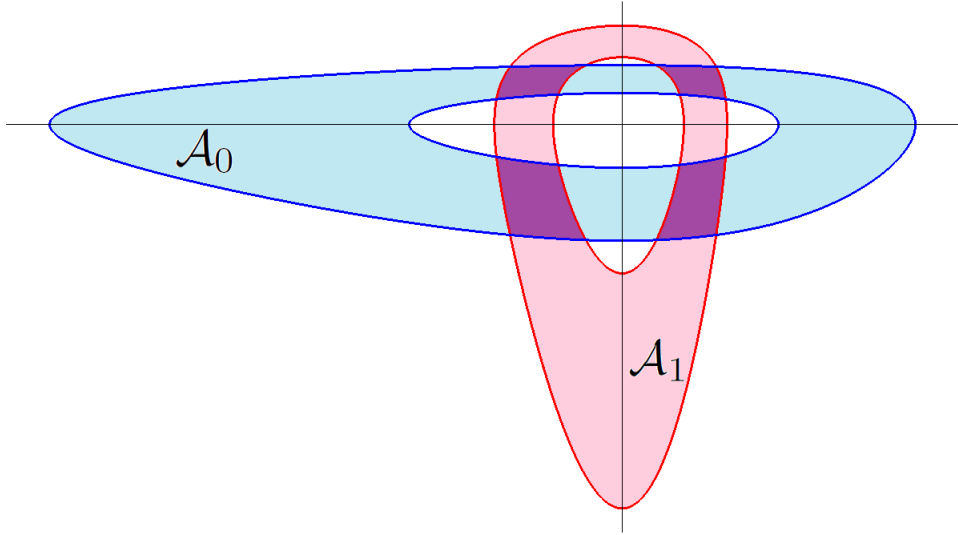


Figure 14: Two linked annuli \mathcal{A}_0 and \mathcal{A}_1 filled in by the periodic orbits of (3.24)-(I) and (3.24)-(II), respectively, and crossing to each other into four rectangular regions.

In general, to describe in a precise manner the construction of the two linked annuli, we denote by \mathcal{E}_i the energy functions for the pair (α_i, β_i) ($i = 0, 1$), so that

$$\mathcal{A}_i := \{(x, y) \in \mathbb{R}^2 : c_i \leq \mathcal{E}_i(x, y) \leq d_i\},$$

for

$$d_i > c_i > \min \mathcal{E}_i = \mathcal{E}_i(0, 0) = \alpha_i + \beta_i.$$

We also denote by $x_i^-(\ell) < 0 < x_i^+(\ell)$ the abscissas of the intersection points of the level line $\mathcal{E}_i = \ell \in [c_i, d_i]$ with the x -axis and, symmetrically, by $y_i^-(\ell) < 0 < y_i^+(\ell)$ the ordinates of the intersection points of the level line $\mathcal{E}_i = \ell \in [c_i, d_i]$ with the y -axis. Then \mathcal{A}_0 and \mathcal{A}_1 are *linked* provided that

$$x_0^-(c_0) < x_1^-(d_1); \quad x_1^+(d_1) < x_0^+(c_0), \quad y_1^-(c_1) < y_0^-(d_0); \quad y_0^+(d_0) < y_1^+(c_1).$$

This definition corresponds to that considered by Margheri, Rebelo and Zanolin [79] (see also Papini, Villari and Zanolin [91, Def. 3.2]). The regions obtained as intersections of the

two annuli, are the four components of

$$\{(x, y) \in \mathbb{R}^2 : c_0 \leq \mathcal{E}_0(x, y) \leq d_0 \wedge c_1 \leq \mathcal{E}_1(x, y) \leq d_1\},$$

each one lying in a different quadrant. They are all homeomorphic to the unit square. Now, if we denote by \mathcal{Q} and \mathcal{R} any pair chosen among these four intersections, we define the following orientations

$$\begin{aligned}\mathcal{Q}^- &:= \{(x, y) \in \mathcal{Q} : \mathcal{E}_0(x, y) = c_0\} \cup \{(x, y) \in \mathcal{Q} : \mathcal{E}_0(x, y) = d_0\}, \\ \mathcal{R}^- &:= \{(x, y) \in \mathcal{R} : \mathcal{E}_1(x, y) = c_1\} \cup \{(x, y) \in \mathcal{R} : \mathcal{E}_1(x, y) = d_1\},\end{aligned}$$

not being relevant the order in which the names “left” and “right” in these components of $[\cdot]^-$ are assigned. Finally, if we denote by Φ_1 and Φ_2 the Poincaré maps associated with (3.24)-(I) and (3.24)-(II), respectively, by the monotonicity of the period map (already exploited as, for instance, in Remark 3.1), we can prove that $\Phi_1(\mathcal{Q})$ crosses ℓ -times \mathcal{R} or, more precisely, $\Phi_1 : \widehat{\mathcal{Q}} \rightsquigarrow^\ell \widehat{\mathcal{R}}$, provided that T_0 is sufficiently large. Similarly, one can prove that $\Phi_2 : \widehat{\mathcal{R}} \rightsquigarrow^m \widehat{\mathcal{Q}}$, for sufficiently large T_1 . Thus, a chaotic dynamics on $\ell \times m$ symbols is produced for the map Φ in the set \mathcal{Q} . Equivalently, instead of taking sufficiently large T_0 and T_1 , one can put a parameter λ in front of α and β , with T_0 and T_1 fixed, to obtain complex dynamics on $\ell \times m$ symbols for all $\lambda > \lambda^*$, where λ^* depends on (ℓ, m) , as well as on the several coefficients of the equation.

Here the geometrical configuration is the same as that considered by Burra and Zanolin [15], and later generalized by Margheri, Rebelo and Zanolin [79] and Papini, Villari and Zanolin [91]. The reader is sent to these references for any further technical details.

3.3 Ideal horseshoe dynamics for weights (3.6)

In this section, we will perform a schematic construction of the Smale’s horseshoe inspired on the numerical simulations of model (3.2) with an stepwise configuration of α and β as in (3.6). These simulations show that there is *transversal intersection* between the sets $\mathcal{H}_0, \mathcal{H}_1$ and $\Phi(\mathcal{H}_0), \Phi(\mathcal{H}_1)$ in the sense that, for $i, j \in \{1, 2\}$, the intersection

$$\mathcal{H}_i \cap \Phi(\mathcal{H}_j)$$

is a unique connected set. Assuming that this is the behavior for all forward and backward iterates of the Poincaré map Φ , implies that Φ is not only semi-conjugated to the Bernouilli shift, as proved in the previous subsections (also for the general case of Theorem 3.1), but also conjugated. Figures 19-20-21 give evidence of these facts.

We will assume that there are two disjoint proper *horizontal* topological squares, $\mathcal{H}_0, \mathcal{H}_1 \subsetneq \mathcal{Q}$, such that

$$\Phi(\mathcal{H}_i) := \mathcal{V}_i \quad \text{for } i \in \{0, 1\}. \quad (3.26)$$

By *horizontal*, we mean that the lateral sides of \mathcal{H}_0 and \mathcal{H}_1 lie on the lateral sides of the square \mathcal{Q} , as sketched in Figure 15. In this figure, as in the remaining figures of this section,

we will represent any topological square as an homeomorphic square quadrangle. In order to have (3.26), it is assumed that

$$\Phi_{T_0}(\mathcal{Q}) \cap \mathcal{R} = \mathcal{R}_0 \cup \mathcal{R}_1$$

and, setting

$$\mathcal{V}_i := \Phi_{T_1}(\mathcal{R}_i) \cap \mathcal{Q}, \quad i \in \{0, 1\},$$

it follows that

$$\Phi_{T_1}(\Phi_{T_0}(\mathcal{Q}) \cap \mathcal{R}) \cap \mathcal{Q} = \Phi_{T_1}(\mathcal{R}_0 \cup \mathcal{R}_1) \cap \mathcal{Q} = \mathcal{V}_0 \cup \mathcal{V}_1.$$

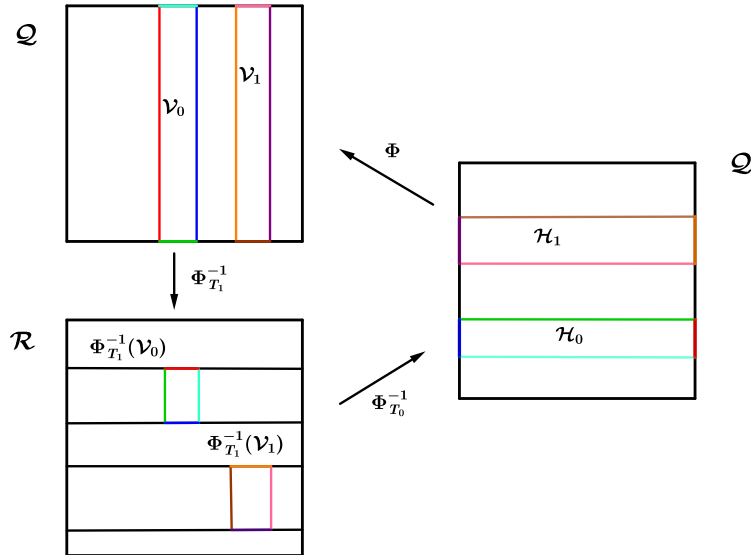


Figure 15: Φ establishes an homeomorphism between \mathcal{H}_i and \mathcal{V}_i , $i \in \{0, 1\}$.

By simply having a look at Figure 15, it is easily realized that, for every $i \in \{0, 1\}$, $\mathcal{S}_i := \Phi_{T_1}^{-1}(\mathcal{V}_i)$ is a *vertical* sub-square of \mathcal{R}_i ; vertical in the sense that it is a portion of \mathcal{R}_i linking the upper and lower sides of \mathcal{R}_i . It turns out that Φ_{T_0} sends $\mathcal{R}_i \setminus \mathcal{S}_i$ outside \mathcal{Q} . Since

$$\mathcal{H}_i := \Phi_{T_0}^{-1}(\mathcal{S}_i) = \Phi_{T_0}^{-1}(\Phi_{T_1}^{-1}(\mathcal{V}_i)) = \Phi^{-1}(\mathcal{V}_i), \quad i \in \{0, 1\},$$

it is apparent that, for every $i \in \{0, 1\}$, Φ establishes an homeomorphism between \mathcal{H}_i and \mathcal{V}_i . In particular,

$$\Phi(\mathcal{H}_i) = \mathcal{V}_i \text{ and } \Phi^{-1}(\mathcal{V}_i) = \mathcal{H}_i \text{ for each } i \in \{0, 1\}.$$

This feature is pivotal in the next construction. The intersection (in \mathcal{Q}) of the *vertical squares* \mathcal{V}_i with the *horizontal squares* \mathcal{H}_j , $i, j \in \{0, 1\}$, generates $2^2 = 4$ topological squares in \mathcal{Q} , namely

$$\mathcal{Q}_{(i,j)} := \mathcal{V}_i \cap \mathcal{H}_j, \quad i, j \in \{0, 1\},$$

which have been represented in Figure 16.

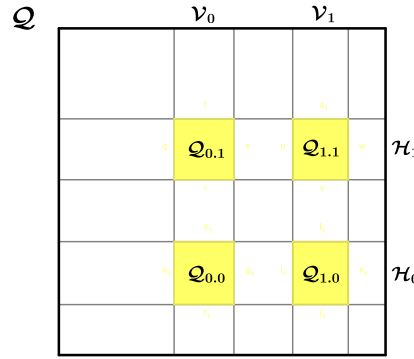


Figure 16: The invariant squares $\mathcal{Q}_{(i,j)}$, $i, j \in \{0, 1\}$.

Subsequently, we will denote Φ^0 the identity map. By construction, for every $s_{-1}, s_0 \in \{0, 1\}$ and

$$z \in \mathcal{Q}_{(s_{-1}, s_0)} = \mathcal{V}_{s_{-1}} \cap \mathcal{H}_{s_0},$$

we have that

$$\Phi^0(z) = z \in \mathcal{H}_{s_0} \text{ and } \Phi^{-1}(z) \in \Phi^{-1}(\mathcal{V}_{s_{-1}}) = \mathcal{H}_{s_{-1}}. \quad (3.27)$$

In other words,

$$\Phi^0(\mathcal{Q}_{(s_{-1}, s_0)}) = \mathcal{Q}_{(s_{-1}, s_0)} \subset \mathcal{H}_{s_0}, \quad \Phi^{-1}(\mathcal{Q}_{(s_{-1}, s_0)}) \subset \mathcal{H}_{s_{-1}}. \quad (3.28)$$

Naturally, the previous *duplication process* can be repeated for each of the topological squares \mathcal{V}_i , $i \in \{0, 1\}$. Much like \mathcal{Q} , for each $i \in \{0, 1\}$, the upper and lower sides of \mathcal{V}_i consist of two arcs of trajectory of $\Gamma(\ell_2)$ and $\Gamma(\ell_1)$, respectively. Thus, replacing \mathcal{Q} by \mathcal{V}_i we can generate the four vertical topological squares

$$\mathcal{V}_{(i,j)} := \Phi(\mathcal{V}_i) \cap \mathcal{V}_j, \quad i, j \in \{0, 1\}. \quad (3.29)$$

Then, as in \mathcal{Q} , \mathcal{V}_0 and \mathcal{V}_1 , for every $i, j \in \{0, 1\}$, $\mathcal{V}_{(i,j)}$ provides us with a vertical topological square linking $\Gamma(\ell_1)$ to $\Gamma(\ell_2)$; vertical in the sense that their upper and lower sides consist

of certain arcs of trajectory of $\Gamma(\ell_2)$ and $\Gamma(\ell_1)$, respectively. According to (3.29), it becomes apparent that, for every $i, j \in \{0, 1\}$,

$$\begin{aligned}\Phi^{-1}(\mathcal{V}_{(i,j)}) &= \Phi^{-1}(\Phi(\mathcal{V}_i) \cap \mathcal{V}_j) \subsetneq \Phi^{-1}(\mathcal{V}_j) = \mathcal{H}_j, \\ \Phi^{-2}(\mathcal{V}_{(i,j)}) &= \Phi^{-2}(\Phi(\mathcal{V}_i) \cap \mathcal{V}_j) \subsetneq \Phi^{-2}(\Phi(\mathcal{V}_i)) = \Phi^{-1}(\mathcal{V}_i) = \mathcal{H}_i.\end{aligned}\quad (3.30)$$

Similarly, we can duplicate the horizontal squares by setting

$$\mathcal{H}_{(i,j)} := \Phi^{-1}(\mathcal{H}_j) \cap \mathcal{H}_i, \quad i, j \in \{0, 1\}. \quad (3.31)$$

By construction, for every $i, j \in \{0, 1\}$, $\mathcal{H}_{(i,j)}$ is an horizontal topological square connecting the lateral sides of \mathcal{Q} , i.e., linking $\{(x, y) \in \mathcal{Q} : x = 0\}$ to $\{(x, y) \in \mathcal{Q} : x = x_1\}$. By (3.31), we have that, for every $i, j \in \{0, 1\}$,

$$\begin{aligned}\Phi^0(\mathcal{H}_{(i,j)}) &= \mathcal{H}_{(i,j)} = \Phi^{-1}(\mathcal{H}_j) \cap \mathcal{H}_i \subsetneq \mathcal{H}_i, \\ \Phi(\mathcal{H}_{(i,j)}) &= \Phi(\Phi^{-1}(\mathcal{H}_j) \cap \mathcal{H}_i) \subsetneq \Phi(\Phi^{-1}(\mathcal{H}_j)) = \mathcal{H}_j.\end{aligned}\quad (3.32)$$

Therefore, we can consider the $2^4 = 16$ topological squares in \mathcal{Q} defined as

$$\mathcal{Q}_{(s_{-2}, s_{-1}, s_0, s_1)} := \mathcal{V}_{(s_{-2}, s_{-1})} \cap \mathcal{H}_{(s_0, s_1)}, \quad s_{-2}, s_{-1}, s_0, s_1 \in \{0, 1\}. \quad (3.33)$$

We claim that, for every $s_{-2}, s_{-1}, s_0, s_1 \in \{0, 1\}$,

$$\Phi^\kappa(\mathcal{Q}_{(s_{-2}, s_{-1}, s_0, s_1)}) \subsetneq \mathcal{H}_{s_\kappa}, \quad \kappa \in \{-2, -1, 0, 1\}. \quad (3.34)$$

Indeed, by (3.33) and (3.32), we have that

$$\Phi(\mathcal{Q}_{(s_{-2}, s_{-1}, s_0, s_1)}) \subsetneq \Phi(\mathcal{H}_{(s_0, s_1)}) \subsetneq \mathcal{H}_{s_1}.$$

Thus, (3.34) holds for $\kappa = 1$. Moreover, by (3.33) and (3.31),

$$\Phi^0(\mathcal{Q}_{(s_{-2}, s_{-1}, s_0, s_1)}) = \mathcal{Q}_{(s_{-2}, s_{-1}, s_0, s_1)} \subset \mathcal{H}_{(s_0, s_{-1})} \subset \mathcal{H}_{s_0},$$

which establishes (3.34) for $\kappa = 0$. Similarly, according to (3.33) and (3.30)

$$\Phi^{-1}(\mathcal{Q}_{(s_{-2}, s_{-1}, s_0, s_1)}) \subsetneq \Phi^{-1}(\mathcal{V}_{(s_{-2}, s_{-1})}) \subsetneq \mathcal{H}_{s_{-1}},$$

and

$$\Phi^{-2}(\mathcal{Q}_{(s_{-2}, s_{-1}, s_0, s_1)}) \subsetneq \Phi^{-2}(\mathcal{V}_{(s_{-2}, s_{-1})}) \subsetneq \mathcal{H}_{s_{-2}},$$

which shows (3.34) for $\kappa = -1, -2$, which ends the proof of (3.34).

The first picture of Figure 17 represents the sixteen topological squares $\mathcal{Q}_{(s_{-2}, s_{-1}, s_0, s_1)}$, $s_i \in \{0, 1\}$, $i \in \{-2, -1, 0, 1\}$, as defined by (3.33), while the second one provides a magnification of $\mathcal{Q}_{(0,0)}$ where the dyadic fractal behavior of this process can be appreciated.

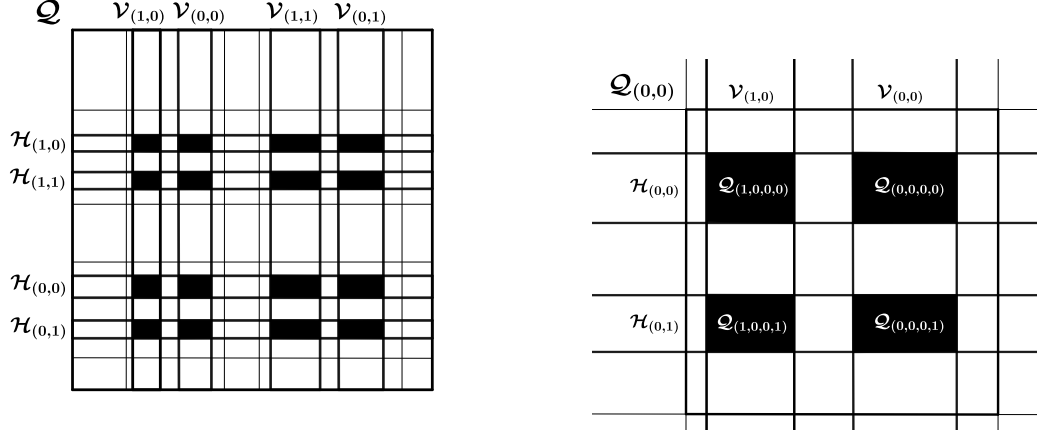


Figure 17: The squares $\mathcal{Q}_{(s_{-2}, s_{-1}, s_0, s_1)}$ (left), and a zoom of $\mathcal{Q}_{(0,0)}$ (right).

Iterating m times the previous process, it turns out that we can generate 2^m vertical rectangles. Namely, for $v_m := (s_{-m}, \dots, s_{-2}, s_{-1}) \in \{0, 1\}^m$,

$$\mathcal{V}_{v_m} := \Phi(\mathcal{V}_{(s_{-m}, \dots, s_{-2})}) \cap \mathcal{V}_{s_{-1}} = \Phi(\cdots (\Phi(\mathcal{V}_{s_{-m}}) \cap \mathcal{V}_{s_{-m+1}}) \cdots) \cap \mathcal{V}_{-2}) \cap \mathcal{V}_{-1}.$$

Thus, by definition, for $\kappa \in \{-1, -2, \dots, -m\}$,

$$\Phi^\kappa(\mathcal{V}_{v_m}) \subsetneq \Phi^{-1}(\mathcal{V}_{s_\kappa}) = \mathcal{H}_{s_\kappa}. \quad (3.35)$$

Similarly, there exists 2^m horizontal rectangles such that for $h_m = (s_0, s_1, \dots, s_{m-1}) \in \{0, 1\}^m$,

$$\mathcal{H}_{h_m} := \Phi(\mathcal{H}_{(s_1, \dots, s_{m-1})}) \cap \mathcal{H}_{s_0} = \Phi^{-1}(\cdots (\Phi^{-1}(\mathcal{H}_{s_{m-1}}) \cap \mathcal{H}_{s_{m-2}}) \cdots) \cap \mathcal{H}_{s_1}) \cap \mathcal{H}_{s_0}.$$

and, hence, for $\kappa \in \{0, 1, \dots, m-1\}$,

$$\Phi^\kappa(\mathcal{H}_{h_m}) \subsetneq \mathcal{H}_{s_\kappa}. \quad (3.36)$$

Figure 18 shows the steps $m = 2$ and $m = 3$ of this process for both the vertical and horizontal squares.

Then, setting

$$\mathcal{Q}_{\Sigma_m} := \mathcal{V}_{v_m} \cap \mathcal{H}_{h_m},$$

where

$$\Sigma_m := (v_m, h_m) = (s_{-m}, \dots, s_{-1}, s_0, \dots, s_{m-1}) \in \{0, 1\}^{2m},$$

it becomes apparent that, by (3.35) and (3.36), for every integer $\kappa \in [-m, m-1]$,

$$\Phi^\kappa(\mathcal{Q}_{\Sigma_m}) \subset \mathcal{H}_{s_\kappa}.$$

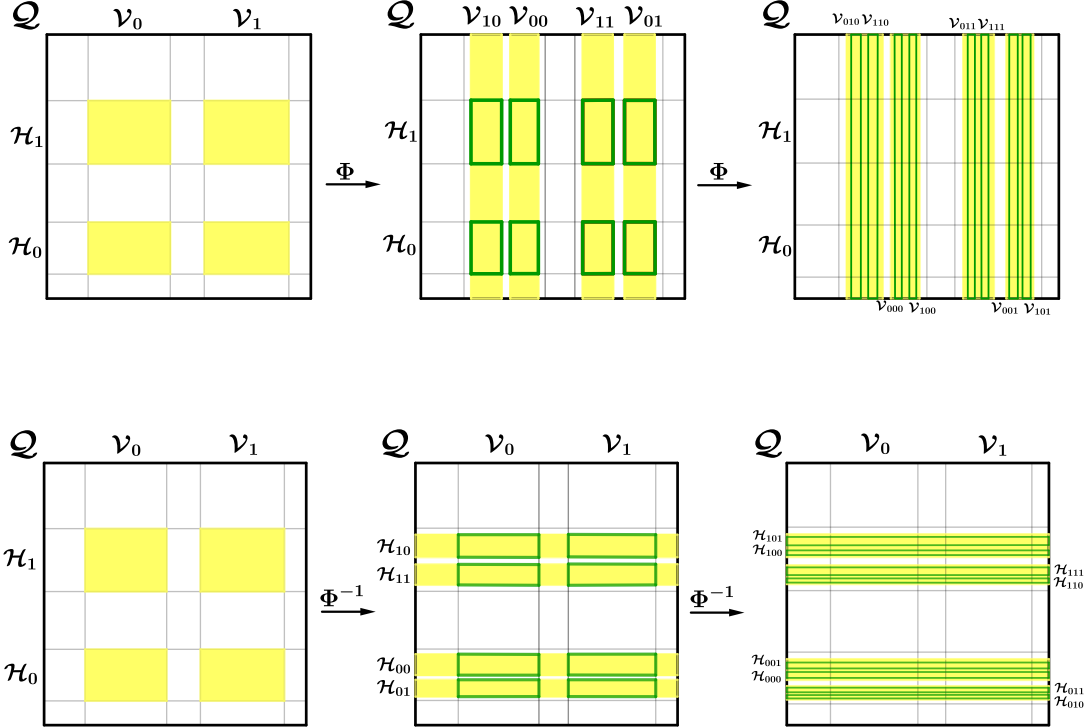


Figure 18: Dyadic fragmentation in horizontal and vertical lines.

As we have constructed two sequences of nonempty compact, connected nested topological squares, \mathcal{V}_{v_m} , \mathcal{H}_{h_m} , by the Cantor principle,

$$\mathcal{V}_{s_v} := \lim_{m \rightarrow +\infty} \mathcal{V}_{v_m} \quad \text{and} \quad \mathcal{H}_{s_h} := \lim_{m \rightarrow +\infty} \mathcal{H}_{h_m}$$

are two nonempty continua with

$$s_v = (\dots, s_{-2}, s_{-1}) \in \{0, 1\}^{\mathbb{N}}, \quad s_h = (s_0, s_1, \dots) \in \{0, 1\}^{\mathbb{N}}.$$

Moreover, by the transversality assumptions, the intersection $\mathcal{V}_{s_v} \cap \mathcal{H}_{s_h}$ is a point and $(s_v, s_h) \in \{0, 1\}^{\mathbb{Z}}$. Furthermore,

$$\Lambda := \bigcup_{s_v, s_h \in \{0, 1\}^{\mathbb{N}}} \mathcal{V}_{s_v} \cap \mathcal{H}_{s_h}$$

is the invariant set of Φ . Therefore, thanks to the choice of the labels s_v and s_h that we have done, it becomes apparent that Φ is conjugated to the Bernoulli full shift in two symbols.

We conclude this section with some geometrical and numerical schemes illustrating the actual occurrence of the theoretical horseshoe framework described above. To simplify the exposition, we consider the case of an annular region under the effect of the composition of a twist map with a vertical shear map. Even if the geometry of the level lines associated with the predator-prey system does not consist of circumferences, nonetheless this can be assumed as a reasonable approximation if we consider small orbits around the equilibrium point (as in [62]) or we suppose to have performed an action-angle transformation leading to an equivalent planar system where the radial component is constant.

The following pictures describe the geometric effect of the composition of a twist map Φ_{T_0} and a vertical shear map Φ_{T_1} on a domain in the first quadrant which is defined like the set \mathcal{Q} in Section 3.1, and denoted again by \mathcal{Q} . Actually, we describe the effect of the maps and their composition $\Phi = \Phi_{T_1} \circ \Phi_{T_0}$, with respect to the homeomorphic unit square $[0, 1]^2$, considered as a reference domain, where we can transfer the geometry. Figure 19 shows \mathcal{Q} , its image through a twist map (with a sufficiently large twist, corresponding to a sufficiently large time T_0) and the effect on the unit square. More precisely, if we denote by $\eta = (\eta_1, \eta_2)$ the homeomorphism from the unit square to \mathcal{Q} , the two bands in the third panel of Figure 19 represent the sets $[0, 1]^2 \cap (\hat{\eta}^{-1} \circ \Phi_{T_0} \circ \eta)^{-1}([0, 1]^2)$ where $\hat{\eta} = (\eta_1, -\eta_2)$ is the homeomorphism from the unit square to \mathcal{R} , which is the target set in the fourth quadrant symmetric to \mathcal{Q} . As a next step, Figure 20 shows the effect on the vertical shear mapping on the set \mathcal{R} and we also show the set of points in the unit square which are mapped into \mathcal{Q} , that is $[0, 1]^2 \cap (\eta^{-1} \circ \Phi_{T_1} \circ \hat{\eta})^{-1}([0, 1]^2)$.

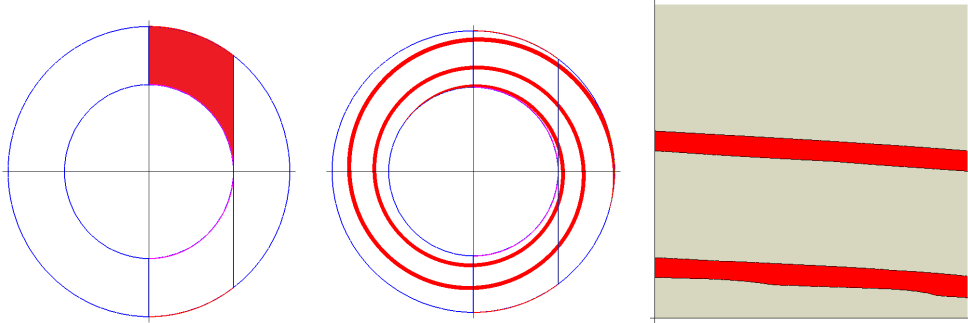


Figure 19: Example of an annular region under the action of a twist map. From left to right: a rectangular domain \mathcal{Q} in the first quadrant, its evolution by a twist map, the part of the unit square (homeomorphic to \mathcal{Q}) which is mapped to the region in the fourth quadrant which is symmetric to \mathcal{Q} .

Finally, Figure 21 puts in evidence the set of points of \mathcal{Q} , represented in the unit square, which come back to \mathcal{Q} after $\Phi = \Phi_{T_1} \circ \Phi_{T_0}$, that is $[0, 1]^2 \cap (\eta^{-1} \circ \Phi \circ \eta)^{-1}([0, 1]^2)$. Obviously, this is a subset of the two bands domain appearing in the third panel of Figure 19.

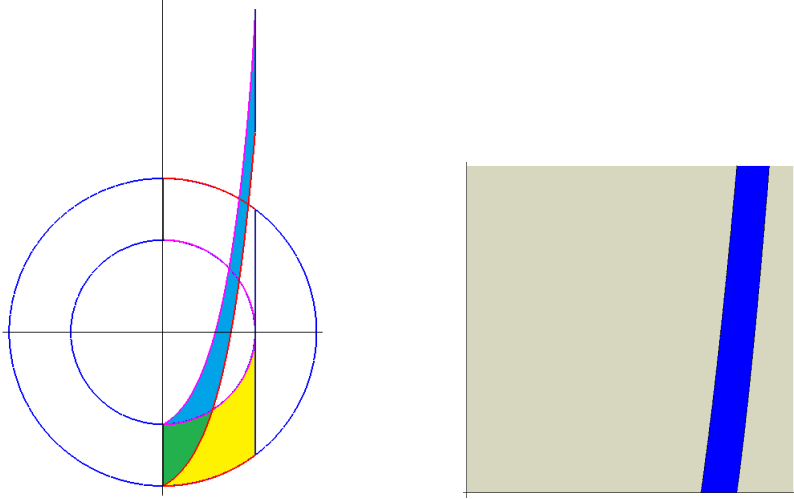


Figure 20: The region in the fourth quadrant (symmetric to \mathcal{Q}) and its transformation by a vertical shear map as in Section 3.1 (left panel). The right panel put in evidence, with respect to the homeomorphic unit square, the part of the region which arrives to \mathcal{Q} .

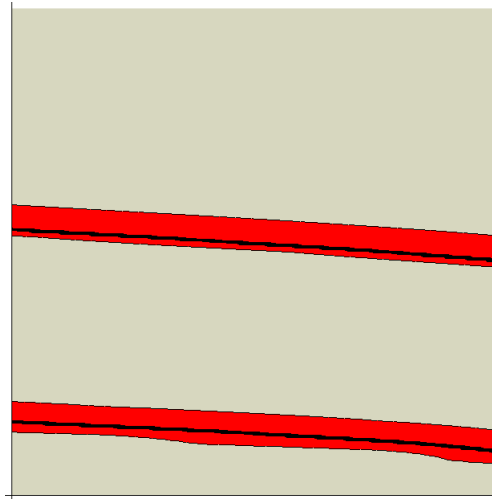


Figure 21: The final effect of the twist map and the vertical shear map, as viewed from the unit square. The larger horizontal bands represent the set of points in \mathcal{Q} which are moved to \mathcal{R} under the action of the twist map. The narrow darker bands represent the set of points which come back to \mathcal{Q} after the application of the vertical shear map.

If we consider the inverse homeomorphism $\Phi^{-1} = \Phi_{T_0}^{-1} \circ \Phi_{T_1}^{-1}$ and look for the sets of points of \mathcal{Q} which remain in the domain after the first iteration, we can repeat, symmetrically the same argument as before. As a first step, passing to the unit square, we will consider the set of the points $w \in [0, 1]^2$ such that $(\hat{\eta}^{-1} \circ \Phi_{T_1}^{-1} \circ \eta)(w) \in [0, 1]^2$, which clearly equals

$[0, 1]^2 \cap (\eta^{-1} \circ \Phi_{T_1} \circ \hat{\eta})^{-1}([0, 1]^2)$, that is, the blue set appearing in the second panel of Figure 20. Next we will consider the set of points of \mathcal{R} which belong to \mathcal{Q} after the action of the inverse twist $\Phi_{T_0}^{-1}$, which transferred to the unit square is $[0, 1]^2 \cap (\eta^{-1} \circ \Phi_{T_0}^{-1} \circ \hat{\eta})^{-1}([0, 1]^2)$. This is exactly the set described in the third panel of Figure 19. At the end, the set $[0, 1]^2 \cap (\eta^{-1} \circ \Phi^{-1} \circ \eta)^{-1}([0, 1]^2)$ will be made by two narrow bands inside the rectangular region in the second panel of Figure 20.

From these numerical outcomes it is apparent that the “real dynamics” follows precisely the abstract scheme of the Smale’s horseshoe map.

References

- [1] A. Abbondandolo. *Morse theory for Hamiltonian systems*, volume 425 of *Chapman & Hall/CRC Research Notes in Mathematics*. Chapman & Hall/CRC, Boca Raton, FL, 2001.
- [2] R. L. Adler, A. G. Konheim, and M. H. McAndrew. Topological entropy. *Trans. Amer. Math. Soc.*, 114:309–319, 1965.
- [3] H. N. Agiza, E. M. ELabbasy, H. EL-Metwally, and A. A. Elsadany. Chaotic dynamics of a discrete prey-predator model with Holling type II. *Nonlinear Anal. Real World Appl.*, 10(1):116–129, 2009.
- [4] D. K. Arrowsmith and C. M. Place. *Dynamical systems*. Chapman and Hall Mathematics Series. Chapman & Hall, London, 1992. Differential equations, maps and chaotic behaviour.
- [5] B. Aulbach and B. Kieninger. On three definitions of chaos. *Nonlinear Dyn. Syst. Theory*, 1(1):23–37, 2001.
- [6] H. Baek and Y. Do. Seasonal effects on a Beddington-DeAngelis type predator-prey system with impulsive perturbations. *Abstr. Appl. Anal.*, pages Art. ID 695121, 19, 2009.
- [7] J.L. Begon, M. Harper and C.R. Townsend. *Ecology, Individual, Populations and Communities*. Blackwell Scientific-Publications, Cambridge, Massachusetts, 1990.
- [8] P. Benevieri and M. Furi. A simple notion of orientability for Fredholm maps of index zero between Banach manifolds and degree theory. *Ann. Sci. Math. Québec*, 22:131–148, 1998.
- [9] P. Benevieri and M. Furi. On the concept of orientability for Fredholm maps between real Banach manifolds. *Top. Meth. Nonl. Anal.*, 16:279–306, 2000.
- [10] A. Boscaggin. Subharmonic solutions of planar Hamiltonian systems: a rotation number approach. *Adv. Nonlinear Stud.*, 11(1):77–103, 2011.
- [11] A. Boscaggin and E. Muñoz-Hernández. Planar Hamiltonian systems: Index theory and applications to the existence of subharmonics. *Nonlinear Analysis*, 226:113142, 2023.
- [12] M. Braun. *Differential equations and their applications*. Springer-Verlag, New York-Berlin, 1983. Third edition (short version).
- [13] H. W. Broer, V. Naudot, R. Roussarie, and K. Saleh. A predator-prey model with non-monotonic response function. *Regul. Chaotic Dyn.*, 11(2):155–165, 2006.
- [14] K. Burns and H. Weiss. A geometric criterion for positive topological entropy. *Comm. Math. Phys.*, 172(1):95–118, 1995.

- [15] L. Burra and F. Zanolin. Chaotic dynamics in a simple class of Hamiltonian systems with applications to a pendulum with variable length. *Differential Integral Equations*, 22(9-10):927–948, 2009.
- [16] G. J. Butler and H. I. Freedman. Periodic solutions of a predator-prey system with periodic coefficients. *Math. Biosci.*, 55(1-2):27–38, 1981.
- [17] R. C. Cantrell and C. Cosner. *Spatial Ecology via Reaction-Diffusion Equations*. Wiley, 2004.
- [18] M. C. Carbinatto, J. Kwapisz, and K. Mischaikow. Horseshoes and the Conley index spectrum. *Ergodic Theory Dynam. Systems*, 20(2):365–377, 2000.
- [19] S. N. Chow and J. K. Hale. *Methods of bifurcation theory*, volume 251 of *Grundlehren der Mathematischen Wissenschaften [Fundamental Principles of Mathematical Sciences]*. Springer-Verlag, New York-Berlin, 1982.
- [20] C. Conley and E. Zehnder. Subharmonic solutions and Morse theory. *Physica A*, 124:649–657, 1984.
- [21] M. G. Crandall and P. H. Rabinowitz. Bifurcation from simple eigenvalues. *J. Functional Analysis*, 8:321–340, 1971.
- [22] M. G. Crandall and P. H. Rabinowitz. Bifurcation, perturbation of simple eigenvalues and linearized stability. *Arch. Rational Mech. Anal.*, 52:161–180, 1973.
- [23] J. M. Cushing. Periodic time-dependent predator-prey systems. *SIAM J. Appl. Math.*, 32(1):82–95, 1977.
- [24] J. M. Cushing. Two species competition in a periodic environment. *J. Mathematical Biology*, 10:385–390, 1980.
- [25] F. Dalbono and C. Rebelo. Poincaré-Birkhoff fixed point theorem and periodic solutions of asymptotically linear planar Hamiltonian systems. *Rend. Sem. Mat. Univ. Politec. Torino*, 60(4):233–263, 2002.
- [26] R. L. Devaney. Subshifts of finite type in linked twist mappings. *Proc. Amer. Math. Soc.*, 71(2):334–338, 1978.
- [27] R. L. Devaney. *An introduction to chaotic dynamical systems*. Addison-Wesley Studies in Nonlinearity. Addison-Wesley Publishing Company, Advanced Book Program, Redwood City, CA, second edition, 1989.
- [28] R. Dieckerhoff and E. Zehnder. Boundedness of solutions via the twist-theorem. *Ann. Scuola Norm. Sup. Pisa Cl. Sci. (4)*, 14(1):79–95, 1987.
- [29] T. R. Ding and F. Zanolin. Harmonic solutions and subharmonic solutions for periodic Lotka-Volterra systems. In *Dynamical systems (Tianjin, 1990/1991)*, volume 4 of *Nankai Ser. Pure Appl. Math. Theoret. Phys.*, pages 55–65. World Sci. Publ., River Edge, NJ, 1993.
- [30] T. R. Ding and F. Zanolin. Periodic solutions and subharmonic solutions for a class of planar systems of Lotka-Volterra type. In *World Congress of Nonlinear Analysts '92, Vol. I-IV (Tampa, FL, 1992)*, pages 395–406. De Gruyter, Berlin, 1996.
- [31] W. Y. Ding. Fixed points of twist mappings and periodic solutions of ordinary differential equations. *Acta Math. Sinica*, 25(2):227–235, 1982.

- [32] T. Dondè and F. Zanolin. Multiple periodic solutions for one-sided sublinear systems: a refinement of the Poincaré-Birkhoff approach. *Topol. Methods Nonlinear Anal.*, 55(2):565–581, 2020.
- [33] J. Esquinias. Optimal multiplicity in local bifurcation theory, II: General case. *J. Differential Equations*, 75:206–215, 1988.
- [34] J. Esquinias and J. López-Gómez. Optimal multiplicity in local bifurcation theory. I. Generalized generic eigenvalues. *J. Differential Equations*, 71(1):72–92, 1988.
- [35] G. Feltrin. Positive subharmonic solutions to superlinear ODEs with indefinite weight. *Discrete Contin. Dyn. Syst. Ser. S*, 11(2):257–277, 2018.
- [36] P. M. Fitzpatrick and J. Pejsachowicz. Parity and generalized multiplicity. *Trans. Amer. Math. Soc.*, 326:281–305, 1991.
- [37] P. M. Fitzpatrick, J. Pejsachowicz, and P. J. Rabier. Orientability of Fredholm families and topological degree for orientable nonlinear Fredholm mappings. *J. Funct. Anal.*, 124(1):1–39, 1994.
- [38] A. Fonda and A. C. Lazer. Subharmonic solutions of conservative systems with nonconvex potentials. *Proc. Amer. Math. Soc.*, 115(1):183–190, 1992.
- [39] A. Fonda, M. Sabatini, and F. Zanolin. Periodic solutions of perturbed Hamiltonian systems in the plane by the use of the Poincaré-Birkhoff theorem. *Topol. Methods Nonlinear Anal.*, 40(1):29–52, 2012.
- [40] A. Fonda and R. Toader. Subharmonic solutions of Hamiltonian systems displaying some kind of sublinear growth. *Adv. Nonlinear Anal.*, 8(1):583–602, 2019.
- [41] A. Fonda and A. J. Ureña. A higher dimensional Poincaré-Birkhoff theorem for Hamiltonian flows. *Ann. Inst. H. Poincaré C Anal. Non Linéaire*, 34(3):679–698, 2017.
- [42] J. Franks. Generalizations of the Poincaré-Birkhoff theorem. *Ann. of Math. (2)*, 128(1):139–151, 1988.
- [43] M. Garrione, A. Margheri, and C. Rebelo. Nonautonomous nonlinear ODEs: nonresonance conditions and rotation numbers. *J. Math. Anal. Appl.*, 473(1):490–509, 2019.
- [44] C. F. Gauss. *Disquisitiones arithmeticae*. Springer-Verlag, New York, 1986. Translated and with a preface by Arthur A. Clarke, Revised by William C. Waterhouse, Cornelius Greither and A. W. Grootendorst and with a preface by Waterhouse.
- [45] P. Gidoni and A. Margheri. Lower bounds on the number of periodic solutions for asymptotically linear planar Hamiltonian systems. *Discrete Contin. Dyn. Syst.*, 39(1):585–606, 2019.
- [46] M. Golubitsky and D. G. Schaeffer. *Singularities and Groups in Bifurcation Theory*. Applied Mathematical Sciences vol. 51, Springer Verlag, New York University, 1985.
- [47] J. Guckenheimer and P. Holmes. *Nonlinear oscillations, dynamical systems, and bifurcations of vector fields*, volume 42 of *Applied Mathematical Sciences*. Springer-Verlag, New York, 1983.
- [48] A. R. Hausrath. Periodic integral manifolds for periodically forced Volterra-Lotka equations. *J. Math. Anal. Appl.*, 87(2):474–488, 1982.
- [49] A. R. Hausrath and R. F. Manásevich. Periodic solutions of a periodically perturbed Lotka-Volterra equation using the Poincaré-Birkhoff theorem. *J. Math. Anal. Appl.*, 157(1):1–9, 1991.

- [50] M. Hénon. Numerical study of quadratic area-preserving mappings. *Quart. Appl. Math.*, 27:291–312, 1969.
- [51] P. Hess. *Periodic Parabolic Boundary Value Problems and Positivity*. Longman Scientific and Technical, 1991.
- [52] V. Hutson, J. López-Gómez, K. Mischaikow, and G. Vickers. Limit behaviour for a competing species problem with diffusion. In *Dynamical systems and applications*, volume 4 of *World Sci. Ser. Appl. Anal.*, pages 343–358. World Sci. Publ., River Edge, NJ, 1995.
- [53] J. Kennedy and J. A. Yorke. Topological horseshoes. *Trans. Amer. Math. Soc.*, 353(6):2513–2530, 2001.
- [54] U. Kirchgraber and D. Stoffer. On the definition of chaos. *Z. Angew. Math. Mech.*, 69(7):175–185, 1989.
- [55] M. A. Krasnosel'skii. *Topological methods in the theory of nonlinear integral equations*. A Pergamon Press Book. The Macmillan Company, New York, 1964. Translated by A. H. Armstrong; translation edited by J. Burlak.
- [56] Y. A. Kuznetsov, S. Muratori, and S. Rinaldi. Bifurcations and chaos in a periodic predator-prey model. *Internat. J. Bifur. Chaos Appl. Sci. Engrg.*, 2(1):117–128, 1992.
- [57] I. S. Labouriau and E. Sovrano. Chaos in periodically forced reversible vector fields. *J. Singul.*, 22:227–240, 2020.
- [58] S. Laederich and M. Levi. Invariant curves and time-dependent potentials. *Ergodic Theory Dynam. Systems*, 11(2):365–378, 1991.
- [59] M. Levi. Quasiperiodic motions in superquadratic time-periodic potentials. *Comm. Math. Phys.*, 143(1):43–83, 1991.
- [60] T. Y. Li and J. A. Yorke. Period three implies chaos. *Amer. Math. Monthly*, 82(10):985–992, 1975.
- [61] D. Liberzon. *Switching in systems and control*. Systems & Control: Foundations & Applications. Birkhäuser Boston, Inc., Boston, MA, 2003.
- [62] B. Liu. The stability of harmonic solutions of Lotka–Volterra systems. *J. Math. Anal. Appl.*, 194(3):727–740, 1995.
- [63] Y. Long. *Index theory for symplectic paths with applications*, volume 207 of *Progress in Mathematics*. Birkhäuser Verlag, Basel, 2002.
- [64] J. López-Gómez. Positive periodic solutions of Lotka–Volterra reaction-diffusion systems. *Differential and Integral Equations*, 5(1):55–72, 1992.
- [65] J. López-Gómez. Permanence under strong competition. *World Scientific Series in Applied Analysis*, 4(4):473–488, 1995.
- [66] J. López-Gómez. A bridge between operator theory and mathematical biology. In *Operator theory and its applications (Winnipeg, MB, 1998)*, volume 25 of *Fields Inst. Commun.*, pages 383–397. Amer. Math. Soc., Providence, RI, 2000.
- [67] J. López-Gómez. *Spectral theory and nonlinear functional analysis*, volume 426 of *Chapman & Hall/CRC Research Notes in Mathematics*. Chapman & Hall/CRC, Boca Raton, FL, 2001.

- [68] J. López-Gómez. *Metasolutions of Parabolic Equations in Population Dynamics*. CRC Press, Boca Raton, 2015.
- [69] J. López-Gómez and M. Molina-Meyer. The competitive exclusion principle versus biodiversity through segregation and further adaptation to spatial heterogeneities. *Theoretical Population Biology*, 69:94–109, 2006.
- [70] J. López-Gómez and M. Molina-Meyer. Superlinear indefinite systems: beyond Lotka-Volterra models. *J. Differ. Equations*, 221(2):343–411, 2006.
- [71] J. López-Gómez and C. Mora-Corral. Counting zeroes of C^1 Fredholm maps of index 1. *Bull. London Math. Soc.*, 37:778–792, 2005.
- [72] J. López-Gómez and C. Mora-Corral. *Algebraic multiplicity of eigenvalues of linear operators*, volume 177 of *Operator Theory: Advances and Applications*. Birkhäuser Verlag, Basel, 2007.
- [73] J. López-Gómez and E. Muñoz-Hernández. Global structure of subharmonics in a class of periodic predator-prey models. *Nonlinearity*, 33(1):34–71, 2020.
- [74] J. López-Gómez, E. Muñoz-Hernández, and F. Zanolin. On the applicability of the Poincaré-Birkhoff twist theorem to a class of planar periodic predator-prey models. *Discrete Contin. Dyn. Syst.*, 40(4):2393–2419, 2020.
- [75] J. López-Gómez, E. Muñoz-Hernández, and F. Zanolin. The Poincaré-Birkhoff theorem for a class of degenerate planar Hamiltonian systems. *Adv. Nonlinear Stud.*, 21(3):489–499, 2021.
- [76] J. López-Gómez, R. Ortega, and A. Tineo. The periodic predator-prey Lotka-Volterra model. *Adv. Differential Equations*, 1(3):403–423, 1996.
- [77] A. J. Lotka. *Analytical theory of biological populations*. The Plenum Series on Demographic Methods and Population Analysis. Plenum Press, New York, 1998. Translated from the 1939 French edition and with an introduction by David P. Smith and Hélène Rossert.
- [78] A. Margheri, C. Rebelo, and F. Zanolin. Maslov index, Poincaré-Birkhoff theorem and periodic solutions of asymptotically linear planar Hamiltonian systems. *J. Differential Equations*, 183(2):342–367, 2002.
- [79] A. Margheri, C. Rebelo, and F. Zanolin. Chaos in periodically perturbed planar Hamiltonian systems using linked twist maps. *J. Differential Equations*, 249(12):3233–3257, 2010.
- [80] R. M. May. Simple mathematical models with very complicated dynamics. *Nature*, 261:459–467, 1976.
- [81] A. Medio, M. Pireddu, and F. Zanolin. Chaotic dynamics for maps in one and two dimensions: a geometrical method and applications to economics. *Internat. J. Bifur. Chaos Appl. Sci. Engrg.*, 19(10):3283–3309, 2009.
- [82] R. Michalek and G. Tarantello. Subharmonic solutions with prescribed minimal period for nonautonomous Hamiltonian systems. *J. Differential Equations*, 72(1):28–55, 1988.
- [83] K. Mischaikow and M. Mrozek. Isolating neighborhoods and chaos. *Japan J. Indust. Appl. Math.*, 12(2):205–236, 1995.
- [84] J. Moser. On invariant curves of area-preserving mappings of an annulus. *Nachr. Akad. Wiss. Göttingen Math.-Phys. Kl. II*, 1962:1–20, 1962.

- [85] J. Moser. *Stable and random motions in dynamical systems*. Annals of Mathematics Studies, No. 77. Princeton University Press, Princeton, N. J.; University of Tokyo Press, Tokyo, 1973. With special emphasis on celestial mechanics, Hermann Weyl Lectures, the Institute for Advanced Study, Princeton, N. J.
- [86] J. D. Murray. *Mathematical Biology. I*, volume 17 of *Interdisciplinary Applied Mathematics*. Springer-Verlag, New York, third edition, 2002.
- [87] S. Nakaoka, Y. Saito, and Y. Takeuchi. Stability, delay, and chaotic behavior in a Lotka-Volterra predator-prey system. *Math. Biosci. Eng.*, 3(1):173–187, 2006.
- [88] W. D. Neumann. Generalizations of the Poincaré Birkhoff fixed point theorem. *Bull. Austral. Math. Soc.*, 17(3):375–389, 1977.
- [89] W. M. Ni. *The Mathematics of Diffusion*. SIAM, Philadelphia, 2011. CBMS-NSF Regional Conf. Ser. in Appl. Math., vol. 82.
- [90] L. Nirenberg. *Topics in Nonlinear Functional Analysis*. Courant Institute of Mathematical Sciences, New York University, 1974.
- [91] D. Papini, G. Villari, and F. Zanolin. Chaotic dynamics in a periodically perturbed Liénard system. *Differential Integral Equations*, 32(11-12):595–614, 2019.
- [92] D. Papini and F. Zanolin. Fixed points, periodic points, and coin-tossing sequences for mappings defined on two-dimensional cells. *Fixed Point Theory Appl.*, (2):113–134, 2004.
- [93] D. Papini and F. Zanolin. On the periodic boundary value problem and chaotic-like dynamics for nonlinear Hill’s equations. *Adv. Nonlinear Stud.*, 4(1):71–91, 2004.
- [94] A. Pascoletti, M. Pireddu, and F. Zanolin. Multiple periodic solutions and complex dynamics for second order ODEs via linked twist maps. In *The 8th Colloquium on the Qualitative Theory of Differential Equations*, volume 8 of *Proc. Colloq. Qual. Theory Differ. Equ.*, pages No. 14, 32. Electron. J. Qual. Theory Differ. Equ., Szeged, 2008.
- [95] M. Pireddu and F. Zanolin. Chaotic dynamics in the Volterra predator-prey model via linked twist maps. *Opuscula Math.*, 28(4):567–592, 2008.
- [96] M. Pireddu and F. Zanolin. Fixed points, periodic points and chaotic dynamics for continuous maps with applications to population dynamics. In *Lotka-Volterra and related systems*, volume 2 of *De Gruyter Ser. Math. Life Sci.*, pages 123–233. De Gruyter, Berlin, 2013.
- [97] D. Qian and P. J. Torres. Periodic motions of linear impact oscillators via the successor map. *SIAM J. Math. Anal.*, 36(6):1707–1725, 2005.
- [98] P. H. Rabinowitz. Some global results for nonlinear eigenvalue problems. *J. Functional Analysis*, 7:487–513, 1971.
- [99] P. H. Rabinowitz. Some aspects of nonlinear eigenvalue problems. *Rocky Mountain J. Math.*, 3:161–202, 1973.
- [100] P. H. Rabinowitz. On subharmonic solutions of Hamiltonian systems. *Comm. Pure Appl. Math.*, 33(5):609–633, 1980.
- [101] C. Rebelo. A note on the Poincaré-Birkhoff fixed point theorem and periodic solutions of planar systems. *Nonlinear Anal.*, 29(3):291–311, 1997.

- [102] S. Rosenblat. Population models in a periodically fluctuating environment. *J. Math. Biol.*, 9(1):23–36, 1980.
- [103] F. Rothe. The periods of the Volterra-Lotka system. *J. Reine Angew. Math.*, 355:129–138, 1985.
- [104] A. Ruiz-Herrera. Chaos in predator-prey systems with/without impulsive effect. *Nonlinear Anal. Real World Appl.*, 13(2):977–986, 2012.
- [105] R. Schaaf. A class of Hamiltonian systems with increasing periods. *J. Reine Angew. Math.*, 363:96–109, 1985.
- [106] E. Serra, M. Tarallo, and S. Terracini. Subharmonic solutions to second-order differential equations with periodic nonlinearities. *Nonlinear Anal.*, 41(5-6, Ser. A: Theory Methods):649–667, 2000.
- [107] J. Shi and X. Wang. On global bifurcation for quasilinear elliptic system on bounded domains. *J. Differential Equations*, 124:1–39, 1994.
- [108] S. Smale. Diffeomorphisms with many periodic points. In *Differential and Combinatorial Topology (A Symposium in Honor of Marston Morse)*, pages 63–80. Princeton Univ. Press, Princeton, N.J., 1965.
- [109] S. Smale. Differentiable dynamical systems. *Bull. Amer. Math. Soc.*, 73:747–817, 1967.
- [110] S. Smale. Finding a horseshoe on the beaches of Rio. *Math. Intelligencer*, 20(1):39–44, 1998.
- [111] R. Srzednicki. A generalization of the Lefschetz fixed point theorem and detection of chaos. *Proc. Amer. Math. Soc.*, 128(4):1231–1239, 2000.
- [112] R. Srzednicki and K. Wójcik. A geometric method for detecting chaotic dynamics. *J. Differential Equations*, 135(1):66–82, 1997.
- [113] R. Sturman, J. M. Ottino, and S. Wiggins. *The mathematical foundations of mixing*, volume 22 of *Cambridge Monographs on Applied and Computational Mathematics*. Cambridge University Press, Cambridge, 2006.
- [114] P. Táboas. Periodic solutions of a forced Lotka-Volterra equation. *J. Math. Anal. Appl.*, 124(1):82–97, 1987.
- [115] Y. Takeuchi and N. Adachi. Influence of predation on species coexistence in Volterra models. *Math. Biosci.*, 70(1):65–90, 1984.
- [116] Y. Takeuchi, N. H. Du, N. T. Hieu, and K. Sato. Evolution of predator-prey systems described by a Lotka-Volterra equation under random environment. *J. Math. Anal. Appl.*, 323(2):938–957, 2006.
- [117] J. Vandermeer, L. Stone, and B. Blasius. Categories of chaos and fractal basin boundaries in forced predator-prey models. *Chaos, Solitons & Fractals*, 12(2):265–276, 2001.
- [118] V. Volterra. *Variazioni e fluttuazioni del numero d'individui in specie animali conviventi*. Mem. Acad. Lincei, Società anonima tipografica Leonardo da Vinci, 1926.
- [119] V. Volterra. *Leçons sur la théorie mathématique de la lutte pour la vie*. Les Grands Classiques Gauthier-Villars. [Gauthier-Villars Great Classics]. Éditions Jacques Gabay, Sceaux, 1990. Reprint of the 1931 original.

- [120] J. Waldvogel. The period in the Lotka-Volterra system is monotonic. *J. Math. Anal. Appl.*, 114(1):178–184, 1986.
- [121] S. Wiggins. *Introduction to applied nonlinear dynamical systems and chaos*, volume 2 of *Texts in Applied Mathematics*. Springer-Verlag, New York, second edition, 2003.
- [122] K. Wójcik and P. Zgliczyński. Isolating segments, fixed point index, and symbolic dynamics. *J. Differential Equations*, 161(2):245–288, 2000.
- [123] P. Zgliczyński. Fixed point index for iterations of maps, topological horseshoe and chaos. *Topol. Methods Nonlinear Anal.*, 8(1):169–177, 1996.
- [124] P. Zgliczyński and M. Gidea. Covering relations for multidimensional dynamical systems. *J. Differential Equations*, 202(1):32–58, 2004.